***Highlights (for review)**

Highlights

- RSL histories were reconstructed for four regions in the New Zealand archipelago
- Northern sites experience RSL rise earlier compared to southern sites
- Northern sites experience a higher-magnitude highstand compared to southern sites
- Long-wavelength signals from Antarctica cannot explain the observed variation in RSL
- A range of processes potentially drive the observed variation in RSL

*Manuscript
Click here to view linked References

An examination of spatial variability in the timing and magnitude of Holocene relative sea-level changes in the New Zealand archipelago

Alastair J.H. Clement[1*], Pippa L. Whitehouse[2] and Craig R. Sloss[3]

1 Physical Geography Group, Institute of Agriculture and Environment, Massey University, Private Bag 11-222, Palmerston North 4442, New Zealand

2 Department of Geography, Durham University, South Road, Durham, DH1 3LE, UK

3 School of Earth and Environmental Sciences, Queensland University of Technology, GPO Box 2434, Brisbane Q 4001, Australia

* Corresponding author: Tel: + 64 6 3569099 extn 84847; Email address: a.clement@massey.ac.nz

Abstract

Holocene relative sea-level (RSL) changes have been reconstructed for four regions within the New Zealand archipelago: the northern North Island (including Northland, Auckland, and the Coromandel Peninsula); the southwest coast of the North Island; the Canterbury coast (South Island); and the Otago coast (South Island). In the North Island the RSL highstand commenced c. 8,100-7,2400 cal yr BP when present mean sea-level (PMSL) was first attained. This is c. 600-1,400 years earlier than has been previously indicated for the New Zealand region as a whole, and is consistent with recent Holocene RSL reconstructions from Australia. In North Island locations the early-Holocene sea-level highstand was quite pronounced, with RSL up to 2.75 m higher than present. In the South Island the onset of highstand conditions was later, with the first attainment of PMSL being between 7,000-6,400 cal yr BP. In the mid-Holocene the northern North Island experienced the largest sea-level highstand, with RSL up to 3.00 m higher than present. This is demonstrably higher than the highstand recorded for the southwest North Island and Otago regions. A number of different drivers operating at a range of scales may be responsible for the spatial and temporal variation in the timing and magnitude of RSL changes within the New Zealand archipelago. One possible mechanism is the north-south gradient in RSL that would arise in the intermediate field around Antarctica in response to the reduced gravitational attraction of the Antarctic Ice Sheet (AIS) as it lost mass during the Holocene. This gradient would be enhanced by the predicted deformation of the lithosphere in the intermediate field of the Southern Ocean around Antarctica due to hydro-isostatic loading and mass loss of the AIS. However, no such long-wavelength signals in sea-surface height or solid Earth deformation are evident in glacial isostatic adjustment (GIA) model predictions for the New Zealand region, while research from Australia has suggested that north-south variations in Holocene RSL changes due to hydro-isostatic influences are limited or non-existent. At the regional- to local-scale, post-glacial meltwater loading on the continental shelf around New Zealand is predicted by GIA modelling to have a significant effect on the timing and magnitude of RSL changes through the phenomenon of continental levering. The spatial variation in continental levering is controlled by the configuration of the coast and the width of the adjacent continental shelf, with continental levering providing a robust explanation for the observed spatial and temporal variations in RSL changes. Further research is required to characterise the regional and local effects of different tectonic regimes, wave climates, and sediment regimes. These are potentially very significant drivers of RSL variability at the regional- to local-scale. However, the magnitude of their potential effects remains equivocal.

Highlights

- RSL histories were reconstructed for four regions in the New Zealand archipelago
- Northern sites experience RSL rise earlier compared to southern sites
- Northern sites experience a higher-magnitude highstand compared to southern sites
- Long-wavelength signals from Antarctica cannot explain the observed variation in RSL
- A range of processes potentially drive the observed variation in RSL

Keywords relative sea-level change, New Zealand, Holocene, coastal geomorphology, continental levering, hydro-isostatic loading, glacial isostatic adjustment

1 Introduction and background

Over the past 30 years studies of coastal environments in New Zealand have drawn heavily on the Holocene sea-level reconstruction presented by Gibb (1986). This work revised and refined earlier studies (Gibb, 1979, 1983), and found that present mean sea level (PMSL) in New Zealand was attained approximately 6,500 years BP, with sea levels thereafter remaining largely static.

Gibb (1986) was highly significant at the time it was published, being the first systematic attempt to reconstruct the Holocene sea-level history of New Zealand. As a result Gibb (1986) has been widely utilised, to such an extent that it has been described as the "de facto" Holocene sea-level reconstruction for New Zealand (Hesp et al., 1999; Kennedy, 2008; Clement, 2011).

A number of studies have since investigated the evolution of Holocene coastal environments within the context of the sea-level history presented by Gibb (1986), and have recovered new palaeo sea-level indicators (e.g., Davis and Healy, 1993; Brown, 1995; Heap and Nichol, 1997; Wilson et al., 2007a, b; Abrahim et al., 2008; Kennedy 2008; Nichol et al., 2009). However, these studies were undertaken almost entirely in isolation of each other, and little consideration has been made of the coherent Holocene sea-level history of New Zealand beyond that presented by Gibb (1986). No attempt has been made to draw the results of these separate investigations together. As a result, Hayward et al. (2010a, c) have rightly described the state of knowledge of Holocene sea-level change in New Zealand as highly fragmented, and in its infancy.

The advancement of the state of knowledge of Holocene sea-level change in New Zealand therefore requires that the findings of these individual investigations be brought together to resolve this fragmentation. The wide utilisation of the Holocene sea-level reconstruction presented by Gibb (1986) has occurred in a vacuum devoid of a robust review of that study. Only Pirazzoli (1991) and

Clement (2011) have presented any critical analysis of Gibb (1986). As a result, there are a number of largely unrecognised assumptions and limitations present in the study by Gibb (1986), as well as those subsequent investigations that have adopted that sea-level reconstruction, which should be considered:

No mid-Holocene sea-level highstand or late-Holocene sea-level change. Gibb (1986) attempted to separate the effects of tectonics and eustasy on the elevations of palaeo sea-level indicators used to reconstruct past sea levels. To achieve this, indicators from two sites assessed to be tectonically stable (Blueskin Bay and Weiti River Estuary) were adopted as a 'zero datum', predicated on the assumption that sea level in the New Zealand region had been stable about the present level for the past 6,500 years (c. 6,700 cal yr BP, Clement 2011). Gibb (1986) fitted the elevations of relative sea-level (RSL) index points from tectonically unstable locations to the zero datum, and suggested that this allowed rates of long-term tectonic deformation (uplift or subsidence) to be estimated for these tectonically unstable sites. These deformation rates were then used to adjust the observed elevations of these same indicators for tectonic movement, supposedly yielding a RSL signal unaffected by tectonic deformation. This is a circular argument, and the base assumption of stable Late Holocene sea level no longer holds, as a mid-Holocene sea-level highstand is indicated by a large number of studies of Holocene RSL change in New Zealand, including glacial-isostatic adjustment (GIA) models of Holocene sea-level change in New Zealand (e.g., Peltier, 1988; Nakada and Lambeck, 1989; Gehrels et al., 2012), geomorphic studies from a number of New Zealand locations (e.g., Hull, 1985; Hicks and Nichol, 2007; Kennedy, 2008; Schallenberg et al., 2012), and other New Zealand Holocene sea-level reconstructions (e.g., Hayward et al., 2010a, b, c; Clement 2011). In the wider context of the southwest Pacific a large number of studies show a mid-Holocene sea-level highstand (e.g., Nunn, 1995, 1998; Woodroffe et al., 1995; Baker and Haworth, 1997, 2000a, b; Baker et al., 2001a, b; Woodroffe, 2009; Lewis et al., 2013). Studies from the east coast of Australia, at similar latitudes to the northern North Island, also show a highstand, and indicate an earlier culmination of the Holocene marine transgression at c. 7,700 cal yr BP (e.g., Sloss et al., 2007;

Horton et al., 2007; Lewis et al., 2013). These findings are significant in a New Zealand context as both New Zealand and Australia lie within the same regional sea-level zone (e.g., Clark et al., 1978; Clark and Lingle, 1979; Pirazzoli, 1991), in which it is predicted that RSL reconstructions will have a similar form (in the case of New Zealand and Australia in zone V: a sea-level highstand of up to +2 m initiated in the early Holocene, followed by a late-Holocene fall in RSL), though they may differ slightly in magnitude. The Holocene sea-level record presented by Gibb (1986) therefore likely reflects the base assumption of stable sea level after 6,500 years BP, rather than an accurate reconstruction of Holocene sea-level changes in the New Zealand region. Gibb (1986) may have misidentified a mid-Holocene highstand as tectonic uplift, thereby removing the indication of a highstand from the sea-level history.

No spatial variation in sea-level change. The reconstruction presented by Gibb (1986) brought together sea-level index points from around New Zealand. This reflected contemporary practice (e.g., Thom and Chappell, 1975, Thom and Roy, 1983). Also, at that time, age control existed for only a limited number of palaeo sea-level indicators; assembling a sufficient number of index points to reconstruct a sea-level history therefore required drawing them from a wide geographic area. The possibility of regional differences in the timing and amplitude of Holocene sea-level changes has been explored in Australia (e.g., Nakada and Lambeck, 1989; Lambeck and Nakada, 1990; Lambeck et al., 2010; Lewis et al., 2013), but has not been considered in New Zealand. GIA models of Holocene sea-level changes in the New Zealand region indicate that RSL varied both temporally and spatially during the Holocene (e.g., Peltier, 1988; Nakada and Lambeck, 1989). As it groups together index points from across New Zealand, the reconstruction of Holocene RSL presented by Gibb (1986) is therefore a composite of sea-level fluctuations from around the country, and it is unlikely to reliably reconstruct a RSL history that is truly representative of any New Zealand location.

Refinements of earlier studies. Gibb (1986) revised and refined earlier, similar reconstructions of the Holocene sea-level history of New Zealand (cf. Gibb, 1979, 1983). The final reconstruction (Gibb,

1986) features a number of differences in the timing and occurrence of sea-level stillstands and regressions when compared with the two earlier iterations, with no reason or justification given for these changes. As Pirazzoli (1991) observed, the unstated changes between the iterations leaves the impression that the range of vertical uncertainty in the final reconstruction may be much larger than Gibb (1986) inferred. While Gibb (1986) presented indicator points with vertical error bars, the interpreted sea-level history was represented by a single line, seemingly ignoring the inherent uncertainty. A number of subsequent studies have also ignored the uncertainty inherent in Gibb (1986), by presenting only the single line interpreted to represent the sea-level history (e.g., Heap, 1995; Heap and Nichol, 1997; Carter et al., 2002; Thomas, 2000; Ota et al., 1995).

Unconventional dating methods. Recently, a number of studies have attempted to transform the sea-level history presented by Gibb (1986) into sidereal years by calibrating the ages of the index points in order to utilise the sea-level reconstruction in concert with modern radiocarbon age determinations (e.g., Clement et al., 2010; Wilson et al., 2007a; Clark et al., 2011). However, Clement (2011) has noted that the vast majority of the radiocarbon ages presented by Gibb (1986) are not conventional radiocarbon ages (CRAs, cf. Stuvier and Pollach, 1977), and therefore cannot be calibrated to sidereal years. As a result the calibrated sea-level reconstructions presented by these recent studies are inaccurate representations of Gibb (1986) and must not be used.

Use of unreliable sea-level indicators. A number of the index points utilised by Gibb (1986) are not reliable indicators of palaeo sea-level (cf. Kidson, 1982). For example, carbonaceous muds (cf. Gibb and Cox, 2009) and rafted wood fragments.

Taken together, these limitations and assumptions preclude the continued use of the Holocene sea-level history for New Zealand presented by Gibb (1986). It should not be overlooked that the population of sea-level indicators presented by Gibb (1986) is the most significant collection of sea-level index points assembled for the New Zealand region to date. The continued, high degree of utilisation of Gibb (1986) and the readiness of recent studies to calibrate the history to sidereal years indicates considerable demand for understanding the Holocene sea-level history of New Zealand. This study advances the state of knowledge of Holocene sea-level change in New Zealand and meets this demand by:

i. drawing together Holocene palaeo sea-level indicators from recent studies of New Zealand coastal environments;
ii. in order to produce a set of Holocene RSL reconstructions for regions within New Zealand calibrated to sidereal years;
iii. so as to assess differences in the Holocene RSL histories of different regions within New Zealand;
iv. and evaluate the drivers behind any regional variation in Holocene RSL;
v. while understanding and avoiding the limitations of previous studies.

2 Methods

2.1 Selection of palaeo sea-level indicators

A total of 206 radiocarbon-dated palaeo sea-level indicators were compiled from 38 published and unpublished reports, papers, and theses (Table 1). The locations of sites from which sea-level indicators were recovered are shown on Figure 1. Selected indicators were restricted to studies that presented both an accurate description of the sedimentary facies from which the indicator was recovered, and related the dated indicator to an established vertical datum. Palaeo sea-level indicators from regions with complex tectonic histories, such as the east coast of the North Island, were not included. Studies that presented only a few indicator points from areas where no other palaeo sea-level index points have been recovered have also been excluded, as they provide too few points to reconstruct a meaningful sea-level history on their own, and are too far removed from other studies to permit the regional sea-level history to be determined. Table 1 is therefore not a comprehensive list of all radiocarbon-dated palaeo sea-level indicators recovered in the New Zealand region.

2.2 Treatment of radiocarbon ages

Many of the radiocarbon ages presented in Table 1 were not originally reported as conventional radiocarbon ages (CRAs; cf. Stuvier and Pollach, 1977; see Clement, 2011 for a summary of this issue), and therefore they cannot be calibrated to sidereal years. These non-CRA ages have subsequently been recalculated as CRAs by the laboratory that undertook the original dating (Rafter Radiocarbon Laboratory, New Zealand). Table 1 presents both the originally reported ages (suffixed years BP), and recalculated CRAs (suffixed 14C years).

CRAs were calibrated to sidereal years (suffixed cal yr BP) using the radiocarbon calibration program CALIB REV 6.1.1 (Stuvier and Braziunas, 1993; Stuvier and Reimer, 1993). Palaeo sea-level indicators with CRAs outside the range suitable for calibration have been omitted from the dataset. Calibration of fossil molluscs utilised the marine model calibration curve Marine09 (Reimer et al., 2009) with a ΔR value of -7 ± 45 to correct for the marine reservoir effect (e.g., Smith and James-Lee, 2009; Hayward et al., 2010a, b; Goff et al., 2010; Clement, 2011; Tribe and Kennedy, 2010). The CRAs of peat samples were calibrated using the Southern Hemisphere calibration curve SHCal04 (McCormac et al., 2004). All calibrated radiocarbon ages are presented using the 2-sigma uncertainty term (95 per cent degree of confidence).

2.3 Sources of vertical error

Following Gibb (1986), total sample elevation errors are calculated as the root-sum-square of the component errors:

$$\text{Elevation error} = \sqrt{L^2 + D^2 + B^2 + V^2} \qquad \text{(Equation 1)}$$

Where

- L is the accuracy of the measurement of the elevation of the indicator (Table 1). The elevations of some indicators were determined using bathymetric contours; for these samples L is taken as half the bathymetric contour interval.
- D is the magnitude of the present day living range of the dated indicator. For fossil shells this is species-specific (Table 2). The ecological ranges of fossil shell species are briefly summarised below. As tidal ranges vary around the New Zealand coast, D also varies with location. Site-specific tidal ranges have therefore been adopted with reference to the New Zealand Nautical Almanac and other sources of tidal information (Table 3).
- B is the magnitude of the vertical range of the bed or unit from which the dated sample was recovered.
- V is the uncertainty associated with long-term or event tectonic deformation (see Table 4). Long-term tectonic deformation (10^3-10^4 years) of the elevation of a palaeo sea-level indicator is expressed as a rate such as 0.2 ± 0.1 mm a^{-1}, with a range of 0.1-0.3 mm a^{-1}. The uncertainty V associated with the long-term tectonic deformation rate A ± E mm a^{-1} of a sample X is calculated as:

$$V = \frac{(X_{maximum\ sidereal\ age\ (years)} \times (A+E)) - (X_{minimum\ sidereal\ age\ (years)} \times (A-E))}{2}$$

(Equation 2)

2.4 Palaeo sea-level indicators

A summary of the habitats of fossil shell species used as indicators of palaeo sea-level position is given in Table 2. In many cases contradictory, or inconsistent information, exists regarding the habitats of shell species. Gibb (1979) presented a detailed compilation of studies that recorded the living depth ranges of a number of shell species used as palaeo sea-level indicators, and suggested that many studies were unreliable because of insufficient observations. Gibb (1979) concluded that the true ecological ranges of many New Zealand fossil shell species may not be definitively recognised. Numerous other studies have since commented on the lack of information on the ecology of shell species in New Zealand (e.g., Blackwell, 1984; Roper et al., 1992; Grant, 1994; Hooker and Creese, 1995; Norkko et al., 2001). The ecological ranges presented in Table 2 represent an attempt to find some consensus (where it exists) between published accounts.

The RSL elevations of the estuary tidal flat-dwelling bivalve species *Paphies australis* and the exposed beachface-dwelling bivalve *Paphies subtriangulata* are given with respect to mean sea-level (MSL), with a living depth range (D in Equation 1 and Table 1) from mean high water neaps (MHWN) to mean low water neaps (MLWN). The RSL elevations of samples of *Austrovenus stutchburyi*, *Macta ovata,* and *Macomona liliana,* all estuary lower tidal flat-dwelling species, are given with respect to MSL minus a quarter of the spring tidal range, with a range (D in Table 1) from MSL down to mean low water springs (MLWS). This accounts for bivalves living half-way between mid- and low-tide, with a 95 per cent uncertainty spanning the mid-low tide range (e.g., Wilson et al., 2007b). While the majority occurrence of bivalve species such as *A. stutchburyi*, *M. liliana*, and *P. australis* may be within the intertidal zone, some individuals may be found at greater depths. This study considers that fossil molluscs recovered from sedimentary facies indicative of an estuarine intertidal environment lived (and died) in the intertidal zone. This is consistent with the use of such samples as minimum indicators of RSL. Mollusc shells of known species recovered from intertidal estuarine sediments are classed as “identified estuarine” (IE) index points (Table 1, Figure 2). Correspondingly, unidentified estuarine molluscs are treated the same as known examples of estuarine tidal flat-dwelling species, but are recorded as “unidentified estuarine” (UE) index points (Table 1, Figure 2).

The RSL elevations of samples of deepwater-dwelling mollusc species such as *Dosina zealandica*, *Maoricolpus roseus*, *Dosinia lambata*, and *Mactra discors*, are given with respect to the level at the top of their living depth range, with an error of the neap tidal range at the location where the sample was recovered (cf. intertidal bivalve species). Palaeo sea-level index points from deepwater-dwelling mollusc samples therefore represent minimum indicators of RSL, and are recorded as deepwater/marine (DW) index points (Table 1, Figure 2).

Following Gibb (1986), the elevations of samples presented by Millener (1981), Osborne (1983), and Osborne et al. (1991) from shell bank and beach ridge deposits are given relative to mean high water springs (MHWS). Shell bank, beach ridge, and chenier samples constrain the maximum possible elevation of RSL, and are referred to as maximum indicators (MX) (Table 1, Figure 2). Both Gibb (1986) and Thomas (2000) presented palaeo sea-level indicators with respect to the levels described above; the elevations of these indicators have been retained.

2.5 Regional groupings of indicators

The population of sea-level indicators (Table 1) was grouped into four regions: northern North Island (all sites from Kowhai Beach south to Miranda, Figure 1C); the southwest North Island (the Manawatu River valley south to Kumenga, Figure 1B); Canterbury (Pegasus Bay south to the Kaitorete Barrier, Figure 1B); and Otago (Blueskin Bay Estuary, Pauanui Inlet, and Hoopers Inlet, Figure 1B). Grouping RSL indicators into regional datasets makes it possible to assess spatial and temporal variations in the timing and magnitude of Holocene RSL changes in different regions around New Zealand, with a further view to identifying and evaluating potential drivers behind any such regional variation in Holocene RSL.

2.6 Long-term and event tectonic deformation of sites

In order to isolate regional RSL signals that are free from the effects of local tectonic deformation, adjustments for long-term and event-specific tectonic movements have been made (Table 1). These adjustments are summarised in Table 4. Long-term rates have been applied to samples with respect to the age at the centre of their calibrated age range. The vertical uncertainty associated with long-term rates of tectonic deformation was calculated using Equation 2. Event tectonic deformation was applied to sea-level indicators older than the age of the tectonic event. The vertical uncertainty of tectonic events is recorded in Table 4.

2.7 GIA modelled RSL for New Zealand

A GIA model was used to generate predicted RSL histories for the four regions for which there are palaeo sea-level indicators. These modelled RSL predictions provide useful context to the palaeo reconstructions, and aid in the evaluation of drivers that might underpin any regional variation in Holocene RSL. The GIA model is used to solve the sea-level equation (Farrell and Clark, 1976) following the methods described in Kendall et al. (2005). The model includes consideration of time-dependent shoreline migration, an accurate treatment of sea-level change in regions of marine-grounded ice (Mitrovica and Milne, 2003), and feedbacks between GIA and the rotational state of the Earth (Mitrovica et al., 2005). As well as calculating the predicted RSL change over time in each region, we isolate those components of RSL change that are due to changes in the elevation of the solid Earth and the sea-surface height, respectively. Within the GIA model the solid Earth is modelled as a spherically-symmetric, compressible, Maxwell body. We adopt the radial viscosity profile of VM2 (Peltier, 2004) and use a lithospheric thickness of 90 km. The GIA model predictions were generated using the ICE-5G deglaciation model (Peltier, 2004).

We do not have access to an alternative global deglaciation model, and the focus of this study is not to investigate different melt scenarios that may provide a better fit to the New Zealand RSL data set; however, we do carry out calculations using a small number of alternative rheological models in order to investigate the uncertainty in the RSL predictions. The ICE-5G (VM2) combination has been carefully tuned to fit a suite of global RSL constraints (Peltier, 2004), and the use of an alternative rheological model will reduce the fit to this global data set. Bearing this in mind, results were produced for models in which lithospheric thickness varies in the range 96-120 km, upper mantle viscosity is varied between 0.3×10^{21} Pa s and 10^{21} Pa s, and lower mantle viscosity is varied between

5 x 10^{21} Pas and 10^{22} Pa s. These values cover a reasonable range of mantle viscosities, as inferred from previous GIA studies (e.g., Lambeck et al., 1998; Mitrovica and Forte, 2004).

3 Results

3.1 Palaeo sea-level reconstructions

3.1.1 Northern North Island

A cluster of three radiocarbon-dated fossil molluscs places RSL in the northern North Island at -3.01 ± 1.12 m between 8,360-7,580 cal yr BP (Figure 2A). RSL rose to attain present level sometime between 8,100-7,340 cal yr BP (Figure 2E), as indicated by three fossil shells and one peat sample that are clustered above and below PMSL. Between 7,340-6,830 cal yr BP a cluster of three fossil shells indicate that RSL was in the range--0.84 to +0.41 m (Figure 2A). From 6,830-6,440 cal yr BP there is a 550-year gap in the history during which it is not possible to discern the position of RSL. Index points from four *A. stutchburyi* shells indicate that RSL was most likely higher than present between 6,440-5,470 cal yr BP. Two of the indicators suggest a very broad range for RSL during this period of -0.85 to +3.00 m, while the other two indicators suggest a comparatively more precise range for RSL of +0.52 to +2.18 m. For the period 5,420-4,870 cal yr BP a cluster three fossil shells collectively indicate that RSL was in the range +0.52 to +2.69 m. However, these indicators are accompanied by a maximum indicator that suggests that RSL was no higher than +0.73 to +1.42 m. Between 4,900-3,950 cal yr BP a grouping of three fossil shells and three maximum index points that suggest that RSL was between -0.69 to +1.08 m. However, in the centre of this age range lies an estuarine shell with a very broad error range of 1.61 m; the upper limit of the error range of this index point corresponds with a maximum index point that suggests that RSL was no higher than +1.92 to +2.40 m at 4,385 ± 195 cal yr BP. A cluster of four fossil index points together suggest that RSL was in the range +0.17 to +2.23 m between 3,800-3,200 cal yr BP (Figure 2A). This is not contradicted by a group of maximum indicators between 3,450-3,070 cal yr BP that indicate that RSL was no higher than -0.42 to +1.46 m during this period. There is a gap in the record between 3,000-2,340 cal yr BP that makes it impossible to reconstruct RSL during this period. There are a large number of maximum indicators of RSL with comparatively high precisions that suggest that RSL in northern New Zealand was at or below present between 2,300-300 cal yr BP (Figure 2A). The lowest of these maximum indicators suggest that RSL was no higher than present, and may have been as low as -0.50 to -0.70 m below PMSL. A lower sea level through this period is not contradicted by the minimum sea-level index points as this is within their vertical error ranges.

3.1.2 Southwest North Island

On the southwest coast of the North Island a cluster of three *A. stutchburyi* index points places RSL at -2.29 ± 1.26 m between 8,630-7,850 cal yr BP (Figure 2B). RSL rose to reach the present level between 7,780-7,270 cal yr BP, as indicated by two fossil *A. stutchburyi* valves recovered from Pauatahanui Inlet by Swales et al. (2005) (Figure 2E). Following the attainment of PMSL, a cluster of three fossil shell index points indicates that RSL rose to +0.15 to +2.73 m between 7,240-6,500 cal yr BP (Figure 2B). Given the overlap in both the ages and vertical errors of these samples it is not possible to be more precise. There are too few indicators in the period 6,500-5,600 cal yr BP to reliably reconstruct the precise position of RSL. From 5,660-2,880 cal yr BP nine index points straddle PMSL, indicating that RSL was between -1.33 to +1.71 m. It is not possible to reconstruct the position of RSL between 2,880 cal yr BP and the present as there are no index points for this period.

3.1.3 Canterbury

A broad swath of fossil mollusc and peat index points record the early-Holocene rise of RSL on the Canterbury coast (Figure 2C). A cluster of one peat and four fossil mollusc index points indicates that RSL was at -22.84 ± 4.23 m between 10,590-9,000 cal yr BP. RSL rose from -19.31 to -7.13 m between 9,510-8,190 cal yr BP, with four closely clustered fossil mollusc index points indicating that RSL was at -8.85 ± 3.96 m at 8210 ± 390 cal yr BP. It is not possible to precisely identify the timing of the attainment of PMSL on the Canterbury coast. Two *A. stutchburyi* valves with overlapping age and RSL ranges indicate that RSL was at -4.03 ± 3.14 m at 7,355 ± 325 cal yr BP, while a single valve indicates that RSL was between +0.01 to +4.31 m at 6,590 ± 180 cal yr BP. These three valves therefore indicate that PMSL was attained between 7,030-6,410 cal yr BP (Figure 2E). There are a few scattered indicators of RSL after 6,400 cal yr BP; however they are not of sufficient number to provide a reliable record of RSL on the Canterbury coast in the later Holocene (Figure 2C). The three unidentified fossil shells dated between 4,430-2,360 cal yr BP and a *M. discors* shell dated at 1670 ± 220 cal yr BP were recovered from a progradational beach sequence by Shulmeister and Kirk (1993, 1997). The potential for reworking is unclear as the condition of the shells is not reported; these index points therefore provide only a lower bound for the position of RSL. That the *M. discors* shell indicates that PMSL was ~+2.35 m at c. 1670 ± 220 cal yr BP is highly suggestive of reworking of this indicator. Five maximum index points from 1720 cal yr BP to present indicate that RSL was no higher than +2 m above PMSL (Figure 2C).

3.1.4 Otago

On the Otago coast there are no RSL index points which indicate the position of RSL during the early Holocene at depths greater than -3 m RSL (Figure 2D). Two *A. stutchburyi* valves bracketed above and below PMSL indicate that PMSL was attained in the 730 year window between 7,360-6,630 cal yr BP. The earlier of these two index points indicates RSL was at -0.97 ± 0.5 m at 7,595 ± 235 cal yr BP, while the later index point indicates RSL was at +0.73 ± 0.9 m at 6,815 ± 185 cal yr BP. PMSL was therefore probably attained after 7,360 cal yr BP (Figure 2E). A more precise time window for the timing of the attainment of PMSL requires a greater number of sea-level index points. At 6,375 ± 185 cal yr BP a maximum index point and a minimum index point with overlapping age and height error ranges indicate that RSL was within ±0.9 m of PMSL (Figure 2D). Between 6,050-4,620 a group of three *A. stutchburyi* valves indicates that RSL was between +0.19 to -1.49 m. A cluster of six fossil mollusc index points indicates that RSL was at +0.04 ± 1.47 m between 3,915-3,320 cal yr BP (ignoring the 1,700 year age error on NZ6867 in favour of the more precise 250-450 year age errors of the other five index points; Table 1). Three fossil mollusc and two peat index points indicate that RSL remained within this range until 1,750 cal yr BP. A series of four *A. stutchburyi* valves indicate that RSL was below the present level at -0.72 ± 0.53 m between 1,630-820 cal yr BP. Between 960 cal yr BP and the present, six fossil mollusc index points indicate that RSL lay within 0.67 m of the present level (Figure 2D). However, as the vertical error range of these six index points overlap with the vertical error range of the four index points between 1630-820 cal yr BP, it is not possible to infer any fluctuation in RSL between 1,630 cal yr BP and the present.

3.2 GIA model predictions of Holocene RSL

The GIA model predicts the occurrence of a mid-Holocene sea-level highstand in the New Zealand region, consistent with sea-level zone V of Clark et al. (1978). The highstand is the product of the phenomenon of ocean-siphoning during the deglaciation, where the capacity of the Earth's ocean basins increases due to (a) the subsidence of peripheral forebulge regions adjacent to major glaciation centres, and (b) hydro-isostatic loading on continental shelves (i.e. continental levering) (Mitrovica and Peltier, 1991; Mitrovica and Milne, 2002; Milne and Shennan, 2013). In far-field locations like New Zealand this siphoning effect results in a drop in RSL during the mid-to-late Holocene, producing an early-to-mid Holocene sea-level highstand. The timing and magnitude of the highstand may be modulated at the regional to local scale by effects such as continental levering.

The GIA model predicts that for the northern North Island (Northland, Auckland, and Coromandel) and the Canterbury and Otago coasts, the highstand commenced shortly before 8,000 years BP, when PMSL was first attained (Figure 3A). On the southwest coast of the North Island the highstand is predicted to have commenced with the initial attainment of PMSL c. 300 years earlier at c. 8,300 years BP (Figure 3A). The highstand is predicted to be largest on the southwest coast of the North Island, with a peak at ~2.5 m above present c. 7,000 years BP, which is maintained until c. 4,000 years BP. In the other three regions sea level is predicted to have risen more gradually, reaching a peak at ~2 m above present c. 4,000 years BP. In all four regions RSL is predicted to drop gradually back to the present level after 4,000 years BP. These results were produced using the ICE-5G (VM2) model combination. Results were also produced for a suite of alternative rheological models (i.e. replacing the VM2 model). The timing of events, including the attainment of PSML and the duration of the highstand, does not change when the alternative models are used; however, the magnitude of the highstand can vary by up to ~±0.5 m. This variation is primarily associated with the differing response of the solid Earth to loading when different rheological profiles are adopted. We do not discuss this issue further since the main focus of this study is to analyse the RSL data set. However, we do note that an improvement in the precision of the RSL data is necessary before it will be possible to distinguish between different rheological models.

A change in RSL (ΔRSL), or equivalently water depth, can arise due to a change in the sea-surface height (ΔSSH) or a change in the elevation of the solid Earth (ΔE) (Supplementary Figure 1):

$$\Delta RSL(x,\Delta t) = \Delta SSH(x,\Delta t) - \Delta E(x,\Delta t) \qquad \text{(Equation 3)}$$

SSH change during the Holocene is predicted to have been essentially uniform across New Zealand (dotted lines, Figure 3A); differences between sites are below the resolution of the RSL data. However, solid Earth deformation during the Holocene, driven by spatial variations in water loading, is predicted to have varied across the study region (dashed lines, Figure 3A). From Figure 4 it can be seen that differences in predicted RSL between the four regions are driven by differences in predicted solid earth deformation (ΔE), primarily through the mechanism of continental levering (e.g., Lambeck and Nakada, 1990). Over the course of the Holocene, the GIA model predicts that the southwest coast of the North Island will be tilted upwards by up to 1 m due to its location towards the centre of the continental platform (green dashed line in Figure 3A). This up-tilting increases the apparent height of the highstand predicted there (Figure 3 and Supplementary Figure 2). In contrast, the northern North Island and the Canterbury and Otago coasts are predicted to be downwarped by the hydro-isostatic load (black, red and blue lines in Figure 3A). This downwarping reduces the apparent height of the RSL highstand in these locations (Figures 3A and 6).

4 Discussion

4.1 Comparison between the Holocene sea-level reconstructions and other observations of Holocene sea levels in the New Zealand region

Both Kennedy (2008) and Clement (2011) have noted that little attempt has been made over the last 27 years to integrate the small but growing body of local evidence of Holocene sea-level fluctuations in New Zealand. Post-Gibb (1986) only a small number of investigations have presented new observations of palaeo sea-level changes. Consequently, there are few independent studies of palaeo sea-level fluctuations with which to compare the four regional Holocene sea-level reconstructions (Sections 3.1.1-3.1.4, Figures 2A-D).

Heap and Nichol (1997) studied the geomorphic evolution of Weiti River Estuary (Figure 1) in response to Holocene sea-level change, and noted that the formation of the earliest beach ridge inside the mouth of the estuary was delayed until c. 4,010-3,060 cal yr BP (NZ6479 and NZ1971, Table 1). This is between 5,040-3,330 cal yrs after the initial attainment of PMSL in the Northland-Auckland region (Figure 2A, E). Heap and Nichol (1997) hypothesised that a temporary sea-level high may have controlled the timing of the formation of beach ridges in the estuary. A sea-level highstand would have precluded significant wave reworking of bay-floor deposits. The formation of beach ridges would therefore have been delayed until either the bay floor accreted or sea level dropped sufficiently to allow wave reworking. The Holocene sea-level reconstruction for the northern North Island (Figure 2A) indicates that RSL may have been up to 2.5 m higher than present prior to c. 4,010-3,660 cal yr BP when the earliest beach ridge at Weiti River Estuary began to form. Through the same period the GIA model predicts that RSL for the northern North Island was up to 2 m higher than present, with the peak at +2 m occurring at c. 4,000 cal yr BP (Figure 3A). Beach ridge formation within Weiti River Estuary could therefore have been delayed until after 4,000 cal yr BP, when the GIA model predicts that RSL in the northern North Island began to gradually drop following the highstand. However, the initiation of the formation of the first breach ridge within Weiti River Estuary is coincident with the formation of beach ridges at Kaiaua and Tokerau Beach (Figure 1; Millener, 1981; Gibb, 1986; Osborne et al., 1991). This suggests a regional control on beach ridge formation, such as RSL, rather than a local control, such as bay floor accretion. It may be that fluctuating higher sea levels in the mid-Holocene in northern New Zealand may have eroded beach ridges formed prior to c. 4,000 cal yr BP (when the GIA model predicts the peak of the highstand in the northern North Island), rather than delaying beach ridge formation. However, it is not possible to infer any sea-level fluctuations from the Holocene sea-level reconstruction for the northern North Island, given the 2-3 m vertical error typical of most of the sea-level index points (Figure 2A).

Doherty and Dickson (2012) investigated the influence of sea-level change and storm events on the Holocene evolution of the chenier plain at Miranda, in the Firth of Thames (Figure 1). Ground penetrating radar surveys of the cheniers identified a clear stratigraphic boundary between the chenier beachface and underlying intertidal foreshore muddy sands. Doherty and Dickson (2012) used this boundary as a relative proxy for palaeo RSL, and concluded that regional RSL fell from a mid-Holocene sea-level highstand of +2 m c. 4,000 years BP to the present level by c. 1,000 years BP. This is consistent with the Holocene sea-level reconstruction for the northern North Island (Figure 2A).Hicks and Nichol (2007) used diatoms to examine sedimentary successions in a wetland at Kowhai Beach in Northland (Figure 1). They analysed diatom salinity zones in a core recovered from the wetland, and inferred that the inter-tidal zone at Kowhai Beach c. 3,350 cal yr BP was elevated up to 1.2 m above the modern tidal zone. This is in line with a number of minimum indicators of palaeo sea level which indicate that RSL in the northern North Island was between 0.15-1.77 m above the present level between 3800-3230 (Figure 2A). The GIA model of RSL for the northern North Island also predicts that RSL was ~+1.5 m higher than present c. 3,350 cal yr BP (Figure 3A). This evidence for significantly higher sea levels c. 3,300 cal yr BP contradicts the suggestion by Heap and Nichol (1997) that RSL closer to the present level induced beach ridge formation at this time in Weiti River Estuary. Kennedy (2008) recently suggested that more studies from Northland were required, as differing wave climates and sediment supply regimes between different locations may have affected observations of palaeo sea-level.

Elsewhere in Northland at sites such as Henderson Bay, One Tree Point and Tokerau Beach (Figure 1; e.g., Millener, 1981, Hicks, 1983, Nichol, 2002, Osborne and Nichol, 2006) Holocene dune ridges show significant seaward progradation and decreases in height. These dune sequences may record coastal responses to higher mid-Holocene sea levels (Kennedy 2008), and falling sea levels through the late Holocene. Marks and Nelson (1979) made a similar observation of dune ridge heights on the Omaro Spit in Whangapoua Estuary on the Coromandel Peninsula (Figure 1). An overall seaward decrease in the height of successive dune ridges and swales of 2-3 m was noted, which it was suggested reflected a first-order lowering of sea-level during progradation of the barrier. Marks and Nelson (1979) inferred that RSL in Whangapoua Estuary was at least 2 m higher than present 4000-5000 years BP. This is in line with the GIA model prediction of RSL in the northern North Island, which predicts a peak in RSL at ~+2.5 m above present c. 4,000 ka BP, followed by a gradual decline (Figure 3A). However, Marks and Nelson (1979) did not consider the effects of tectonic uplift, which could account for up to 1.5 m of the observed elevated RSL (cf. Table 4).

In the South Island, both Hull (1985) and Schallenberg et al. (2012) have identified peaks in marine influence c. 4000 cal yr BP in sedimentary sequences on opposite sides of the island. Hull (1985) suggested that articulated bivalves recovered from a 3 m thick deposit of well sorted silty sand and sandy silt exposed in a river cutting at Lake McKerrow (Figure 1) on the West Coast of the south Island recorded a ~2 m rise in sea level c. 4,400 cal yr BP. Bivalves from the base of the deposit, which was inferred to be an estuarine sequence, were dated at 4413 ± 71 cal. yr BP (NZ6367) and 4,448 ± 81 cal. yr BP (NZ6369); these ages are statistically similar to the age of a bivalve 2 m above, which was dated at 4,468 ± 39 cal yr BP (NZ5398). Hull (1985) inferred that this sequence indicated swift RSL rise, and suggested that as the Lake McKerrow area had been subject to tectonic uplift through the Holocene, the rise was due to ice volume changes rather than tectonics. On the opposite side of the South Island Schallenberg et al. (2012) identified a peak in marine influence c. 4000 cal yr BP in Lake Waihola, a coastal freshwater lake ~50 km southwest of the Otago peninsula (Figure 1). Schallenberg et al. (2012) identified a marked change in palaeoenvironmental conditions in the lake c. 4,000 cal yr BP, marked by a layer of articulated estuarine bivalves (*A. stutchburyi*). No other estuarine shells were found, and the lake is currently inhabited by freshwater shell fish. As *A. stutchburyi* prefers saline conditions, Schallenberg et al. (2012) interpreted the presence of the shell bed as indicative of a peak in marine influence in the lake associated with a mid-Holocene sea level highstand c. 4,000 cal yr BP. Unfortunately there is very sparse coverage of RSL index points for both the Canterbury and Otago regions c. 4,000 cal yr BP (Figures 2C and D). It is therefore not possible to discern either an episode of sea-level rise or a sea-level highstand c. 4,000 cal yr BP in either sea-level history. The RSL predictions for the Canterbury and Otago coasts produced by the GIA model both show RSL rising to a peak c. 4,000 years BP (Figure 3A), coincident with the observations of both Hull (1985) and Schallenberg et al. (2012). However, the magnitude of the predicted rise is much smaller in magnitude (0.3-0.5 m) than the ~2 m RSL rise identified on the West Coast of the South Island (cf. Hull, 1985).

A number of studies have utilised saltmarsh foraminifera from sites in the southern South Island to reconstruct RSL changes over the past 600 years. Gehrels et al. (2008) used saltmarsh foraminifera to reconstruct a proxy sea-level history for the past 500 years for Pounawea, approximately 100 km southwest of the Otago Peninsula (Figure 1). The sea-level reconstruction showed that RSL at Pounawea was ~-0.40 m below present c. 500 years BP, rising to the present level by 1990. Approximately 0.28 m of this sea-level rise occurred during the 20th century. Saltmarsh cores recovered by Hayward et al. (2007) from Akatore Estuary and Catlins Lake (Figure 1) record a similar rate of sea-level rise to that recorded at Pounawea. Foraminifera recovered from these sites, which are both within 50 km of Pounawea, documented ~0.3 m of sea-level rise over the last 150 years.

Hayward et al. (2012) later investigated the marine immersion of an archaic Maori occupation site at the Shag River estuary, approximately 50 km north of the Otago Peninsula (Figure 1). There, fossil saltmarsh foraminifera assemblages record a rise in RSL of 0.59 ± 0.05 m over the past 600 years. While all the fossil mollusc sea-level index points from the past 900 years BP from the Otago area lie within 0.03 m of PMSL, the error range is considerably greater, up to 2 m (Figure 2D). The sea-level changes suggested by Gehrels et al. (2008) and Hayward et al. (2007, 2012) therefore fall below the level of detection possible using the fossil mollusc index points from Otago. RSL 0.3-0.5 m below present on the southeast coast of the South Island during the past 600 years is therefore in no way contraindicated by the Holocene sea-level record for Otago (Figure 2D).

Gehrels et al. (2012) recently presented a GIA model-derived prediction of Holocene RSL at Pounawea (Figure 3C), and compared the modelled RSL history to the proxy sea-level history produced using the saltmarsh foraminifera (Gehrels et al., 2008). Both the model prediction presented by Gehrels et al. (2012), and the ICE-5G-derived prediction for the Otago coast (this study, Figure 3A), over-predict the observed sea-level positions at Pounawea (cf. Gehrels et al., 2008). However, it is important to note that GIA models do not consider ice melt during the 20th Century, which increases the degree of overprediction by ~0.3 m (cf. Gehrels et al., 2008). The GIA models also over-predict RSL compared to the majority of the fossil mollusc index points from the Otago Holocene sea level reconstruction (Figure 2D). However, the model prediction presented by Gehrels et al. (2012) shows close agreement with fossil mollusc index points at c. 6,600 cal yr BP and 3,400 cal yr BP, while the ICE-5G model prediction for the Otago coast (Figure 3A) predicts a much earlier timing for the attainment of PMSL (c. 8,000 cal yr BP).

4.2 Sea-level fluctuations in the New Zealand region: Australasian context

While the sea-level history presented by Gibb (1986) has become the (de facto) benchmark or standard reconstruction of Holocene sea-level change for New Zealand, it contrasts with much recent research from the wider southwest Pacific region (Hicks and Nichol, 2007; Clement, 2011).

For example, while many studies from the southwest Pacific have documented higher than present mid-Holocene sea levels (e.g., Nunn, 1995, 1998; Woodroffe et al., 1995; Baker and Haworth, 1997, 2000a, b; Baker et al., 2001a, b; Horton et al., 2007; Sloss et al., 2007; Woodroffe, 2009; Lewis et al., 2013), New Zealand workers have been noticeably reticent on the subject (Hicks and Nichol, 2007). Kennedy (2008) noted that sea-level histories from southeast Australia and the Tasman Sea in particular may be significant in the New Zealand context, as these records come from within the same oceanic region as New Zealand (e.g., Clark and Lingle, 1979; Pirazzoli, 1991), and so may be expected to yield similar histories of Holocene sea-level fluctuations. It is therefore prudent to briefly consider the findings of studies that have reconstructed Holocene sea-level changes in the Australasian region proximal to New Zealand.

Baker and Haworth (1997, 2000a, b) and Baker et al. (2001a, b) undertook studies of late Holocene sea levels along the southeast Australian coast (28-36 degrees South) using fixed biological indicators as a proxy to discern sea-level fluctuations. Baker et al. (2001b) considered the biostratigraphical implications of various fixed biological indicators, and presented an oscillating, or stepped, model of late Holocene sea-level fluctuations. This model indicated that the Holocene marine transgression culminated with sea levels +2 m above PMSL. During the last 5,000 cal yr BP, the model shows sea levels falling to PMSL in a series of oscillations, with minor peaks in sea-level between 4,000-3,200 cal yr BP and at c. 2,000 cal yr BP. However, both Sloss et al. (2007) and Lambeck et al. (2010) have criticised the findings of Baker, Haworth, and others, noting that the some of the sea-level indicators used in those studies cannot be accurately related to mean sea-level. Lambeck et al. (2010) also suggested that the conclusion of oscillating sea levels during the mid- to late-Holocene may be due not to accurate reconstructions of the RSL signal, but rather to the use of sea-level indicators from spatially removed geographic areas that may be subject to different hydro-isostatic loading histories. Lambeck et al. (2010) therefore concluded that it was premature to revise the RSL history for the southeast coast of Australia to include these oscillations.

Sloss et al. (2007) presented a revised Holocene sea-level curve for the southeast coast of Australia (34-36 degrees South), based on a review of previously published geochronological results for fossil molluscs, organic-rich mud, mangrove roots, and fixed biological indicators such as wormtubes and barnacles. The RSL history presented by Sloss et al. (2007) indicated that sea level on the southeast Australian coast had risen to at least -5 m below present c. 8,500 cal yr BP, with PMSL being attained between 7,900-7,700 cal yr BP. Following this, sea level continued to rise, reaching +1.5 above PMSL by 7,400 cal yr BP. Sloss et al. (2007) indicated that this higher sea-level was sustained until c. 2,000 cal yr BP, after which sea level fell slowly and smoothly to PMSL. Sloss et al. (2007) noted that RSL may have fluctuated during the sea-level highstand between 7,700-2,000 cal yr BP, but concluded that significant oscillations like those identified by Baker and Haworth (1997, 2000a, b) and Baker et al. (2001a, b) were due to the adjustment of fixed biological indicator species to changing wave and climatic conditions, rather than external driving by climate of ice volume fluctuations.

Horton et al. (2007) utilised subtidal foraminifera recovered in cores collected on the continental shelf near Townsville to reconstruct Holocene sea-level fluctuations for the central Great Barrier Reef. Horton et al. (2007) developed a transfer function to infer the water depths of sediment samples based on their foraminiferal content. These sediment samples were used to produce ten sea-level index points. The index points indicated that RSL in the central Great Barrier Reef area had reached -8.8 ± 4.5 m below PMSL between 9300-8600 cal yr BP. A mid-Holocene sea-level highstand of +1.7 ± 3.9 m above PMSL was inferred for the period 6900-6400 cal yr BP, before sea-level fell steadily back to PMSL by the present day.

Woodroffe (2009) also presented a sea-level history for the Great Barrier Reef coastline of northern Australia using a foraminifera-based transfer function in conjunction with a review of other palaeo sea-level indicators from the area. Woodroffe (2009) suggested that sea levels rose above PMSL between 8000-6200 cal yr BP, with the peak of the sea-level highstand being ~+2.8 m above PMSL c. 5000 cal yr BP. Woodroffe (2009) posited that sea-level remained relatively stable above +1.5 m above present from 6200-2300 cal yr BP, before falling to PMSL during the past 1000 cal yr BP. Woodroffe (2009) suggested that there was no evidence in northern Australia for sea-level oscillations during the Holocene, though they were not ruled out entirely. Woodroffe (2009) further noted that geophysical models of sea level changes for the region predict a smooth decline in sea level from the peak of the mid-Holocene highstand.

4.3 Spatial and temporal variations between the four regional RSL histories for New Zealand

The four regional Holocene palaeo sea-level reconstructions for New Zealand (Figures 2A-D) show demonstrable spatial variability in the timing of the attainment of PMSL, and the magnitude and duration of the mid-Holocene sea-level highstand. Comparison of clusters of palaeo sea-level index points from the two North Island RSL histories with clusters from the two South Island RSL histories (Figure 2A-E, Sections 3.1.1-3.1.4), shows that that the timing of the attainment of PMSL was at a minimum 240-340 years earlier at sites in the North Island compared to sites in the South Island (Figures 2E, and 5). In the North Island, PMSL was attained prior to 7,240 cal yr BP (Figures 2E and 5); this is c. 500-700 years earlier than has been suggested for the New Zealand region as a whole (e.g., Gibb, 1986). In Canterbury and Otago PMSL was attained after c. 7,000 cal yr BP; though later than in the North Island this is still 300-500 years earlier than previous reconstructions have suggested (e.g., Gibb, 1986). There is no demonstrable difference in the timing of the attainment of PMSL between the two North Island regions, or between the two South Island regions (Figures 2E and 5).

Between 7,250-6,750 cal yr BP a cluster of three index points mark the peak of the early-Holocene sea-level highstand for the southwest North Island coast (Figures 2B and 5). This highstand is up to 0.56-1.24 m higher than the cluster of three index points that delineate RSL in the northern North Island at this time, and up to 0.85-1.10 m higher than the cluster of three index points that mark the timing of the attainment of PMSL on the Otago coast. However, all three clusters vertically overlap with each other; the differences in RSL between the clusters therefore represent maximum possible values (Figure 5).

The mid-Holocene sea-level highstand reaches its peak in the northern North Island between 6,500-4,500 cal yr BP, as delineated by two separate clusters of sea-level index points (Figures 2A and 5). The earlier cluster, between 6,500-5,500 cal yr BP, clearly shows that prior to 6,250 cal yr BP RSL in the northern North Island was up to 0.30-1.37 m higher than in the Otago region, when compared to the Otago cluster between 7,000-6,250 cal yr BP that marks the timing of the attainment of PMSL on the Otago coast. Between 6,250-4,750 cal yr BP a cluster of three broadly-spaced index points suggests that RSL in the Otago region dropped to -0.65 ± 0.84 m (Figures 2D and 5). As a result, the difference in RSL between the northern North Island and Otago increases, with RSL in the northern North Island being 1.09-2.81 m higher than in the Otago region during this period. At the same time RSL in the northern North Island is up to is up to 1.49-1.80 m higher compared to RSL in the southwest North Island. Given the complete overlap of the clusters from the southwest North Island and Otago during this period it is not possible to definitively infer a difference in RSL. However, it cannot be ruled out that RSL was up to ~1.01 m higher in the southwest North Island compared to Otago (Figures 2B, 2D, and 5).Between 4,750-3,750 cal yr BP sea-level clusters for the northern North Island, southwest North Island, and Otago region all overlap (Figures 2A-D and 5). A cluster of four index points between 3,750-3,250 cal yr BP from the northern North Island indicates that RSL in that region was up to 1.20-2.03 m higher than on the southwest coast of the North Island and in the Otago region. As the clusters from all three regions overlap this represents the maximum possible difference in RSL between the regions during this period. Between 3,250 cal yr BP and present the RSL histories for the northern North Island and Otago overlap, both indicating that RSL was at or slightly below present (Figure 2A and D).

4.4 Drivers of spatial and temporal variation between the four regional RSL histories for New Zealand

The four Holocene palaeo sea-level reconstructions for New Zealand (Figures 2A-D) show significant spatial variability in the timing of the attainment of PMSL, and the magnitude and duration of the mid-Holocene sea-level highstand. There are a number of potential mechanisms that may drive this spatial and temporal variation, with a considerable range in spatial scale, temporal duration, and magnitude of effect.

The GIA model predictions for the four New Zealand regional SL sites show almost no inter-regional variation in sea surface height in the New Zealand region during the Holocene (Figure 3A, Supplementary Figure 3). Some variation with longitude is evident between 8,000-4,000 years BP, due to a long wavelength gradient related to feedbacks in the rotational state of the Earth, but this accounts for less than 0.2 m of the inter-regional variation observed in the GIA predictions (Figure 3A, Supplementary Figure 3).

Land-based ice sheets influence the local height of the sea surface through the gravitational attraction exerted on ocean water by the mass of ice (e.g., J.A. Clark et al., 1978; P.U. Clark et al., 2002; Tamisiea et al., 2003; Whitehouse, 2009; Milne and Shennan, 2013). This results in a predicted long-wavelength signal emanating from any large ice sheet, such as Antarctica, with sea levels proximal to the ice sheet expected to fall as ice melts, due to the decreased gravitational attraction of the ice sheet, while sea levels rise at distal sites. Antarctica is thought to have continued to lose ice mass into the mid-Holocene. In intermediate locations such as New Zealand, which would have been experiencing RSL fall at the time due to ocean siphoning, the net effect of Antarctic mass loss would have been to reduce the magnitude of mid-to-late-Holocene RSL fall at northern sites relative to southern sites, leading to lower highstands being recorded in the north. The palaeo sea-level reconstructions do not reflect such a pattern (Figures 2A-D), with the lowest highstand being recorded in the south, and hence Antarctic mass loss during the Holocene cannot explain the observed distribution of Holocene highstands around New Zealand. We note that out GIA model predictions for this period do not indicate a strong latitudinal gradient in the magnitude of the Holocene highstand across New Zealand, and this may be because the magnitude of Holocene Antarctic ice loss in our model is too small to produce a detectable gradient in sea-level change, or alternatively the signal may have been swamped by the rotational feedback signal in the GIA model or a competing signal from the Greenland Ice Sheet.

There is also a predicted intermediate-field effect on RSL due to the deformation of the Earth's crust in the region surrounding Antarctica as a result of the latitudinal gradient in the loading of meltwater on the lithosphere (e.g., Nakada and Lambeck, 1988; Lambeck and Nakada, 1990; Lambeck et al., 2010). The collapse of the peripheral forebulge as the AIS loses mass would also contribute to this deformation (e.g., Farrell and Clark, 1976; Clark et al., 1978; Davis and Mitrovica, 1996; Conrad, 2013). Such southern latitude deformation has been shown to produce a north-south effect in RSL signals around Australia and New Zealand (e.g., Nakada and Lambeck, 1988; Lambeck and Nakada, 1990). However, both Bryant (1992) and Haworth et al. (2002) have tested the suggestion of southern latitude deformation during the Holocene, and found that there was sufficient evidence to indicate that north-south differences in Holocene sea levels due to hydro-isostatic influences were either limited or non-existent. The GIA model results for New Zealand do not predict a demonstrable north-south effect in solid Earth deformation (Figures 3 and 5), supporting the conclusions of Bryant (1992) and Haworth et al. (2002).

At the local to regional scale hydro-isostatic deformation of the lithosphere is also expected to have a significant effect on RSL. Studies by Nakada and Lambeck (1989) and Lambeck and Nakada (1990) have shown that considerable spatial variation in RSL can be expected as a result of meltwater loading across the Australian continental shelf, resulting in subsidence of offshore locations and the upward tilting of onshore locations (continental levering, e.g., Wolcott, 1972; Milne and Shennan, 2013; Murrary-Wallace and Woodroffe, 2014). Around New Zealand, the GIA model predicts a significant effect on observed RSL during the Holocene due to continental levering. In most locations around the New Zealand coast the comparatively narrow continental shelf means that coastal sites (for example, the Otago and Canterbury coasts, Figures 3A-B and 5) are sufficiently close to the shelf margin to be tilted downwards, while upward tilting occurs further inland away from the shelf margin (for example, along the southwest of the North Island, Figures 3A-B and 5). As a result of continental levering, the GIA model predicts that the magnitude of the mid-Holocene sea-level highstand will be largest on the southwest coast of the North Island (Manawatu River mouth), and somewhat less in the northern North Island (Auckland), Canterbury (Lyttleton), and Otago (Dunedin Harbour) (Figure 3A-B). This is consistent with the palaeo reconstructions of RSL for the four regions in the early Holocene (Figure 2A-D). Prior to 6,500 cal yr BP it is possible that the highstand on the southwest coast of the North Island may be greater in magnitude than in the northern North Island; however, the indicator points used in both RSL reconstructions lack sufficient precision to state this definitively (Figures 2A, D, and 5). The magnitude of the highstand in Otago is much less than is indicated for the two North Island regions (Figure 5; there is insufficient evidence to comment on the magnitude of the highstand on the Canterbury coast). However, in the mid-Holocene, the palaeo RSL histories indicate that only the northern North Island experienced a significant sea-level highstand, with no demonstrable difference in the magnitude of the highstand experienced in the southwest North Island or Otago regions. Analysis of the effects of continental levering at the regional-to-local scale shows that continental levering can induce potentially significant differences in predicted RSL histories over distances as small as 50-70 km (Figure 6). In the northern North Island the predicted response to hydro-isostatic loading of the continental shelf is spatially quite complex (Figure 6). The narrow landmass surrounded by a narrow continental shelf results in subsidence along the length of the peninsula (Figure 4). At Henderson Bay, at the northern end of the peninsula, subsidence due to hydro-isostatic adjustment is predicted to be 7.76 m over the past 10,000 years (Figure 6B). This reduces progressively with increasing distance to the south, with 0.59 m of subsidence predicted for the past 10,000 years at Miranda (Figure 6B). The effect of this spatial variation in subsidence on the timing and magnitude of predicted RSL changes is dramatic. At Miranda the mid-Holocene sea-level highstand is predicted to begin with the attainment of PMSL shortly before 8,000 years BP. The timing of the onset of highstand conditions is increasingly delayed with increasing distance to the north, with the highstand at Henderson Bay predicted to begin with the attainment of PMSL c. 5,000 years BP. The magnitude of the predicted highstand is also spatially variable as a consequence of the variation in predicted hydro-isostatic subsidence (Figure 6D). More southerly sites which are predicted to experience smaller amounts of subsidence are consequently predicted to experience higher magnitude highstands compared to more northerly locations which are predicted to experience lower magnitude highstands as a consequence of greater amounts of subsidence. At Miranda the highstand is predicted to have a maximum magnitude of +2.38 m above PMSL at 4,000 years BP, compared to Henderson Bay where the highstand is predicted to have a maximum magnitude of +0.93 m above PMSL.

RSL indicators from the northern North Island show moderately close agreement with the GIA model-predicted spatial patterns in the timing and magnitude of RSL changes (Figure 6E-N). In locations such a Matarui Bay, Kaituna Bay, Bream Bay, and Southern Kaitoke, single RSL indicators fit well with the GIA-predicted RSL histories (Figure 6F-I). At Mahurangi Estuary, Okahu Bay, and Miranda there is reasonable agreement between the GIA-predicted RSL histories and the palaeo sea level index points, although in all three areas the GIA-predicted RSL histories appear to over-estimate RSL with respect to a small number of maximum indicators of palaeo sea-level (beach ridges and cheniers; Figure 6J, L, and M). The RSL histories for both Mahurangi Estuary and Okahu Bay display a vertical spread of palaeo sea-level index points between c. 8,000-6,000 cal yr BP. This is consistent with recent palaeo sea-level reconstructions from Australia that show a similar vertical spread (e.g., Sloss et al., 2007; Lewis et al., 2013). The sea-level index points plotted for the Mahurangi Estuary and Okahu Bay RSL histories have been recovered from relatively deeply-incised drowned-valley settings (Mahurangi Estuary, Weiti River Estuary, Puhoi River Estuary, Tamaki Estuary, and the Waitamata Harbour; e.g., Heap and Nichol, 1997; Swales et al., 1997; Wratt, 1999; Abrahim et al., 2008). Given the lack of tectonic deformation in the northern North Island (Section 2.6, Table 4), this vertical spread most likely represents the effects of the compaction of the sediments that have infilled these incised-valleys (e.g., Gehrels, 1999; Goodbred and Kuehl, 1999; Tornqvist et al., 2008; Mazzotti et al., 2009; Yuill et al., 2009; Bartholdy et al., 2010).

For Henderson Bay the peak of the GIA-predicted mid-Holocene sea-level highstand coincides with a number of palaeo sea-level indicators, though there are a few maximum indicators of palaeo sea-level within the last 2,000 cal yr BP that are at significant elevations about the predicted RSL history. There is a very poor fit between the GIA model-predicted RSL histories and the populations of palaeo sea-level indicators from both Coromandel Harbour and Whitianga, with the GIA model-predicted RSL history significantly overestimating RSL changes compared to the palaeo sea-level indicators from these areas (Figure 6K and M). This is potentially explained by sediment compaction (e.g., Gehrels, 1999; Goodbred and Kuehl, 1999; Tornqvist et al., 2008; Mazzotti et al., 2009; Yuill et al., 2009; Bartholdy et al., 2010), or an overestimation in tectonic uplift rates for the Coromandel Peninsula (cf. Table 4).

Local and regional tectonism may also be a factor in the variation observed in the four main RSL histories reconstructed for New Zealand. Regional features associated with the Hikurangi subduction zone may have altered observed RSL histories in some locations. For example, the Wanganui Basin is a 200 by 200 km ovoid back-arc subsiding sedimentary basin located on the southwest margin of the North Island. Subsidence in the basin was initiated during the Pliocene as the Pacific Plate exerted a downward pull on the Australian Plate (Stern et al., 1992, 1993). The rate of subsidence of the basin since the Pliocene has been estimated to be ~1.0 m ka^{-1} (e.g., Wilson and McGuire, 1995; Journeaux et al., 1996; Kamp and McIntyre, 1998; Carter et al., 1999; Proust et al., 2005). However, this is a maximum rate based on the depth of fill in the basin depocenter; onshore sites, from which palaeo sea-level indicators were recovered, are likely to have experienced only half this rate of subsidence. Another reason why this should be regarded as a maximum rate is that while the southern portion of the basin has been subsiding, the northern periphery of the basin has been consequently flexed upward (e.g., Stern et al., 1992). Subsidence of the basin has had a demonstrable effect on Holocene sedimentary successions at the top of the South Island (e.g., Hayward et al., 2010a, b, c). However, the effect on sites at the top of the South Island may be greater than might be observed on the southwest coast of the North Island as the depocenter of the Wanganui Basin has moved progressively southward throughout the Quaternary. Regardless, it is expected that some regional down-warping will have occurred at southwest North Island sites on the periphery of the basin. As a result, the observed magnitude of the mid-Holocene sea-level highstand would be reduced relative to that observed at other New Zealand locations, effectively reducing or reversing the observed effect of continental levering.

Local-scale tectonics may also have an effect in inducing variation in regional RSL histories. For example, sites in the southern North Island and northern South Island, proximal to the subduction interface of the Hikurangi Margin, are subject to coseismic subsidence (e.g., Clark et al., 2011). Coseismic uplift may also occur. For example, mid-to-late Holocene marine terraces are extensively preserved along the east coast of the North Island, recording sudden episodes of uplift (e.g., Hull, 1987; Ota et al., 1991; Berryman, 1993; Wilson et al., 2007a, b). In contrast, regions that are relatively far removed from the Hikurangi Margin's subduction interface (such as the northern North Island) will not have experienced coseismic movement. Varying regional tectonic histories therefore have the potential to introduce regional variations in RSL reconstructions, particularly where regional tectonic histories are poorly understood.

Variations between the regional RSL reconstructions may also be introduced because of regional and local variations in the apparent radiocarbon age of ocean and estuarine waters around New Zealand (the marine reservoir effect). The marine reservoir effect is corrected for when marine and estuarine shell ^{14}C ages are calibrated using the modelled marine ^{14}C calibration curve (Marine09, Reimer et al., 2009). This curve represents a global average of the surface seawater ^{14}C flux over time. Local and regional deviations from this global average are corrected for using a ΔR value, which represents the difference between the modelled radiocarbon age of the surface seawater and the actual radiocarbon age of the seawater in that locality. Around New Zealand, a number of ΔR values have been derived from different shell samples. These ΔR values range from -107 ± 61 to $+77 \pm 57$ (e.g., Petchley et al., 2008). These ΔR values imply that the median age of a calibrated radiocarbon age from a marine shell may vary by c. 180 years depending upon location. Studies from Australia have clearly shown that the marine reservoir effect and variation in ΔR values can be very significant at the scale of individual estuaries (e.g., Spenneman and Head, 1996; Ulm, 2002). The potential for variation in the calibration of estuarine and marine shell ^{14}C ages is similarly significant in a New Zealand context. However, in the absence of a systematic study of the radiocarbon signatures of estuarine and coastal waters around New Zealand, it is impossible to ascertain what degree of temporal variation may exist due to localised variations in surface seawater ^{14}C flux, as such variations are essentially random (Ulm, 2002).

Variations in RSL histories may also be introduced by the post-depositional compression of Holocene sediments (sometimes referred to as auto-compaction), a widely observed phenomenon in coastal environments (e.g., Gehrels, 1999; Goodbred and Kuehl, 1999; Tornqvist et al., 2008; Mazzotti et al., 2009; Yuill et al., 2009; Bartholdy et al., 2010). Sediment consolidation can be significant in fine-grained organic rich sediments (e.g., Pizzuto and Schwendt, 1997; Haslett et al., 1998; Allen, 1999, 2000; Gehrels, 1999; Massey et al., 2006), with Holocene compaction ratios of ~0.2-0.8 reported (e.g., Bloom, 1964; Kaye and Barghoorn, 1964; Belknap, 1975; Pizzuto and Schwendt, 1997; Hayward et al., 2002). Sea-level index points collected from thick sequences of unconsolidated intertidal sediments in estuaries and marshes are therefore likely to require correction to account for sediment compaction (Allen, 1995, 2000; Gehrels, 1999; Shennan and Horton, 2002; Massey et al., 2006). However, there is a current lack of applied theory and a shortage of models available to quantify the consolidation of Holocene sediments (e.g., Paul et al., 1995; Pizzuto and Schwendt, 1997; Paul and Barras, 1998; Rybczyk et al., 1998; Allen, 1999, 2000; Tovey and Paul, 2002; Williams, 2003; Bird et al., 2004; Massey et al., 2006). Sediment compaction is a likely explanation for the vertical spread in palaeo sea-level index points in the mid-Holocene shown on the RSL histories for Mahurangi Estuary, Okahu Bay (Figure 6), and the southwest North Island (Figure 2B; e.g., Clement, 2011), as all include index points recovered from thick sedimentary sequences that have infilled deeply-incised drowned-valley estuaries.

Kennedy (2008) has suggested that differing wave climates and sediment supply regimes in different New Zealand locations may have affected the evolution of depositional features such as dune ridges and barriers, thereby modifying observed sea-level records preserved in different locations. Kennedy (2008) also noted that the sea-level signal recorded by a sedimentary system will be influenced by its infilling history. For example, Clement (2011) reported that the Manawatu estuary, on the southwest coast of the North Island, was almost completely infilled by 4,700 cal yr BP. If other systems on the southwest coast of the North Island infilled at a similarly rapid rate, then this would explain why no sea level index points from the last 3000 cal yr BP have been recovered from this region.

5 Conclusions

The four RSL reconstructions for regions within the New Zealand archipelago each record different Holocene sea-level histories (Figures 2A-D and 5). While there is overlap between the two North Island regional RSL reconstructions and the two South Island regional RSL reconstructions in terms of the timing of the initial attainment of PMSL, it is clear that the Holocene marine transgression culminated at sites in the North Island before sites in the South Island (Figure 2E). In the North Island the RSL highstand commenced c. 8,100-7,240 cal yr BP, when PMSL was first attained. This is 600-1,400 years earlier than has been suggested by Gibb (1986), but is in line with RSL reconstructions from the east coast of Australia. In the South Island the RSL highstand commenced c. 7,000-6,400 cal yr BP, when PMSL was first attained. Unfortunately there are only eleven index points in the dataset that delineate the timing of the initial attainment of PMSL (and therefore the initiation of the mid-Holocene sea-level highstand) across the four regions. As a result, the four regional time windows for the initial attainment of PMSL vary in length from 540 years (the southwest coast of the North Island), to 760 years (the northern North Island). Clearly, many more indicators are required to more robustly delimit the timing of the initiation of the RSL highstand around New Zealand.

The magnitude and duration of the early- to mid-Holocene sea-level highstand also varied between regions. In the northern North Island highstand sea level was up to 3.0 m higher than present, with the highstand persisting until at least c. 3,000 cal yr BP. On the southwest coast of the North Island the early-Holocene sea-level highstand was up to 2.73 m higher than present, with a lower-magnitude highstand of up to 1.20-1.50 m above present persisting until at least 3,000 cal yr BP. The precise duration of the highstand on the southwest coast of the North Island is not clear, as the rapid evolution of coastal environments there means that there are no palaeo sea-level indicators from the late Holocene. The occurrence of a highstand in both North Island regions is contrary to the RSL reconstruction presented by Gibb (1986), but is consistent with predictions of Holocene RSL changes in the New Zealand region and RSL reconstructions from the east coast of Australia and the South Pacific. There are too few mid- and late-Holocene palaeo sea-level indicators in the Canterbury region to reach robust conclusions about the occurrence and magnitude of a highstand there. On the Otago coast early- and mid-Holocene sea levels were lower than in the North Island. There may have been a brief highstand c. 6,700 cal yr BP when PMSL was first attained; however, for the remainder of the Holocene RSL was not higher than ~1.40 m above present.

There are a number of mechanisms that are potentially driving the observed and predicted spatial variation in Holocene RSL changes around the New Zealand archipelago. One possible driver is a decrease in the gravitational attraction of the AIS during the Holocene, resulting in a shift in ocean water northwards away from the AIS. This would have the effect of raising RSL in more northern New Zealand locations relative to southern New Zealand locations, which would lead to a lower Holocene highstand being recorded in the north, in disagreement with the palaeo sea-level reconstructions. Another possible driving mechanism is solid Earth deformation predicted in southern latitudes as a result of meltwater loading in the Southern Ocean around Antarctica. However, this effect remains equivocal, with studies from Australia that have considered this effect finding it to be limited or non-existent. It is therefore unlikely that the observed and predicted spatial variation in the timing, magnitude, and duration of Holocene RSL changes in the New Zealand archipelago is being driven by these long-wavelength signals emanating from the Antarctic region.

At the regional- to local-scale spatial variations in Holocene RSL changes may be driven by different local and regional tectonic regimes, and different wave climates and sediment regimes. These are potentially very significant drivers. However, the magnitude of their potential effects is equivocal. It is therefore difficult to make an informed assessment as to the degree to which tectonic, wave, and sediment regime may be driving observed spatial variations in Holocene RSL histories from around New Zealand. Similarly, sediment compaction is likely to be a strong driver of variation in sea-level index points for RSL reconstructions that include index points recovered from deeply-incised drowned-valley sequences. The potential magnitude of the effect of sediment compaction is unclear, and it is presently not possible to precisely determine or account for this effect. Regional differences in hydro-isostatic loading and continental tilting drive considerable spatial variation in the timing, magnitude, and duration of Holocene RSL changes predicted by GIA modelling. The configuration of the coast and the width of the adjacent continental shelf has a significant effect on RSL histories around New Zealand. At the regional scale, subsidence due to continental levering suitably explains why the magnitude of the highstand observed on the Otago coast is less than in the two North Island regions. It is also possible that the early-Holocene highstand on the southwest coast of the North Island may be greater in magnitude than in the northern North Island, in line with predictions that the southwest coast experienced uplift induced by the mechanism of continental levering. At the regional- to local-scale GIA modelling further predicts that continental levering drives significant differences in RSL histories over distances as small as 50-70 km. Substantial differences are predicted in the timing, magnitude, and duration of RSL changes throughout the northern North Island. Palaeo sea-level indicators from this region are in broad agreement with these predictions. However, it is difficult to precisely and conclusively identify actual effects of continental levering in palaeo sea-level observations from the northern North Island given the poor precision and often sparse coverage of palaeo sea-level index points. More research is clearly needed to understand the clearly significant effect that continental levering has had on Holocene RSL histories in the New Zealand region. The analysis of the effects of continental levering clearly demonstrates that palaeo sea-level indicators from around New Zealand should not be grouped into national-scale datasets, and considerable thought should be given to the merit of regional-scale datasets.

Despite the limited vertical precision of the fossil mollusc palaeo sea-level index points used, and some temporal gaps in the RSL reconstructions, this study represents a significant advancement of the state of knowledge of Holocene RSL changes in the New Zealand region. However, there remain considerable gaps in the understanding of Holocene RSL changes in New Zealand, and many areas in which improvements may be made. A major challenge remains resolving the potential uncertainties in the RSL reconstructions. While we have taken every possible care in assembling this dataset, the vertical spread of indicators on some of the reconstructions suggests that the true uncertainties may be broader that we assess (e.g., Pirazzoli, 1991). There is clearly considerable scope for studies to target the recovery of palaeo sea-level indicators to fill gaps in the current dataset. These gaps are most evident in the Canterbury region through the last 6,700 cal yrs BP, and the southwest North Island through the last 3,000 cal yrs BP. Further index points are also needed for all regions to better delineate the timing, magnitude, and duration of the mid-Holocene RSL highstand. Collectors of such index points must take care to clearly document and minimise potential errors to maximise precision, potentially allowing for future analysis to quantitatively compare palaeo sea-level observations and predictions. Further detailed study of local and regional RSL histories should be pursued to improve the limited knowledge of the significant effects continental levering and different wave climates and sediment supply regimes may have on local and regional RSL histories.

Acknowledgements

This research was undertaken as part of a PhD by AJHC, supported by a Top Achievers' Doctoral Scholarship, the Massey University Research Fund, the Geoscience Society of New Zealand Wellman Research Award, and funding from the Institute of Agriculture and Environment, Massey University.

PLW is supported by a NERC Independent Research Fellowship (grant ref: NE/K009958/1). Many people freely provided data, both published and unpublished, and information borne of their own expertise, which is gratefully acknowledged: Scott Nichol (Geoscience Australia), unpublished measurements of cores from Great Barrier Island; Christine Prior (GNS Science), advice on radiocarbon age determinations; Louise Chick (formerly University of Waikato), unpublished data on tectonic movements of the Kerepehi Fault; John Ogden (University of Auckland), unpublished information of cores recovered from Whangapaoa Estuary; John Oldman (NIWA), advice and information on cores recovered from Mahurangi Estuary; Alan Hogg (Waikato Radiocarbon Laboratory), advice regarding conventional radiocarbon ages; Fiona Petchley (Waikato Radiocarbon Laboratory), advice on marine reservoir age corrections and identification of fossil mollusc species; Helen Bostock (NIWA), advice on complications of the marine reservoir effect; Roland Gehrels (University of York), details of GIA model predictions for Pounawea. This manuscript benefitted from valuable discussions with Louise Callard, Natasha Barlow, Ed Garrett, and Ian Fuller, and reviews by Colin Murray-Wallace, Aron Meltzner, and an anonymous reviewer. This research is a contribution to the INQUA Commission for Coastal and Marine Processes.

References

Abrahamson, L., 1987. Aspects of Late Quaternary stratigraphy and evolution of some coastal embayments on the east Coromandel Peninsula, New Zealand. Unpublished MSc Thesis, University of Waikato, Hamilton.

Abrahim, G.M.S., Nichol, S.L., Parker, R.J., Gregory, M.R., 2008. Facies depositional setting, mineral maturity and sequence stratigraphy of a Holocene drowned valley, Tamaki Estuary, New Zealand. Estuarine, Coastal and Shelf Science 79, 133-142.

Allen, J.R.L., 1999. Geological impacts on coastal wetland landscapes: some general effects of sediment autocompaction in the Holocene of northwest Europe. The Holocene 9, 1-12.

Allen, J.R.L., 2000. Morphodynamics of Holocene salt marshes: a review sketch from the Atlantic and southern North Sea coasts of Europe. Quaternary Science Reviews 19, 1155-1231.

Allmon, W.D., Jones, D., Aiello, R.L., Gowlett-Holmes, K., Probert, P.K., 1994. Observations on the biology of Maoricolpus roseus (Quoy and Gaimard) (Prosobranchia: Turritellidae) from New Zealand and Tasmania. Veliger 37, 267-279.

Baker, R.G.V., Haworth, R.J., 1997. Further evidence from relic shellcrust sequences for a Late Holocene higher sea level for eastern Australia. Marine Geology 141, 1-9.

Baker, R.G.V., Haworth, R.J., 2000. Smooth or oscillating Late Holocene sea-level curve? Evidence from cross-regional statistical regressions of fixed biological indicators. Marine Geology 163, 353-365.

Baker, R.G.V., Haworth, R.J., 2000. Smooth or oscillating Late Holocene sea-level curve? Evidence from the palaeo-zoology of fixed biological indicators in east Australia and beyond. Marine Geology 163, 367-386.

Baker, R.G.V., Haworth, R.J., Flood, P.G., 2001. Inter-tidal fixed indicators of former Holocene sea levels in Australia: a summary of sites and a review of methods and models. Quaternary International 83-85, 257-273.

Baker, R.G.V., Haworth, R.J., Flood, P.G., 2001. Warmer or cooler Late Holocene marine palaeoenvironments?: interpreting southeast Australian and Brazilian sea-level changes using fixed biological indicators and their δ18O composition. Palaeogeography, Palaeoclimatology, Palaeoecology 168, 249-272.

Barlow, N.L.M., Shennan, I., Long, A.J., Gehrels, W.R., Saher, M.H., Woodroffe, S.A., Hillier, C. 2013. Salt marshes as late Holocene tide gauges. Global and Planetary Change 106, 90-110.

Bartholdy, J., Pedersen, J.B.T., Bartholdy, A.T., 2010. Autocompaction of shallow silt and marsh clay. Sedimentary Geology 223, 310-319.

Bax, N.J., McEnnulty, F.R., Gowlett-Holmes, K.L., 2003. Distribution and biology of the introduced gastropod, Maoricolpus roseus (Quoy and Gamard, 1834) (Caenogastropoda: Turritellidae) in Australia (Centre for Research on Introduced Marine Pests Technical Report 25). Centre for Research on Introduced Marine Pests, CSIRO Marine Research, Hobart.

Beavan, R.J., Litchfield, N.J., 2012. Vertical land movement around the New Zealand coastline: implications for sea-level rise (GNS Science Report 2012/29). GNS Science, Lower Hutt.

Belknap, D.F., 1975. Dating of late Pleistocene and Holocene relative sea levels in coastal Delaware. Unpublished MSc Thesis, University of Delaware, Newark.

Beu, A.G., Kitamura, A., 1998. Exposed coasts vs sheltered bays: contrast between New Zealand and Japan in the molluscan record of temperature change in Plio–Pleistocene cyclothems. Sedimentary Geology 122, 129-149.

Beu, A.G., Maxwell, P.A., 1990. Cenozoic mollusca of New Zealand (NZGS Paleontological Bulletin 58). New Zealand Geological Survey, Lower Hutt.

Bird, M.I., Fifield, L.K., Chua, S., Goh, B., 2004. Calculating sediment compaction for radiocarbon dating of intertidal sediments. Radiocarbon 46, 421-435.

Blackwell, R.G., 1984. Aspects of the population dynamics of Chione stutchburyi in Ohiwa Harbour, Bay of Plenty, New Zealand. Unpublished PhD Thesis, University of Auckland, Auckland.

Bloom, A.L., 1964. Peat accumulation and compaction in a Connecticut salt marsh. Journal of Sedimentary Petrology 34, 599-603.

Brook, F.J., 1999. Stratigraphy and landsnail faunas of Late Holocene coastal dunes, Tokerau Beach, northern New Zealand. Journal of the Royal Society of New Zealand 29, 337-359.

Brook, F.J., Grace, R.V., 1981. Soft-bottom benthic faunal associations of Tutukaka Harbour, Northland, New Zealand, part 1: macrofauna. Tane 27, 69-80.

Brown, L.J., 1995. Holocene shoreline depositional processes at Poverty Bay, a tectonically active area, northeastern North Island, New Zealand. Quaternary International 26, 21-33.

Bryant, E., 1992. Last Interglacial and Holocene trends in sea-level maxima around Australia: implications for modern rates. Marine Geology 108, 209-217.

Carroll, J.L., Wells, R.M.G., 1995. Strategies of anaerobiosis in New Zealand infaunal bivalves: adaptations to environmental and functional hypoxia. New Zealand Journal of Marine and Freshwater Research 29, 137-146.

Carter, L., Manighetti, B., Elliot, M., Trustrum, N., Gomez, B., 2002. Source, sea level and circulation effect on the sediment flux to the deep ocean over the past 15 ka off eastern New Zealand. Global and Planetary Change 33, 339-355.

Carter, R.M., Abbott, S.T., Naish, T.R., 1999. Plio-Pleistocene cyclothems from Wanganui Basin, New Zealand: type locality for an astrochronologic time scale, or template for recognising ancient glacio-eustasy. Philosophical Transactions of the Royal Society of London, Series A 357, 1861-1872.

Carter, R.M., Carter, L., Johnson, D.P., 1986. Submergent shorelines in the SW Pacific: evidence for an episodic post-glacial transgression. Sedimentology 33, 629-649.

Clark, J.A., Farrell, W.E., Peltier, W.R., 1978. Global changes in postglacial sea level: a numerical calculation. Quaternary Research 9, 265-287.

Clark, J.A., Lingle, C.S., 1979. Predicted relative sea-level changes (18,000 years BP to present) caused by late-glacial retreat of the Antarctic Ice Sheet. Quaternary Research 11, 279-298.

Clark, K.J., Hayward, B.W., Cochran, U.A., Grenfell, H.R., Hemphill-Haley, E., Mildenhall, D.C., Hemphill-Haley, M.A., Wallace, L.M., 2011. Investigating subduction earthquake geology along the southern Hikurangi margin using palaeoenvironmental histories of intertidal inlets. New Zealand Journal of Geology and Geophysics 54, 255-271.

Clark, P.U., Mitrovica, J.X., Milne, G.A., Tamisiea, M.E., 2002. Sea-level fingerprinting as a direct test for the source of global meltwater pulse 1A. Science 295, 2438-2441.

Clement, A.J.H., 2011. Holocene sea-level change in the New Zealand archipelago and the geomorphic evolution of a Holocene coastal plain incised-valley system: the lower Manawatu valley, North Island, New Zealand. Unpublished PhD Thesis, Massey University, Palmerston North.

Clement, A.J.H., Sloss, C.R., Fuller, I.C., 2010. Late Quaternary geomorphology of the Manawatu coastal plain, North Island, New Zealand. Quaternary International 221, 36-45.

Conrad, C.P., 2013. The solid Earth's influence on sea level. Geological Society of America Bulletin 125, 1027-1052.

Cranfield, H.J., Michael, K.P., 2001. Growth rates of five species of surf clams on a southern North Island beach, New Zealand. New Zealand Journal of Marine and Freshwater Research 35, 909-924.

Cranfield, H.J., Michael, K.P., 2001. The surf clam fishery in New Zealand: description of the fishery, its management, and the biology of surf clams (New Zealand Fisheries Assessment Report 2001/62). Ministry of Fisheries, Wellington.

Cranfield, H.J., Michael, K.P., Stotter, D., Doonan, I.J., 1994. Distribution, biomass and yield estimates of surf clams off New Zealand beaches (New Zealand Fisheries Assessment Research Document 94/1). Ministry of Agriculture and Fisheries, Wellington.

Cummings, V.J., Thrush, S.F., 2004. Behavioural response of juvenile bivalves to terrestrial sediment deposits: implications for post-disturbance recolonisation. Marine Ecology Progress Series 278, 179-191.

Davis, R.A., Jr, Healy, T.R., 1993. Holocene coastal depositional sequences on a tectonically active setting: southeastern Tauranga Harbour, New Zealand. Sedimentary Geology 84, 57-69.

Davis, J.L., Mitrovica, J.X., 1996. Glacial isostatic adjustment and the anomalous tide gauge record of eastern North America. Nature 379, 331-333.

Dougherty, A.J., Dickson, M.E., 2012. Sea level and storm control on the evolution of a chenier plain, Firth of Thames, New Zealand. Marine Geology 307-310, 58-72.

Eiby, G.A., 1990. Changes in Porirua Harbour in about 1855: historical tradition and geological evidence. Journal of the Royal Society of New Zealand 20, 233-248.

Ensor, M.J., 1986. Sedimentology of Blueskin Bay. Unpublished MSc Thesis, University of Otago, Dunedin.

Estcourt, I.N., 1967. Distributions and associations of benthic invertebrates in a sheltered water soft-bottom environment (Marlborough sounds, New Zealand). New Zealand Journal of Marine and Freshwater Research 1, 352-370.

Farrell, W.E., Clark, J.A., 1976. On postglacial sea level. Geophysical Journal of the Royal Astronomical Society 46, 647-667.

Figueira, B., Hayward, B.W., Grenfell, H.R., Gehrels, W.R., 2009. Salt-marsh foraminiferal proxy records from the South Island, New Zealand, IGCP 495 Annual Conference and Field Meeting, Myrtle Beach, South Carolina, USA, Program and Abstracts, p. 38.

Gehrels, W.R., 1999. Middle and Late Holocene sea-level changes in eastern Maine reconstructed from foraminiferal saltmarsh stratigraphy and AMS 14C dates on basal peat. Quaternary Research 52, 350-359.

Gehrels, W.R., Callard, S.L., Moss, P.T., Marshall, W.A., Blaauw, M., Hunter, J., Milton, J.A., Garnett, M.H., 2012. Nineteenth and twentieth century sea-level changes in Tasmania and New Zealand. Earth and Planetary Science Letters 315-316, 94-102.

Gehrels, W.R., Hayward, B.W., Newnham, R.M., Southall, K.E., 2008. A 20th century acceleration of sea-level rise in New Zealand. Geophysical Research Letters 35, L02717.

Gibb, J.G., 1979. Late Quaternary shoreline movements in New Zealand. Unpublished PhD Thesis, Victoria University of Wellington, Wellington.

Gibb, J.G., 1983. Sea levels during the past 10000 years BP from the New Zealand region - South Pacific Ocean, Abstracts of International Symposium on Coastal Evolution in the Holocene, August 29-31, Tokyo, Japan. Japan Society for the Promotion of Science, Tokyo, pp. 28-31.

Gibb, J.G., 1986. A New Zealand regional Holocene eustatic sea-level curve and its application to determination of vertical tectonic movements. Royal Society of New Zealand Bulletin 24, 377-395.

Gibb, J.G., Aburn, J.H., 1986. Shoreline fluctuations and an assessment of a coastal hazard zone along Pauanui Beach, eastern Coromandel Peninsula, New Zealand (Water \& Soil Technical Publication 27). National Water Soil Conservation Authority and Water and Soil Directorate, Ministry of Works and Development, Wellington.

Gibb, J.G., Cox, G.J., 2009. Patterns and rates of sedimentation within Porirua Harbour (Coastal Management Consultancy Report CR 2009/1). Coastal Management Consultants, Kerikeri.

Goff, J.R., Pearce, S., Nichol, S.L., Chague-Goff, C., Horrocks, M., Strotz, L., 2010. Multi-proxy records of regionally-sourced tsunamis, New Zealand. Geomorphology 118, 369-382.

Goff, J.R., Rouse, H.L., Jones, S.L., Hayward, B.W., Cochran, U., McLea, W., Dickinson, W.W., Morley, M.S., 2000. Evidence for an earthquake and tsunami about 3100-3400 yr ago, and other catastrophic saltwater inundations recorded in a coastal lagoon, New Zealand. Marine Geology 170, 231-249.

Goodbred, S.L., Kuehl, S.A., 1999. Holocene and modern sediment budgets for the Ganges-Brahmaputra river system: evidence for highstand dispersal to floodplain, shelf, and deep-sea depocenters. Geology 27, 559-562.

Grant, C.M., 1994. Demographics and reproduction of the tuatua - Paphies subtriangulata. Unpublished MSc Thesis, University of Auckland, Auckland.

Grant, C.M., Hay, B.E. 2003. A review of issues related to depletion of populations of selected infaunal bivalve species in the Hauraki Gulf Marine Park. Report prepared for the Hauraki Gulf Forum by AquaBio Consultants Ltd. AquaBio Consultants Ltd., Auckland.

Grant-Taylor, T.L., Rafter, T.A., 1971. New Zealand radiocarbon age measurements - 6. New Zealand Journal of Geology and Geophysics 14, 364-402.

Grapes, R., Downes, G., 1997. The 1855 Wairarapa, New Zealand, earthquake - analysis of historical data. New Zealand National Society for Earthquake Engineering Bulletin 30, 272-368.

Haddon, M., Willis, T.J., Wear, R.G., Anderlini, V.C., 1996. Biomass and distribution of five species of surf clam of an exposed west coast North Island beach, New Zealand. Journal of Shellfish Research 15, 331-339.

Haworth, R.J., Baker, R.G.V., Flood, P.G., 2002. Predicted and observed Holocene sea-level in the Australian coast: what do they indicate about hydro-isostatic models in far-field sites? Journal of Quaternary Science 17, 581-591.

Hayward, B.W., Grenfell, H.R., Sabaa, A.T., 2012. Marine submersion of an archaic moa-hunter occupational site, Shag River estuary, North Otago. New Zealand Journal of Geology and Geophysics 55, 127-136.

Hayward, B.W., Grenfell, H.R., Sabaa, A.T., Kay, J., Daymond-King, R., Cochran, U., 2010a. Holocene subsidence at the transition between strike-slip and subduction on the Pacific-Australian plate boundary, Marlborough Sounds, New Zealand. Quaternary Science Reviews 29, 648-661.

Hayward, B.W., Wilson, K., Morley, M.S., Cochran, U., Grenfell, H.R., Sabaa, A.T., Daymond-King, R., 2010b. Microfossil record of the Holocene evolution of coastal wetlands in a tectonically active region of New Zealand. The Holocene 20, 405-421.

Hayward, B.W., Grenfell, H.R., Sabaa, A.T., Kay, J., 2010c. Using foraminiferal faunas as proxies for low tide level in the estimation of Holocene tectonic subsidence, New Zealand. Marine Micropaleontology 76, 23-36.

Hayward, B.W., Grenfell, H.R., Sabaa, A.T., Southall, K.E., Gehrels, W.R., 2007. Foraminiferal evidence of Holocene fault displacements in coastal south Otago, New Zealand. Journal of Foraminiferal Research 37, 344-359.

Hayward, B.W., Grenfell, H.R., Sandiford, A., Shane, P.R., Morley, M.S., Alloway, B.V., 2002. Foraminiferal and molluscan evidence for the Holocene marine history of two breached maar lakes, Auckland, New Zealand. New Zealand Journal of Geology and Geophysics 45, 467-479.

Hayward, B.W., Stephenson, A.B., Morley, M.S., Blom, W., Grenfell, H.R., Brook, F.J., Riley, J.L., Thompson, F., Hayward, J.J., 2001. Marine biota of Parengarenga Harbour, Northland, New Zealand. Records of the Auckland Museum 37-38, 45-80.

Healy, W.B., 1980. Pauatahanui Inlet - an environmental study (DSIR Information Series 141). Science Information Division, Department of Scientific and Industrial Research, Wellington.

Heap, A.D., 1995. Stratigraphic reconstruction of an incised valley system, Weiti River estuary, New Zealand. Unpublished MSc Thesis, University of Auckland, Auckland.

Heap, A.D., Nichol, S.L., 1997. The influence of limited accommodation space on the stratigraphy of an incised-valley succession: Weiti River estuary, New Zealand. Marine Geology 144, 229-252.

Herzer, R.H., 1981. Late Quaternary stratigraphy and sedimentation of the Canterbury continental shelf, New Zealand (NZOI Memoir 89). Department of Scientific and Industrial Research, Wellington.

Hesp, P.A., Shepherd, M.J., 1978. Some aspects of the late Quaternary geomorphology of the lower Manawatu valley, New Zealand. New Zealand Journal of Geology and Geophysics 21, 403-412.

Hesp, P.A., Shepherd, M.J., Parnell, K., 1999. Coastal geomorphology in New Zealand, 1989-99. Progress in Physical Geography 23, 501-524.

Hicks, D.L., 1983. Landscape evolution in consolidated coastal dunesands. Zeitschrift fur Geomorphologie, Supplement 45, 245-250.

Hicks, H., Nichol, S.L., 2007. A marine to freshwater sediment succession from Kowhai Beach wetland, Northland: implications for Holocene sea level. Journal of the Royal Society of New Zealand 37, 91-107.

Hogg, A.G., Higham, T.F.G., Dahm, J., 1998. 14C dating of modern marine and estuarine shellfish. Radiocarbon 40, 975-984.

Hooker, S.H., Creese, R.G., 1995. The reproductive biology of pipi, Paphies australis (Gmelin, 1790) (Bivalvia: Mesodesmatidae). I. Temporal patterns of the reproductive cycle. Journal of Shellfish Research 14, 7-15.

Horrocks, M., Deny, Y., Ogden, J., Sutton, D.G., 2000. A reconstruction of the history of a Holocene sand dune on Great Barrier Island, northern New Zealand, using pollen and phytolith analyses. Journal of Biogeography 27, 1269-1277.

Horrocks, M., Ogden, J., Nichol, S.L., Alloway, B.V., Sutton, D.G., 1999. The palynology and sedimentology of a coastal swamp at Awana, Great Barrier Island, New Zealand, from c. 7000 yr BP to present. Journal of the Royal Society of New Zealand 29, 213-233.

Horrocks, M., Ogden, J., Nichol, S.L., Alloway, B.V., Sutton, D.G., 2000. A Late Quaternary palynological and sedimentological record from two coastal swamps at southern Kaitoke, Great Barrier Island, New Zealand. Journal of the Royal Society of New Zealand 30, 49-68.

Horton, B.P., Culver, S.J., Hardbattle, M.I.J., Larcombe, P., Milne, G.A., Morigi, C., Whittaker, J.E., Woodroffe, S.A., 2007. Reconstructing Holocene sea-level change for the central Great Barrier Reef (Australia) using subtidal foraminifera. Journal of Foraminiferal Research 37, 327-343.

Hull, A.G., 1985. A possible eustatic sea level rise c. 4500 years BP: evidence from New Zealand coast (note), In: Pillans, B. (Ed.), Proceedings of the second CLIMANZ conference, Harihari, Westland, New Zealand, February 4-8 1985. Geology Department, Victoria University of Wellington, Wellington, pp. 8-12.

Hume, T.M., Dahm, J., 1991. An investigation of the effects of Polynesian and European land use on sedimentation in Coromandel estuaries (Water Quality Center, DSIR, Consultancy Report 7106). Water Quality Centre, Department of Scientific and Industrial Research, Hamilton.

Hume, T.M., McGlone, M.S., 1986. Sedimentation patterns and catchment use change recorded in the sediments of a shallow tidal creek, Lucas Creek, upper Waitamata Harbour, New Zealand. New Zealand Journal of Marine and Freshwater Research 20, 677-687.

Hutcheon, R.L., 2006. Evaluation of evidence of mid-Holocene sea-level in the Auckland region. Unpublished MA Thesis, University of Auckland, Auckland.

Johnston, R.M.S., 1984. Sediments and sedimentary processes in Mahurangi Harbour. Unpublished MSc Thesis, University of Waikato, Hamilton.

Journeaux, T.D., Kamp, P.J.J., Naish, T.R., 1996. Middle Pleistocene cyclothems, Mangaweka region, Wanganui Basin, New Zealand: a lithostratigraphic framework. New Zealand Journal of Geology and Geophysics 39, 135-149.

Kamp, P.J.J., McIntyre, A.P., 1998. The stratigraphic architecture of Late Pliocene (2.8--2.4 Ma) asymmetrical shelf sequences, western Wanganui Basin, New Zealand. Sedimentary Geology 122, 53-67.

Kaye, C.A., Barghoorn, E.S., 1964. Late Quaternary sea-level change and crustal rise at Boston, Massachusetts, with notes on the autocompaction of peat. Geological Society of America Bulletin 75, 63-80.

Kendall, R.A., Mitrovica J.X., Milne, G.A., 2005. On post-glacial sea level – II. Numerical formulation and comparative results on spherically symmetric models. Geophysical Journal International 161, 679-706.

Kennedy, D.M., 2008. Recent a future higher sea levels in New Zealand: a review. New Zealand Geographer 64, 105-116.

Kidson, C., 1982. Sea level changes in the Holocene. Quaternary Science Reviews 162, 121-151.

Lambeck, K., Chappell, J., 2001. Sea level change through the Last Glacial cycle. Science 292, 679-686.

Lambeck, K., Nakada, M., 1990. Late Pleistocene and Holocene sea-level change along the Australian coast. Palaeogeography, Palaeoclimatology, Palaeoecology 89, 143-176.

Lambeck, K., Smither, C., Johnston, P., 1998. Sea-level change, glacial rebound and mantle viscosity for northern Europe. Geophysical Journal International 134, 102-144.

Lambeck, K., Yokoyama, Y., Purcell, T., 2002. Into and out of the Last Glacial Maximum: sea-level change during Oxygen Isotope Stages 3 and 2. Quaternary Science Reviews 21, 343-360.

Lambeck, K., Woodroffe, C.D., Antonioli, F., Anzidei, M., Gehrels, W.R., Laborel, J., Wright, A.J., 2010. Paleoenvironmental records, geophysical modeling, and reconstruction of sea-level trends and variability on centennial and longer timescales, In: Chruch, J.A., Woodworth, P.L., Aarup, T., Wilson, W.S. (Eds.), Understanding sea-level rise and variability. Wiley-Blackwell, Oxford, pp. 61-121.

Leach, B.F., Anderson, A.J., 1974. The transformation from an estuarine to lacustrine environment in the lower Wairarapa. Journal of the Royal Society of New Zealand 4, 267-275.

Lelieveld, S.D., Pilditch, C.A., Green, M.O., 2004. Effects of deposit-feeding bivalve (Macomona liliana) density on intertidal sediment stability. New Zealand Journal of Marine and Freshwater Research 38, 115-128.

Lensen, G.J., 1975. Earth-deformation studies in New Zealand. Tectonophysics 29, 541-551.

Lewis, S.E., Wust, R.A.J., Webster, J.M., Sheilds, G.A., 2008. Mid-late Holocene sea-level variability in eastern Australia. Terra Nova 20, 74-81.

Litchfield, N., Berryman, K., 2007. Relations between postglacial fluvial incision rates and uplift rates in the North Island, New Zealand. Journal of Geophysical Research 111, F02007.

Lundquist, C.J., Pilditch, C.A., Cummings, V.J., 2004. Behaviour controls post-settlement dispersal by the juvenile bivalves Austrovenus stutchburyi and Macomona liliana. Journal of Experimental Marine Biology and Ecology 306, 51-74.

Marks, G.P., Nelson, C.S., 1979. Sedimentology and evolution of Omaro Spit, Coromandel Peninsula. New Zealand Journal of Marine and Freshwater Research 13, 347-372.

Massey, A.C., Paul, M.A., Gehrels, W.R., Charman, D.J., 2006. Autocompaction in Holocene coastal back-barrier sediments from south Devon, southwest England, UK. Marine Geology 226, 225-241.

Mather, N.S., 2004. Coastal sedimentation on the east coast of Auckland: evidence for tsunami. Unpublished MSc Thesis, University of Auckland, Auckland.

Mazzotti, S., Lambert, A., Van der Kooij, M., Mainville, A., 2009. Impact of anthropogenic subsidence on relative sea-level rise in the Fraser River Delta. Geology 37, 771-774.

McCormac, F.G., Hogg, A.G., Blackwell, P.G., Buck, C.E., Higham, T.F.G., Reimer, P.J., 2004. SHCal04 Southern Hemisphere calibration, 0-11.0 cal kyr BP. Radiocarbon 46, 1087-1092.

McFadgen, B.G., Manning, M.R., 1990. Calibrating New Zealand radiocarbon dates of marine shells. Radiocarbon 32, 229-232.

McKnight, D.G., 1969. Infaunal benthic communities of the New Zealand continental shelf. New Zealand Journal of Marine and Freshwater Research 3, 409-444.

Millener, P.R., 1981. The Quaternary avifauna of the North Island, New Zealand (2 volumes). Unpublished PhD Thesis, University of Auckland, Auckland.

Milne, G.A., Shennan, I., 2013. Isostasy: glaciation-induced sea-level change. In: Elias, S.A., Encyclopaedia of Quaternary Sciences, 2nd Edition. Elsevier, Amsterdam, 452-459.

Mitrovica, J.X., Forte, A.M., 2004. A new inference of mantle viscosity based upon joint inversion of convection and glacial isostatic adjustment data. Earth and Planetary Science Letters 225, 177-189.

Mitrovica, J.X., Milne, G.A., 2002. On the origin of late Holocene sea-level highstands within equatorial ocean basins. Quaternary Science Reviews 21, 2179-2190.

Mitrovica, J.X., Milne, G.A., 2003. On post-glacial sea level: I. General theory. Geophysical Journal International 154, 253-267.

Mitrovica, J.X., Peltier, W.R., 1991. On postglacial geoid subsidence over the equatorial oceans. Journal of Geophysical Research 96, 20053-20071.

Mitrovica, J.X., Wahr, J., Matsuyama, I., Paulson, A. 2005. The rotational stability of an ice-age earth. Geophysical Journal International 161, 491–506.

Morton, J.E., Miller, M.C., 1968. The New Zealand sea shore. Collins, Auckland.

Murray-Wallace, C.V., Woodroffe, C.D., 2014. Quaternary sea-level changes: a global perspective. Cambridge University Press, Cambridge.

Nakada, M., Lambeck, K., 1988. The melting history of the late Pleistocene Antarctic ice sheet. Nature 333, 36-40.

Nakada, M., Lambeck, K., 1989. Late Pleistocene and Holocene sea-level change in the Australian region and mantle rheology. Geophysical Journal 96, 497-517.

Nichol, S.L., 2002. Morphology, stratigraphy and origin of Last Interglacial beach ridges at Bream Bay, New Zealand. Journal of Coastal Research 18, 149-159.

Nichol, S.L., Deny, Y., Horrocks, M., Zhou, W., Hume, T.M., 2009. Preservation of a Late Glacial terrestrial and Holocene estuarine record on the margins of Kaipara Harbour, Northland, New Zealand. Journal of the Royal Society of New Zealand 39, 1-14.

Nipper, M.G., Roper, D.S., 1995. Growth of an amphipod and a bivalve in uncontaminated sediments: implications for chronic toxicity assessments. Marine Pollution Bulletin 31, 424-430.

Norkko, A., Cummings, V.J., Thrush, S.F., Hewitt, J.E., Hume, T., 2001. Local dispersal of juvenile bivalves: implications for sandflat ecology. Marine Ecology Progress Series 212, 131-144.

Nunn, P.D., 1995. Holocene sea-level changes in the south and west Pacific. Journal of Coastal Research SI17, 311-319.

Nunn, P.D., 1998. Sea-level changes over the past 1,000 years in the Pacific. Journal of Coastal Research 14, 23-30.

Osborne, N.M., 1983. Holocene coastal depositional landforms: Bream Bay, Northland. Unpublished MA Thesis, University of Auckland, Auckland.

Osborne, N.M., Enright, N.J., Parnell, K.E., 1991. The age and stratigraphic significance of sea-rafted Loisels Pumice in northern New Zealand. Journal of the Royal Society of New Zealand 21, 357-371.

Osborne, N.M., Nichol, S.L., 2006. Geomorphology and evolution of Te Aupouri Peninsula and Karikari Peninsula: a summary. Mid-conference field trip guide, 12th Australia and New Zealand Geomorphology Group Conference, Taipa Bay, Northland, 12-17 February 2006. University of Auckland, Auckland.

Ota, Y., Brown, L.J., Berryman, K.R., Fujimori, T., Miyauchi, T., 1995. Vertical tectonic movement in northeastern Marlborough: stratigraphic, radiocarbon, and paleoecological data from Holocene estuaries. New Zealand Journal of Geology and Geophysics 38, 269-282.

Paul, M.A., Barras, B.F., 1998. A geotechnical correction for post-depositional sediment compression: examples from the Forth Valley, Scotland. Journal of Quaternary Science 13, 171-176.

Paul, M.A., Barras, B.F., Peacock, J.D., 1995. Flandrian stratigraphy and sedimentation in the Bothkennar-Grangemouth area. Quaternary Newsletter 75, 22-35.

Peltier, W.R., 1988. Lithospheric thickness, Antarctic deglaciation history, and ocean basin descretization effects in a global model of postglacial sea level change: a summary of some sources of nonuniqueness. Quaternary Research 29, 93-112.

Peltier, W.R., 2004. Glocal glacial isostasy and the surface of the ice-age Earth: the ICE-5G (VM2) model and GRACE. Annual Review of Earth and Planetary Sciences 32, 111-149.

Petchley, F., Anderson, A., Hogg, A., Zondervan, A., 2008. The marine reservoir effect in the Southern Ocean: an evaluation of extant and new ΔR values and their application to archaeological chronologies. Journal of the Royal Society of New Zealand 38, 243-262.

Pillans, B., 1986. A late Quaternary uplift map for the North Island, New Zealand. Royal Society of New Zealand Bulletin 24, 409-417.

Pillans, B., Huber, P., 1995. Interpreting coseismic deformation using Holocene coastal deposits, Wellington, New Zealand. Quaternary International 26, 87-95.

Pirazzoli, P.A., 1991. World atlas of Holocene sea-level changes. Elsevier, Amsterdam.

Pizzuto, J.E., Schwendt, A.E., 1997. Mathematical modelling of autocompaction of a Holocene transgressive valley-fill deposit, Wolfe Glade, Delaware. Geology 25, 57-60.

Powell, A.W.B., 1979. New Zealand mollusca - marine, land and freshwater shells. Collins, Auckland.

Probst, T.A., Crawford, C.M., 2008. Population characteristics and planktonic larval stage of the New Zealand screwshell Maoricolpus roseus. Journal of Molluscan Studies 74, 191-197.

Proust, J.-N., Lamarche, G., Nodder, S.D., Kamp, P.J.J., 2005. Sedimentary architecture of a Plio-Pleistocene proto-back-arc basin: Wanganui Basin, New Zealand. Sedimentary Geology 181, 107-145.

Rayns, N.D., 1985. Sedimentation in Hoopers and Papanui Inlets. Unpublished MSc Thesis, University of Otago, Dunedin.

Reimer, P.J., Baillie, M.G.L., Bard, E., Bayliss, A., Beck, J.W., Blackwell, P.G., Bronk Ramsey, C., Buck, C.E., Burr, G.S., Edwards, R.L., Friedrich, M., Grootes, P.M., Guilderson, T.P., Hajdas, I., Heaton, T.J., Hogg, A.G., Hughen, K.A., Kaiser, K.F., Kromer, B., McCormac, F.G., Manning, S.W., Reimer, R.W., Richards, D.A., Southon, J.R., Talamo, S., Turney, C.S.M., van der Plicht, J., Weyhenmeyer, C.E., 2009. IntCal09 and Marine09 radiocarbon age calibration curves, 0–50,000 years cal BP. Radiocarbon 51, 1111-1150.

Roper, D.S., Pridmore, R.D., Thrush, S.F., 1992. Recruitment to the macrobenthos of Macomona liliana (Bivalvia: Tellinidae) in Manakau Harbour, New Zealand. New Zealand Journal of Marine and Freshwater Research 26, 385-392.

Rybczyk, J.M., Callaway, J., Day Jr, J.W., 1998. A relative elevation model (REM) for a subsiding coastal forested wetland receiving wastewater effluent. Ecological Modelling 112, 23-44.

Schallenberg, M., Goff, J., Harper, M.A., 2012. Gradual, catastrophic and human induced environmental changes from a coastal lake, southern New Zealand. Sedimentary Geology 273-274, 48-57.

Schofield, J.C., 1960. Sea level fluctuations during the last 4000 years as recorded by a chenier plain, Firth of Thames, New Zealand. New Zealand Journal of Geology and Geophysics 3, 467-485.

Schofield, J.C., 1973. Post-glacial sea levels of Northland and Auckland. New Zealand Journal of Geology and Geophysics 16, 359-366.

Shennan, I., Milne, G., Bradley, S. 2012. Late Holocene vertical land motion and relative sea-level changes: lessons from the British Isles. Journal of Quaternary Science 27, 64-70.

Shepherd, M.J., Gibb, J.G., Johnson, M., 1986. Geological Society of New Zealand 16th annual conference field excursions guide book (GSNZ Miscellaneous Publication 35B). Geological Society of New Zealand, Wellington.

Shepherd, M.J., Lees, C.M., 1987. Holocene alluviation and transgressive dune activity in the lower Manawatu Valley, New Zealand. New Zealand Journal of Geology and Geophysics 30, 175-187.

Shulmeister, J., Kirk, R.M., 1993. Evolution of a mixed sand and gravel barrier system in North Canterbury, New Zealand, during Holocene sea-level rise and still-stand. Sedimentary Geology 87, 215-235.

Shulmeister, J., Kirk, R.M., 1997. Holocene fluvial-coastal interactions on a mixed sand and sand and gravel beach system, North Canterbury, New Zealand. Catena 30, 337-355.

Sloss, C.R., Murray-Wallace, C.V., Jones, B.G., 2007. Holocene sea-level change on the southeast coast of Australia: a review. The Holocene 17, 999-1014.

Smith, I., James-Lee, T., 2009. Data for an archaeozoological analysis of marine resource use in two New Zealand study areas. Otago Archaeological Laboratory, Anthropology Department, University of Otago (Laboratory Report 6), Dunedin.

Soons, J.M., Shulmeister, J., Holt, S., 1997. The Holocene evolution of a well nourished gravelly barrier and lagoon complex, Kaitorete "Spit", Canterbury, New Zealand. Marine Geology 138, 69-90.

Spennemann, D.H.R., Head, M.J., 1996. Reservoir modification of radiocarbon signatures in coastal and near-shore waters of eastern Australia: the state of play. Quaternary Australasia 14, 32-39.

Stephenson, W., Shulmeister, J., 1999. A Holocene progradation record from Okains Bay, Banks Peninsula, Canterbury, New Zealand. New Zealand Journal of Geology and Geophysics 42, 11-19.

Stern, T.A., Quinlan, G.M., Holt, W.E., 1992. Basin formation behind an active subduction zone: 3D flexural modelling of Wanganui Basin. Basin Research 4, 197-214.

Stern, T.A., Quinlan, G.M., Holt, W.E., 1993. Crustal dynamics associated with the formation of Wanganui Basin, New Zealand, In: Ballance, P.F. (Ed.), South Pacific sedimentary basins (Sedimentary Basins of the World, 2). Elsevier, Amsterdam, pp. 213-223.

Stuiver, M., Braziunas, T.F., 1993. Modelling atmospheric 14C influences and 14C ages of marine samples to 10,000 BC. Radiocarbon 35, 137-189.

Stuiver, M., Polach, H.A., 1977. Reporting of 14C data. Radiocarbon 19, 355-363.

Stuiver, M., Reimer, P.J., 1993. Extended 14C database and revised CALIB radiocarbon calibration program. Radiocarbon 35, 215-230.

Swales, A., Bentley, S.J., McGlone, M.S., Ovenden, R., Hermanspahn, N., Budd, R., Hill, A., Pickmere, S., Haskew, R., Okey, M.J., 2005. Pauatahanui Inlet: effects of historical catchment landcover changes on inlet sedimentation (NIWA Client Report HAM2004-149). National Institute of Water and Atmospheric Research, Hamilton.

Swales, A., Hume, T.M., Oldman, J.W., Green, M.O., 1997. Mahurangi Estuary: sedimentation history and recent human impacts (NIWA Client Report ARC60210). National Institute of Water and Atmospheric Research, Hamilton.

Tamisiea, M.E., Mitrovica, J.X., Davis, J.L., Milne, G.A., 2003. Long wavelength sea level and solid surface perturbations driven by polar ice mass variations: fingerprinting Greenland and Antarctica ice sheet flux. Space Science Reviews 108, 81-93.

Thom, B.G., Chappell, J., 1975. Holocene sea levels relative to Australia. Search 6, 90-93.

Thom, B.G., Roy, P.S., 1983. Sea-level change in New South Wales over the past 15,000 years, In: Hopley, D. (Ed.), Australian sea levels in the last 15000 years: a review. Department of Geography, James Cook University, Townsville, Australia, pp. 64-84.

Thomas, D., 2000. Holocene stratigraphy and sequence architecture of the Blueskin Bay estuary, East Otago (2 volumes). University of Otago, Dunedin.

Thrush, S.F., Lawrie, S.M., Hewitt, J.E., Cummings, V.J., 1999. The problem of scale: uncertainties and implications for soft-bottom marine communities and the assessment of human impacts, In: Gray, J.S., Ambrose, W.G., Szaniawska, A. (Eds.), Biogeochemical cycling and sediment ecology. Kluwer Academic Publishers, Dordrecht, pp. 195-210.

Tornqvist, T.E., Wallace, D.J., Storms, J.E.A., Wallinga, J., van Dam, R.L., Blaauw, M., Derksen, M.S., Klerks, C.J.W., Miejneken, C., Snijders, E.M.A., 2008. Mississippi Delta subsidence primarily caused by compaction of Holocene strata. Nature Geoscience 1, 173-176.

Tovey, N.K., Paul, M.A., 2002. Modelling self-weight consolidation in Holocene sediments. Bulletin of the International Association of Engineering Geologists 61, 21-33.

Tribe, H.M., Kennedy, D.M., 2010. The geomorphology and evolution of a large barrier spit: Farewell Spit, New Zealand. Earth Surface Processes and Landforms 35, 1751-1762.

Ulm, S. 2002. Marine and estuarine reservoir effects in central Queensland, Australia: determination of ΔR values. Geoarchaeology 17, 319-348.

Wellman, H.W., 1979. An uplift map for the South Island of New Zealand, and a model for uplift of the Southern Alps. Royal Society of New Zealand Bulletin 18, 13-20.

Whitehouse, P., 2009. Glacial isostatic adjustment and sea level change: state of the art report. Svensk Kärnbränslehantering, Stockholm.

Williams, H., 2003. Modelling shallow autocompaction in coastal marshes using Cesium-137 fallout: preliminary results from the Trinity River Estuary, Texas. Journal of Coastal Research 19, 180-188.

Williams, P.W., 1991. Tectonic geomorphology, uplift rates and geomorphic response in New Zealand. Catena 18, 439-452.

Wilson, G.S., McGuire, D.M., 1995. Distributed deformation due to coupling across a subduction thrust: mechanism of young tectonic rotation within the south Wanganui Basin, New Zealand. Geology 23, 645-648.

Wilson, K., Berryman, K., Cochran, U., Little, T., 2007a. A Holocene incised valley infill sequence developed on a tectonically active coast: Pakarae River, New Zealand. Sedimentary Geology 197, 333-354.

Wilson, K., Berryman, K., Cochran, U., Little, T., 2007b. Holocene coastal evolution and uplift mechanisms of the northeastern Ruakumara Peninsula, North Island, New Zealand. Quaternary Science Reviews 26, 1106-1128.

Wolcott, R.I., 1972. Past sea levels, eustasy and deformation of the Earth. Quaternary Research 2, 1-14.

Woodroffe, C.D., Curtis, R.J., McLean, R.F., 1983. Development of a chenier plain, Firth of Thames, New Zealand. Marine Geology 53, 1-22.

Woodroffe, C.D., Murray-Wallace, C.V., Bryant, E.A., Brooke, B., Heijnis, H., Price, D.M., 1995. Late Quaternary sea-level highstands in the Tasman Sea: evidence from Lord Howe Island. Marine Geology 125, 61-72.

Woodroffe, S.A., 2009. Testing models of mid to late Holocene sea-level change, north Queensland, Australia. Quaternary Science Reviews 28, 2474-2488.

Woods, J.L.D., 2011. The evolution of a Holocene estuarine barrier on the Coromandel Coast, New Zealand. Geographical Research 50, 89-101.

Wratt, C.R.L., 1999. Stratigraphic reconstruction of a cross section in the upper Puhoi River Estuary, Northland. Unpublished MSc Thesis, University of Auckland, Auckland.

Wynne, K.E., 1981. Porirua Harbour Authority harbour investigation May 1981. Unpublished Consulting Report prepared for the Porirua Harbour Authority.

Yuill, B., Lavoie, D., Reed, D.J., 2009. Understanding subsidence processes in coastal Louisiana. Journal of Coastal Research 54, 23-36.

Figure captions

Figure 1: (A) Situation map showing New Zealand's location in the South Pacific relative to Australia. (B) Map of locations in the southern North Island and South Island of New Zealand referred to in the text. (C) Detail map of the northern North Island showing locations referred to in the text.

Figure 2: Palaeo sea-level reconstructions for four regions of New Zealand. (A) Palaeo sea level index points for the northern North Island. (B) Palaeo sea level index points for the southwest North Island. (C) Palaeo sea level index points for Canterbury. (D) Palaeo sea level index points for

Otago. (E) Comparison of the time-windows for the timing of the attainment of PMSL in each of the four regions (NO, northern North Island; SW, southwest North Island; CA, Canterbury; OT, Otago). Grey bars delineate the proposed timing of the attainment of PMSL in each region, and are divided into possible time-window (light grey) and probable time-window (dark grey). GIA-modelled predictions of RSL change are shown for each region. Comparison of the GIA-modelled predictions is shown on Figure 3.

Figure 3: (A) GIA model predictions of Holocene RSL change (solid lines) for the northern North Island (Auckland), the southwestern North Island (Manawatu River mouth), Canterbury (Christchurch), and Otago (Dunedin). The components of RSL change are also shown for each site; predictions for the change in the height of the solid Earth and the sea-surface height are shown as dashed and dotted lines, respectively. (B) GIA model prediction of RSL change for Pounawea (Gehrels et al., 2012). (C) Map showing the bathymetric situation offshore of New Zealand, with locations of GIA-modelled predictions of RSL changes indicated.

Figure 4: Maps of GIA-model-predicted solid Earth deformation for the New Zealand region for 1000 year time slices from 8,000 years BP to 1,000 years BP. Values are given relative to present (e.g., a negative value indicates land was below present at that time), with the 0 m contour shown as a dashed line.

Figure 5: Comparison of clusters of sea-level index points from the four regional palaeo sea-level reconstructions of New Zealand (Figure 2). Clusters correspond to the analysis of the regional palaeo sea-level reconstructions presented in the Results, Sections 3.1.1-3.1.4.

Figure 6: Comparison of GIA-model predictions with RSL indicators for the northern North Island. (A) Map of the northern North Island showing locations from which palaeo sea-level index points were recovered. Indicators have been divided into 10 sub-groups; groupings are indicated by colour. GIA-model predictions have been produced for locations labelled in italic font. (B) GIA-

model-predicted solid Earth deformation for the 10 sub-groups shown in A. (C) GIA-model-predicted sea-surface height for the 10 sub-groups shown in A. Sea-surface height is very similar for all localities in the northern North Island. (D) GIA-model-predicted RSL change for the 10 sub-groupings shown in A. Refer to Supplementary Figure 1 for the relationship between solid Earth deformation, sea-surface height, and RSL. (E) GIA-model-predicted RSL change for Henderson Bay, compared with palaeo sea-level indicators from Henderson Bay, Matai Bay, and Tokerau Beach. (F) GIA-model-predicted RSL change compared with palaeo sea-level indicators from Matauri Bay. (G) GIA-model-predicted RSL change compared with palaeo sea-level indicators from Kaituna Bay. (H) GIA-model-predicted RSL change compared with palaeo sea-level indicators from Bream Bay. (I) GIA-model-predicted RSL change for Southern Kaitoke compared with palaeo sea-level indicators from Southern Kaitoke, Northern Kaitoke, and Awana. (J) GIA-model-predicted RSL change for Mahurangi Estuary compared with palaeo sea-level indicators from Mahurangi Estuary, Mangatawhiri Spit, Christian Bay, Puhoi River Estuary, and Weiti River Estuary. (K) GIA-model-predicted RSL change compared with palaeo sea-level indicators from Coromandel Harbour. (L) GIA-model-predicted RSL change for Okahu Bay compared with palaeo sea-level indicators from Okahu Bay, Waitamata Harbour, Tamaki Estuary, and Kelly’s Beach. (M) GIA-model-predicted RSL change compared with palaeo sea-level indicators from Whitianga Estuary. (N) GIA-model-predicted RSL change for Miranda compared with palaeo sea-level indicators from Miranda and Kaiaua.

Supplementary Figure 1: Conceptual diagram illustrating the relationship between RSL changes, the elevation of the solid Earth (E), and changes in sea-surface height (SSH). Sea-surface height and solid Earth elevation are both measured with respect to the centre of the Earth. At time t1 the surface of the solid Earth is at a-a'; the shoreline is at A(t1). In the time interval t1-t2 the Earth's surface is deformed, such that at t2 the surface of the solid Earth is at b-b', with the original shoreline displaced to A(t2). In the same time interval t1-t2 the ocean volume has increased, so that the sea-surface height has increased: the shoreline therefore lies at B(t2).

The observed change in relative sea level is the difference in elevation between A(t2) and B(t2), which is found by ΔRSL = ΔSSH – ΔE. In the case where an increase in sea-surface height in the interval t1-t2 is not accompanied by deformation of the solid Earth, the original shoreline A(t1) is displaced to C(t2) by a rise in RSL of magnitude ΔSSH. Conversely, uplift of the solid Earth of magnitude ΔE in the interval t1-t2 would result in a fall in RSL of magnitude ΔE and displacement of the original shoreline A(t1) to D(t2). After Lambeck et al. (2010), Shennan et al. (2012).

Supplementary Figure 2: Maps of GIA model-predicted RSL height for the New Zealand region for 1000 year time slices from 8,000 years BP to 1,000 years BP. Values are given relative to present (e.g., a positive value indicates that sea level was higher at that time), with the 0 m contour shown as a dashed line.

Supplementary Figure 3: Maps of the GIA model-predicted sea surface height for the New Zealand region for 1000 year time slices from 8,000 years BP to 1,000 years BP. Values are given relative to present (e.g., a positive value indicates that the sea-surface was higher at that time).

Table captions

Table 1: Details of 206 palaeo sea level index points from New Zealand. Indicator categories are as outlined in section 2.4: MX – maximum index point from beach ridge or shell bank; UE – unidentified estuarine shell; IE – identified estuarine shell; PT – peat; DW – deepwater/marine shell. Columns L, D, and B are sources of error, and are outlined in section 2.3: L is the accuracy of the measurement of the elevation of the indicator; D is the magnitude of the present-day living range of the dated indicator; B is the magnitude of the vertical range of the dated sample. Tectonic corrections are calculated using the rates of tectonic deformation presented in Table 4. The tectonic regime of each locality may be

cross-referenced with Table 4 using the quick-reference letters (A-L) in the 'tectonic regime' column.

Table 2: Summary of the ecological ranges of fossil shell species used as palaeo sea-level indicators.

Table 3: Tidal ranges for each of the sites throughout the New Zealand region from which palaeo sea-level indicators listed in Table 1 were recovered. Ranges from tide gauges are taken from the New Zealand Nautical Almanac unless otherwise indicated. Distance between the tidal gauge and the specific locality is indicated in the 'proximity' column. Where tidal range data is available for specific localities this has been used in favour of remote tidal gauges; this is indicated by a dash in the 'proximity' column.

Table 4: Summary of long-term and event tectonic deformation for localities and regions within the New Zealand archipelago from which the palaeo sea level indicators detailed in Table 1 were recovered. This table may be cross-referenced with Table 1 using the quick-reference letters (A-L) in the left-most column.

Table 1

Table 1: Details of 206 palaeo sea level index points from New Zealand. Indicator categories are as outlined in section 2.4: MX – maximum index point from beach ridge or shell bank; UE – unidentified estuarine shell; IE – identified estuarine shell; PT – peat; DW – deepwater/marine shell. Columns L, D, and B are sources of error, and are outlined in section 2.3: L is the accuracy of the measurement of the elevation of the indicator; D is the magnitude of the present-day living range of the dated indicator; B is the magnitude of the vertical range of the dated sample. Tectonic corrections are calculated using the rates of tectonic deformation presented in Table 4.

Source / Region	Locality	Tectonic regime (cf. Table 4)	Lat/long (Decimal degrees, WGS 1984)	Indicator	Indicator category	Radiocarbon laboratory code	Environment / Facies	Indicated RSL (m)	L (m)	D (m)	B (m)	Tectonic correction (m)	Tectonic correction error, V (m)	Corrected RSL (m)	Total vertical error (m)	Reported age (years BP)	Conventional radiocarbon age (^{14}C years)	Sidereal age range (cal yr BP)
Northern North Island																		
Abrahim et al 2008	Tamaki Estuary	A	-36.8852, 174.8805	*D. zealandica*	DW	WK7053	High energy marine	-2.65 [h]	0.30	0.88	0.10	0.00	0.00	-2.65	0.93	→	4060±110	3790-4430
	Tamaki Estuary	A	-36.8852, 174.8805	*M. roseus*	DW	WK7051	High energy marine	-3.49 [h]	0.30	0.88	0.10	0.00	0.00	-3.49	0.93	→	4670±200	4400-5450
	Tamaki Estuary	A	-36.8715, 174.8973	*A. stutchburyi*	IE	WK6372	Shallow, subtidal marine	-3.35 [h]	0.30	0.71	0.10	0.00	0.00	-3.35	0.78	→	7490±200	7580-8360
	Tamaki Estuary	A	-36.8969, 174.8746	*A. stutchburyi*	IE	WK7826	Shallow, subtidal marine	0.38 [h]	0.30	0.71	0.10	0.00	0.00	0.38	0.78	→	5830±160	5890-6620
	Tamaki Estuary	A	-36.8948, 174.8753	*A. stutchburyi*	IE	WK7827	Channel fill	0.58 [h]	0.30	0.71	0.10	0.00	0.00	0.58	0.78	→	2030±130	1300-1910
	Tamaki Estuary	A	-36.9068, 174.8684	*A. stutchburyi*	IE	WK7943	Shallow, subtidal marine	0.48 [h]	0.30	0.71	0.10	0.00	0.00	0.48	0.78	→	7350±130	7560-8100
	Tamaki Estuary	A	-36.9395, 174.8587	*A. stutchburyi*	IE	WK9557	Shallow, subtidal marine	-1.24 [h]	0.30	0.71	0.10	0.00	0.00	-1.24	0.78	→	6494±114	6710-7270
Brook 1999, Osborne et al 1991	Tokerau Beach	A	-34.9590, 173.3943	Shell	MX	NZ7291	Beach ridge	2.95 [h]	0.32	0.08	0.20	0.00	0.00	2.95	0.38	1030±60	1366±68	730-1100
Gibb & Aburn 1986	Pauanui Beach	B	-37.0247, 175.8711	Shell	UE	NZ6500	Beach	-0.48	0.10	0.45	0.10	-0.53 [s]	0.09	-1.01	0.48	1960±40	2295±35	1780-2080
	Pauanui Beach	B	-37.0247, 175.8711	Shell	UE	NZ6501	Nearshore	-4.18	0.10	0.45	0.10	-0.59 [s]	0.10	-4.77	0.48	2150±50	2491±35	2000-2310
	Pauanui Beach	B	-37.0247, 175.8711	Shell	UE	NZ6502	Nearshore	-5.98	0.10	0.45	0.10	-1.02 [s]	0.13	-7.00	0.49	3410±40	3747±27	3550-3840
	Pauanui Beach	B	-37.0247, 175.8711	Shell	UE	NZ6514	Nearshore	-7.18	0.10	0.45	0.10	-1.05 [s]	0.16	-8.23	0.50	3500±80	3837±65	3580-4020
	Pauanui Beach	B	-37.0263, 175.8681	Shell	UE	NZ6467	Beach	0.33	0.10	0.45	0.10	-1.24 [s]	0.17	-0.91	0.50	4010±70	4344±53	4290-4720
	Pauanui Beach	B	-37.0263, 175.8681	Shell	UE	NZ6521	Nearshore	-3.67	0.10	0.45	0.10	-1.23 [s]	0.17	-4.90	0.50	4220±70	4321±50	4250-4680
	Pauanui Beach	B	-37.0272, 175.8630	Shell	UE	NZ6522	Beach	-0.77	0.10	0.45	0.10	-1.55 [s]	0.18	-2.32	0.50	4920±50	5258±30	5490-5750
Gibb (1986)	Kaiaua	C	-37.1556, 175.2999	Shell	MX	NZ4427	Beach ridge	-0.28	0.24 [a]	-	-	0.00	0.00	-0.28	0.24	450±50	784±40	300-510
	Kaiaua	C	-37.1556, 175.2999	Shell	MX	NZ4426	Beach ridge	-0.17	0.24 [a]	-	-	0.00	0.00	-0.17	0.24	1130±50	1464±42	900-1170
	Kaiaua	C	-37.1556, 175.2999	Shell	MX	NZ4428	Beach ridge	0.59	0.24 [a]	-	-	0.00	0.00	0.59	0.24	1840±50	2179±43	1610-1930
	Kaiaua	C	-37.1556, 175.2999	Shell	MX	NZ4429	Beach ridge	-0.15	0.24 [a]	-	-	0.00	0.00	-0.15	0.24	2210±50	2549±44	2040-2350
	Kaiaua	C	-37.1556, 175.2988	Shell	MX	NZ4430	Beach ridge	0.33	0.24 [a]	-	-	0.00	0.00	0.33	0.24	3070±60	3406±52	3090-3450
	Kaiaua	C	-37.1556, 175.2966	Shell	MX	NZ4431	Beach ridge	0.83	0.24 [a]	-	-	0.00	0.00	0.83	0.24	3450±60	3786±48	3560-3910
	Kaiaua	C	-37.1557, 175.2954	Shell	MX	NZ4432	Beach ridge	0.61	0.24 [a]	-	-	0.00	0.00	0.61	0.24	3660±50	3998±38	3840-4190
	Kelly's Beach	A	-36.8852, 175.0229	*A. stutchburyi*	IE	NZ4425	Beach	0.76	0.24 [a]	-	-	0.00	0.00	0.76	0.24	4550±60	4888±52	4990-5420
	Kelly's Beach	A	-36.8826, 175.0172	*A. stutchburyi*	MX	NZ4423	Beach ridge	0.46	0.24 [a]	-	-	0.00	0.00	0.46	0.24	2170±60	2502±44	2010-2320
	Kelly's Beach	A	-36.8835, 175.0173	*A. stutchburyi*	MX	NZ4424	Beach ridge	-0.28	0.24 [a]	-	-	0.00	0.00	-0.28	0.24	2300±50	2640±45	2140-2540
	Miranda	C	-47.2923, 172.6197	M. ovata	IE	WK408	Upper tidal flat	0.77	0.70 [a]	-	-	0.00	0.00	0.77	0.70	→	1260±50	670-930
	Miranda	C	-47.2939, 172.5378	M. ovata	IE	WK341	Upper tidal flat	1.53	0.70 [a]	-	-	0.00	0.00	1.53	0.70	→	3650±60	3380-3770
	Miranda	C	-47.2545, 172.6119	M. ovata	IE	WK357	Upper tidal flat	0.38	0.70 [a]	-	-	0.00	0.00	0.38	0.70	→	4510±70	4470-4900
	Miranda	C	-47.2833, 172.6223	Shell	MX	NZ265	Chenier 6	-0.03	0.24 [a]	-	-	0.00	0.00	-0.03	0.24	980±60	1341±41	750-1030
	Miranda	C	-47.2842, 172.6171	Shell	MX	NZ267	Chenier 9	0.00	0.24 [a]	-	-	0.00	0.00	0.00	0.24	1540±60	1909±42	1320-1610
	Miranda	C	-47.2851, 172.6131	Shell	MX	NZ268	Chenier 10	0.49	0.24 [a]	-	-	0.00	0.00	0.49	0.24	1960±70	2352±43	1830-2140
	Miranda	C	-47.2860, 172.6065	Shell	MX	NZ270	Chenier 12	1.22	0.24 [a]	-	-	0.00	0.00	1.22	0.24	2730±70	3104±45	2740-3070
	Miranda	C	-47.2877, 172.5999	Shell	MX	NZ272	Chenier 13	2.16	0.24 [a]	-	-	0.00	0.00	2.16	0.24	3900±90	4274±48	4190-4580
	Weiti River Estuary	A	-36.6390, 174.7217	*A. stutchburyi*	IE	NZ6475	Upper tidal flat	0.97	0.80 [a]	-	-	0.00	0.00	0.97	0.80	3140±50	3482±31	3230-3520
	Weiti River Estuary	A	-36.6390, 174.7217	*A. stutchburyi*	IE	NZ6488	Upper tidal flat	0.97	0.80 [a]	-	-	0.00	0.00	0.97	0.80	3360±50	3701±37	3470-3800
	Weiti River Estuary	A	-44.0333, 173.1745	Shell	IE	NZ1970	Tidal flat	0.41	1.61 [a]	-	-	0.00	0.00	0.41	1.61	3970±60	4282±50	4210-4610
	Weiti River Estuary	A	-36.6435, 174.7218	Shell	IE	NZ6510	Upper tidal flat	1.32	0.80 [a]	-	-	0.00	0.00	1.32	0.80	4900±60	5241±41	5470-5740
	Weiti River Estuary	A	-36.6390, 174.7206	*A. stutchburyi*	IE	NZ6461	Upper tidal flat	1.38	0.80 [a]	-	-	0.00	0.00	1.38	0.80	5560±50	5896±34	6200-6440
	Weiti River Estuary	A	-44.0360, 173.1733	Shell	IE	NZ1968	Tidal flat	0.54	1.63 [a]	-	-	0.00	0.00	0.54	1.63	6260±70	6597±59	6940-7280
	Weiti River Estuary	A	-36.6434, 174.7274	Shell	MX	NZ6519	Chenier A	-0.46	0.24 [a]	-	-	0.00	0.00	-0.46	0.24	395±34	732±32	280-480
	Weiti River Estuary	A	-36.6444, 174.7241	Shell	MX	NZ6462	Beach ridge A/B	-0.23	0.22 [a]	-	-	0.00	0.00	-0.23	0.22	365±30	701±28	260-460
	Weiti River Estuary	A	-44.0378, 173.1758	Shell	MX	NZ1965	Chenier B	0.00	0.24 [a]	-	-	0.00	0.00	0.00	0.24	470±50	791±40	300-520
	Weiti River Estuary	A	-44.0360, 173.1770	Shell	MX	NZ1962	Chenier B	0.12	0.23 [a]	-	-	0.00	0.00	0.12	0.23	670±50	984±41	490-660
	Weiti River Estuary	A	-36.6435, 174.7229	Shell	MX	NZ6509	Beach ridge B/C1	0.03	0.23 [a]	-	-	0.00	0.00	0.03	0.23	1150±30	1486±27	920-1170
	Weiti River Estuary	A	-44.0360, 173.1733	Shell	MX	NZ1966	Chenier C	0.11	0.22 [a]	-	-	0.00	0.00	0.11	0.22	1020±50	1341±42	750-1030
	Weiti River Estuary	A	-44.0333, 173.1745	Shell	MX	NZ1770	Chenier D	0.39	0.22 [a]	-	-	0.00	0.00	0.39	0.22	1420±60	1703±61	1080-1410
	Weiti River Estuary	A	-36.6390, 174.7217	Shell	MX	NZ6487	Chenier E	-0.08	0.24 [a]	-	-	0.00	0.00	-0.08	0.24	1445±35	1783±29	1240-1470
	Weiti River Estuary	A	-36.6390, 174.7217	Shell	MX	NZ6493	Chenier E	-0.21	0.23 [a]	-	-	0.00	0.00	-0.21	0.23	1570±50	1907±42	1310-1610
	Weiti River Estuary	A	-44.0315, 173.1720	Shell	MX	NZ1971	Chenier F	0.31	0.22 [a]	-	-	0.00	0.00	0.31	0.22	3050±50	3371±47	3060-3400
	Weiti River Estuary	A	-36.6390, 174.7206	Shell	MX	NZ6479	Chenier F	0.47	0.24 [a]	-	-	0.00	0.00	0.47	0.24	3530±50	3866±38	3660-4010
Goff et al 2010	Kaituna Bay	A	-35.4304, 174.4298	*A. stutchburyi*	IE	WK19433	Estuary	-0.26	0.32	0.48	0.10	0.00	0.00	-0.26	0.58	→	6570±36	6950-7240
Grant-Taylor & Rafter 1971	Okahu Bay	A	-36.8503, 174.8184	Shell	UE	NZ441	Estuary	1.91	0.30	0.71	0.10	0.00	0.00	1.91	0.78	4205±67	4581±50	4580-4970
Heap & Nichol 1997	Weiti River Estuary	A	-36.6175, 174.7270	*A. stutchburyi* [a]	IE	WK3810	Transgressive open bay	-1.95	0.05	0.55	0.10	0.00	0.00	-1.95	0.56	→	7020±170	7190-7860
	Weiti River Estuary	A	-36.6349, 174.7213	*M. lilianna* [a]	IE	WK3812	Transgressive open bay	-2.45	0.05	0.55	0.10	0.00	0.00	-2.45	0.56	→	7440±120	7650-8170
	Weiti River Estuary	A	-36.6393, 174.7252	*A. stutchburyi* [a]	IE	WK3814	Transgressive open bay	-3.15	0.05	0.55	0.10	0.00	0.00	-3.15	0.56	→	7660±80	7950-8320
	Weiti River Estuary	A	-36.6393, 174.7252	*P. australis* [a]	IE	WK3813	Transgressive open bay	-0.80	0.05	0.8	0.10	0.00	0.00	-0.80	0.81	→	5880±150	5940-6640
Hicks and Nichol (2007)	Kowhai Beach	A	-34.7889, 173.1482	Peaty sand	PT	WK17125	Tidal wetland	-1.12 [g]	0.05	0.49	0.10	0.00	0.00	-1.12	0.50	→	6860±134	7440-7870
Horrocks et al 1999	Awana	A	-36.2071, 175.4740	Peat	PT	WK5561	Estuarine salt marsh	-2.77	0.05	0.55	0.10	0.00	0.00	-2.77	0.56	→	6050±80	6640-7030

Source / Region	Locality	Tectonic regime (cf. Table 4)	Lat/long (Decimal degrees, WGS 1984)	Indicator	Indicator category	Radiocarbon laboratory code	Environment / Facies	Indicated RSL (m)	L (m)	D (m)	B (m)	Tectonic correction (m)	Tectonic correction error, V (m)	Corrected RSL (m)	Total vertical error (m)	Reported age (years BP)	Conventional radiocarbon age (^{14}C years)	Sidereal age range (cal yr BP)
Horrocks et al 2000a	Northern Kaitoke	A	-36.2285, 175.4425	*M. ovata*	IE	WK5557	Tidal flat	-5.63	0.30	0.45	0.10	0.00	0.00	-5.63	0.55	→	6800±70	7160-7470
Horrocks et al 2000b	Southern Kaitoke	A	-36.2612, 175.4736	*M. liliana*	IE	WK7381	Tidal flat	-1.12	0.30	0.45	0.10	0.00	0.00	-1.12	0.55	→	4710±150	4550-5390
	Southern Kaitoke	A	-36.2612, 175.4736	*A. stutchburyi*	IE	WK6397	Tidal flat	-5.67	0.30	0.45	0.08	0.00	0.00	-5.67	0.55	→	6960±100	7260-7650
Hume & Dahm 1991	Coromandel Harbour	B	-36.7604, 175.4831	Shell	UE	WK1466	Tidal flat	0.32 (k)	1.00	0.58	0.10	-0.30 (s)	0.07	0.02	1.16	→	1505±60	920-1230
	Coromandel Harbour	B	-36.7604, 175.4831	Shell	UE	WK1376	Tidal flat	0.21 (k)	1.00	0.58	0.10	-1.42 (s)	0.20	-1.22	1.18	→	4869±80	4910-5430
	Coromandel Harbour	B	-36.7604, 175.4831	Shell	UE	WK1377	Tidal flat	0.09 (k)	1.00	0.58	0.10	-1.85 (s)	0.26	-1.77	1.19	→	6239±130	6380-7040
	Coromandel Harbour	B	-36.7659, 175.4755	Shell	UE	WK1467	Tidal flat	-2.82 (k)	1.00	0.58	0.10	-1.02 (s)	0.23	-3.84	1.18	→	3732±190	3210-4210
	Coromandel Harbour	B	-36.7935, 175.4921	Shell	UE	WK1468	Tidal flat	-0.73 (k)	1.00	0.58	0.10	-0.08 (s)	0.05	-0.81	1.16	→	632±50	110-450
	Coromandel Harbour	B	-36.7935, 175.4921	Shell	UE	WK1378	Tidal flat	-0.99 (k)	1.00	0.58	0.10	-0.17 (s)	0.05	-1.16	1.16	→	1020±60	490-720
	Coromandel Harbour	B	-36.7935, 175.4921	Shell	UE	WK1379	Tidal flat	-1.37 (k)	1.00	0.58	0.10	-0.27 (s)	0.09	-1.64	1.16	→	1409±100	730-1210
	Coromandel Harbour	B	-36.7935, 175.4921	Shell	UE	WK1380	Tidal flat	-1.70 (k)	1.00	0.58	0.10	-0.45 (s)	0.10	-2.15	1.16	→	2060±70	1430-1850
	Coromandel Harbour	B	-36.7935, 175.4921	Shell	UE	WK1381	Tidal flat	-2.02 (k)	1.00	0.58	0.10	-0.69 (s)	0.12	-2.71	1.16	→	2789±80	2320-2730
	Whangapoua Estuary	B	-36.7456, 175.6126	Shell	UE	WK1235	Tidal flat	0.43 (l)	0.85	0.43	0.10	-1.78 (s)	0.21	-1.36	0.98	→	6045±70	6290-6660
	Whangapoua Estuary	B	-36.7499, 175.6228	Shell	UE	WK1237	Tidal flat	0.43 (l)	0.85	0.43	0.10	-0.25 (s)	0.07	0.18	0.96	→	1351±65	720-1070
Hume & McGlone 1986	Waitamata Harbour	A	-36.7542, 174.6753	*A. stutchburyi*	IE	WK251	Tidal flat	-1.28 (g)	0.1	0.75	0.14	0.00	0.00	-1.28	0.77	→	5730±60	5950-6290
Hutcheon 2006	Mirada	C	-37.1590, 175.2887	Valve	UE	WK17479	Beach face	1.64	0.3	0.68	0.10	0.00	0.00	1.64	0.75	→	4786±51	4870-5270
	Tapora Flats	A	-36.3790, 174.2558	Valve	UE	WK17480	Sub-tidal	-0.96	0.3	0.83	0.10	0.00	0.00	-0.96	0.88	→	2449±93	1860-2340
Johnston 1984	Mahurangi Estuary	A	-36.4285, 174.6983	*A. stutchburyi*	IE	WK350	Estuarine shell bed	1.75 (i)	1.00	0.75	0.10	0.00	0.00	1.75	1.25	→	5640±80	5870-6260
	Mahurangi Estuary	A	-36.4707, 174.7307	*A. stutchburyi*	IE	WK401	Tidal flat	-0.66 (i)	1.00	0.75	0.10	0.00	0.00	-0.66	1.25	→	6940±40	7340-7560
Mather 2004	Christian Bay	A	-36.3720, 174.7985	*Volutidae spp*	DW	WK15131	Back-barrier	0.48	0.05	0.75	0.10	0.00	0.00	0.48	0.76	→	2070±39	1510-1810
	Christian Bay	A	-36.3720, 174.7985	*A. stutchburyi*	IE	WK15130	Back-barrier	-0.13	0.05	0.53	0.10	0.00	0.00	-0.13	0.54	→	6477±41	6830-7150
Millener 1981	Tokerau Beach	A	-34.9150, 173.3699	Shell	MX	NZ4614	Beach ridge	1.08	0.30	0.08	0.15	0.00	0.00	1.08	0.34	2970±50	3311±37	2990-3330
	Tokerau Beach	A	-34.9168, 173.3721	*Paphies spp.*	MX	NZ4726	Shell bank	0.90	0.30	0.08	0.30	0.00	0.00	0.90	0.43	636±43	973±40	490-660
	Tokerau Beach	A	-34.9168, 173.3721	*Paphies spp.*	MX	NZ4727	Shell bank	0.80	0.30	0.08	0.30	0.00	0.00	0.80	0.43	897±44	1233±28	680-900
	Tokerau Beach	A	-34.9105, 173.3687	Shell	MX	NZ5064	Beach ridge	-0.05	0.30	0.08	0.20	0.00	0.00	-0.05	0.37	2920±50	3257±36	2920-3270
	Tokerau Beach	A	-34.9195, 173.3699	Shell	MX	NZ4610	Beach ridge	1.08	0.30	0.08	0.15	0.00	0.00	1.08	0.34	4360±60	4692±40	4800-5140
	Tokerau Beach	A	-34.9195, 173.3699	Mixed shells	UE	NZ5063	Estuary	1.53	0.30	0.53	0.20	0.00	0.00	1.53	0.64	3170±80	3510±66	3210-3600
Nichol et al 2009	Tauhara	A	-36.3442, 174.1776	*A. stutchburyi* (a)	IE	WK9631	Tidal flat	0.16 (g)	0.14	0.83	0.10	0.00	0.00	0.16	0.84	→	3956±114	3630-4310
Osborne 1983	Bream Bay	A	-35.8723, 174.4647	Mixed shells	UE	GX3840	Estuary/open beach	-1.85	0.10	0.65	0.10	0.00	0.00	-1.85	0.67	→	1440±110	750-1250
	Bream Bay	A	-35.8723, 174.4647	Mixed shells	UE	GX4005	Estuary/open beach	-1.55	0.10	0.65	0.10	0.00	0.00	-1.55	0.67	→	1735±120	1010-1570
	Bream Bay	A	-35.8723, 174.4647	Mixed shells	UE	GX3701	Estuary/open beach	0.65	0.10	0.65	0.10	0.00	0.00	0.65	0.67	→	2080±150	1310-2020
	Bream Bay	A	-35.8504, 174.4808	Mixed shells	UE	NZ6376	Estuary/open beach	0.15	0.10	0.65	0.10	0.00	0.00	0.15	0.67	5750±140	3779±64	3520-3950
	Bream Bay	A	-35.8422, 174.4873	Mixed shells	UE	NZ6377	Low energy estuary	1.65	0.10	0.65	0.10	0.00	0.00	1.65	0.67	2330±50	2663±35	2180-2570
Osborne et al 1991	Matai Bay	A	-34.8291, 173.4107	Mixed shells	MX	NZ7658	Loisels Pumice	0.60 (g)	0.32	0.08	0.10	0.00	0.00	0.60	0.34	762±74	725±90	140-530
	Tokerau Beach	A	-34.9590, 173.3943	*P. subtriangulata*	MX	NZ7613	Shell bank	1.90 (g)	0.32	0.08	0.10	0.00	0.00	1.90	0.34	1441±34	1441±42	880-1160
	Tokerau Beach	A	-34.9590, 173.3943	*A. stutchburyi*	MX	NZ7560	Shell bank	1.57 (g)	0.32	0.08	0.10	0.00	0.00	1.57	0.34	1360±45	1373±50	760-1080
	Tokerau Beach	A	-34.9168, 173.3699	*P. subtriangulata*	MX	NZ7649	Loisels Pumice	3.21 (g)	0.32	0.08	0.10	0.00	0.00	3.21	0.34	1449±52	1450±69	830-1210
	Tokerau Beach	A	-34.9168, 173.3699	*P. subtriangulata*	MX	NZ7648	Loisels Pumice	4.00 (g)	0.32	0.08	0.10	0.00	0.00	4.00	0.34	2383±54	2186±74	1560-1990
Schofield 1973	Mangatawhiri Spit	A	-36.3531, 174.7904	Mixed shells	UE	NZ833	Estuary	2.23 (j)	0.36	0.63	0.10	0.00	0.00	2.23	0.73	6460±60	6768±60	7150-7430
	Matauri Bay	A	-35.0337, 173.9080	Mixed shells	MX	NZ731	Beach ridge	0.90	0.3	0.11	0.10	0.00	0.00	0.90	0.34	1990±63	2297±70	1710-2130
Swales et al 1997	Mahurangi Estuary	A	-36.4825, 174.7022	Shell	UE	(d)	Tidal flat	-3.02	0.32	0.75	0.10	0.00	0.00	-3.02	0.82	→	6735±302	6560-7830
	Mahurangi Estuary	A	-36.4364, 174.7122	Shell	UE	(d)	Tidal flat	-0.83	0.32	0.75	0.10	0.00	0.00	-0.83	0.82	→	1904±217	1000-1980
	Mahurangi Estuary	A	-36.4364, 174.7122	Shell	UE	(d)	Tidal flat	-2.56	0.32	0.75	0.10	0.00	0.00	-2.56	0.82	→	2549±168	1830-2690
	Mahurangi Estuary	A	-36.4223, 174.6884	Shell	UE	(d)	Tidal flat	-2.61	0.32	0.75	0.10	0.00	0.00	-2.61	0.82	→	1085±110	490-890
	Mahurangi Estuary	A	-36.4223, 174.6884	Shell	UE	(d)	Tidal flat	-4.45	0.32	0.75	0.10	0.00	0.00	-4.45	0.82	→	1031±100	450-820
	Mahurangi Estuary	A	-36.4089, 174.6825	Shell	UE	(d)	Tidal flat	-4.81	0.32	0.75	0.10	0.00	0.00	-4.81	0.82	→	7323±122	7550-8050
Woods 2011	Whitianga	B	-36.8422, 175.6833	*A. stutchburyi* (a)	IE	WK21713	Estuary	-0.45	0.60	0.41	0.10	-0.59 (s)	0.10	-1.04	0.74	→	2472±37	1980-2300
	Whitianga	B	-36.8422, 175.6833	*A. stutchburyi* (a)	IE	WK21714	Estuary	-1.03	0.60	0.41	0.10	-1.16 (s)	0.15	-2.19	0.75	→	4143±30	4070-4390
	Whitianga	B	-36.8422, 175.6833	*A. stutchburyi* (c)	IE	WK21715	Estuary	-2.95	0.60	0.41	0.10	-1.97 (s)	0.22	-4.92	0.76	→	6638±41	7000-7300
	Whitianga	B	-36.8458, 175.6928	*A. stutchburyi* (c)	IE	WK21856	Estuary	-1.10	0.60	0.6	0.10	-1.87 (s)	0.22	-2.97	0.88	→	6339±46	6650-6980
	Whitianga	B	-36.8458, 175.6928	*A. stutchburyi* (c)	IE	WK21857	Estuary	-2.05	0.60	0.6	0.10	-1.82 (s)	0.22	-3.87	0.88	→	6189±65	6440-6830
	Whitianga	B	-36.8458, 175.6928	*A. stutchburyi* (c)	IE	WK21716	Estuary	-4.07	0.60	0.6	0.10	-2.01 (s)	0.21	-6.08	0.88	→	6757±31	7180-7410
Wratt 1999	Puhoi River Estuary	A	-36.5310, 174.7071	*A. stutchburyi*	IE	WK7570	Tidal flat	-0.60	0.30	0.55	0.10	0.00	0.00	-0.60	0.63	→	7020±70	7380-7670
	Puhoi River Estuary	A	-36.5310, 174.7071	*A. stutchburyi*	IE	WK7571	Tidal channel	-0.61	0.30	0.55	0.10	0.00	0.00	-0.61	0.63	→	5300±170	5290-6090
Southwest North Island																		
Clark et al (2011)	Pauatahanui Inlet - Ration Point	F	-41.0964, 174.9109	*A. stutchburyi*	IE	NZA29687	Estuary	-0.77	0.10	0.33	0.10	0.00	0.00	-0.77	0.36	→	6547±45	6910-7230
	Pauatahanui Inlet - Ration Point	F	-41.0991, 174.9098	*A. stutchburyi*	IE	NZA30261	Estuary	-2.47	0.10	0.33	0.10	0.00	0.00	-2.47	0.36	→	7495±25	7850-8100
	Pauatahanui Inlet - Ration Point	F	-41.0964, 174.9109	Peat	PT	NZA29752	Estuary	-5.53	0.10	0.43	0.10	0.00	0.00	-5.53	0.45	→	7521±85	8150-8420
Clement (2011)	Manawatu valley	E	-40.5502, 175.3725	*A. stutchburyi*	IE	WK22171	Tidal flat	-1.58 (o)	0.05	0.55	0.04	0.00	0.00	-1.58	0.55	→	7605±105	7850-8320
	Manawatu valley	E	-40.5502, 175.3725	*A. stutchburyi*	IE	WK22172	Tidal flat	-2.99 (o)	0.05	0.55	0.04	0.00	0.00	-2.99	0.55	→	7850±140	7990-8630
	Manawatu valley	E	-40.5502, 175.3724	*A. stutchburyi*	IE	WK22173	Tidal flat	0.70 (o)	0.05	0.55	0.04	0.00	0.00	0.70	0.55	→	6335±125	6500-7140
	Manawatu valley	E	-40.5269, 175.3491	*A. stutchburyi* (a)	IE	WK26357	Tidal flat	-1.46 (o)	0.05	0.55	0.04	0.00	0.00	-1.46	0.55	→	5588±30	5880-6150

Source / Region	Locality	Tectonic regime (cf. Table 4)	Lat/long (Decimal degrees, WGS 1984)	Indicator	Indicator category	Radiocarbon laboratory code	Environment / Facies	Indicated RSL (m)	L (m)	D (m)	B (m)	Tectonic correction (m)	Tectonic correction error, V (m)	Corrected RSL (m)	Total vertical error (m)	Reported age (years BP)	Conventional radiocarbon age (^{14}C years)	Sidereal age range (cal yr BP)
Clement (2011)	Manawatu valley	E	-40.4935, 175.4241	*A. stutchburyi* [a]	IE	WK26360	Tidal flat	-0.87 [o]	0.05	0.55	0.04	0.00	0.00	-0.87	0.55	→	6260±30	6590-6870
	Manawatu valley	E	-40.4863, 175.4270	*A. stutchburyi* [c]	IE	WK26359	Tidal flat	-0.93 [o]	0.05	0.55	0.04	0.00	0.00	-0.93	0.55	→	6365±30	6700-6990
	Manawatu valley	E	-40.5233, 175.4122	*A. stutchburyi* [a]	IE	WK26361	Tidal flat	-1.17 [o]	0.05	0.55	0.04	0.00	0.00	-1.17	0.55	→	6733±30	7160-7390
	Manawatu valley	E	-40.5378, 175.3317	*A. stutchburyi* [a]	IE	WK26364	Tidal flat	-3.27 [o]	0.05	0.55	0.04	0.00	0.00	-3.27	0.55	→	5661±30	5930-6200
	Manawatu valley	E	-40.5431, 175.3185	*A. stutchburyi* [c]	IE	WK26358	Tidal flat	-3.55 [o]	0.05	0.55	0.04	0.00	0.00	-3.55	0.55	→	5343±30	5590-5860
	Manawatu valley	E	-40.5281, 175.3722	*A. stutchburyi* [a]	IE	WK26362	Tidal flat	-2.26 [o]	0.05	0.55	0.04	0.00	0.00	-2.26	0.55	→	5920±30	6240-6470
	Manawatu valley	E	-40.5068, 175.2839	*A. stutchburyi* [a]	IE	WK26363	Tidal flat	-3.13 [o]	0.05	0.55	0.04	0.00	0.00	-3.13	0.55	→	5320±30	5580-5840
	Manawatu valley	E	-40.5378, 175.3317	*A. stutchburyi* [a]	IE	WK28289	Tidal flat	-2.29 [o]	0.05	0.55	0.04	0.00	0.00	-2.29	0.55	→	5717±30	5990-6260
	Manawatu valley	E	-40.5233, 175.4122	*A. stutchburyi* [a]	IE	WK28299	Tidal flat	-0.39 [o]	0.05	0.55	0.04	0.00	0.00	-0.39	0.55	→	6385±32	6710-7020
Gibb (1986)	Kumenga	J	-41.3117, 175.2110	Shell	IE	NZ1634	Estuarine	0.30	0.73 [q]	-	-	-0.25	0.05	0.05	0.73	3470±50	3786±55	3550-3930
	Kumenga	J	-41.3117, 175.2110	Shell	IE	NZ1635	Estuarine	0.20	0.73 [q]	-	-	-0.25	0.05	-0.05	0.73	4120±50	4437±58	4430-4810
	Kumenga	J	-41.3117, 175.2110	*M. ovata*	IE	NZ3106	Estuarine	-0.05	0.73 [q]	-	-	-0.25	0.05	-0.30	0.73	4510±90	4827±77	4850-5330
	Kumenga	J	-41.3117, 175.2110	*M. ovata*	IE	NZ3107	Estuarine	-0.30	0.73 [q]	-	-	-0.25	0.05	-0.55	0.73	4600±60	4895±59	4990-5430
	Pauatahanui Inlet - Motukaraka Point	F	-40.7832, 174.5974	*A. stutchburyi*	IE	NZ3118	Upper tidal flat	2.23	0.50 [q]	-	-	0.00	0.00	2.23	0.50	6230±60	6566±41	6940-7240
	Pauatahanui Inlet - Taupo Swamp	G	-40.7746, 174.5663	*A. stutchburyi*	IE	NZ4866	Tidal flat	2.23	0.80 [q]	-	-	-1.68 [s]	0.49	0.55	0.94	3780±50	4121±32	4020-4380
Goff et al (2000)	Okupe Lagoon	I	-40.8278, 174.9515	*D. lambata*	DW	WK5699	Estuary	0.28 [g]	0.30	0.15	0.15	-2.25 [t]	0.75	-1.97	0.84	→	4780±150	4670-5460
	Okupe Lagoon	I	-40.8265, 174.9461	*D. lambata*	DW	WK6353	Estuary	0.84 [g]	0.30	0.15	0.07	-2.25 [t]	0.75	-1.41	0.82	→	3360±140	2840-3570
	Okupe Lagoon	I	-40.8265, 174.9461	*A. stutchburyi*	IE	WK6351	Estuary	0.36 [g]	0.30	0.33	0.05	-2.25 [t]	0.75	-1.90	0.87	→	4010±100	3740-4360
	Okupe Lagoon	I	-40.8265, 174.9461	*A. stutchburyi*	IE	WK6352	Estuary	0.10 [g]	0.30	0.33	0.13	-2.25 [t]	0.75	-2.16	0.88	→	4510±140	4290-5120
Hesp and Shepherd (1978)	Manawatu valley	D	-40.5497, 175.3923	*A. stutchburyi*	IE	NZ3085	Tidal flat	1.65	0.30	0.55	0.10	-0.21 [s]	0.21	1.44	0.67	6630±70	6475±45	6810-7150
MJ Shepherd (unpublished)	Manawatu valley	E	-40.4965, 175.2572	*A. stutchburyi* [a]	IE	NZ7911	Tidal flat	0.57	0.30	0.55	0.10	0.00	0.00	0.57	0.63	→	4525±43	4530-4860
Shepherd and Lees (1987)	Manawatu valley	E	-40.4591, 175.4140	*A. stutchburyi*	IE	NZ5218 (e)	Tidal flat	-5.05	0.30	0.55	0.10	0.00	0.00	-5.05	0.63	6280±220	6613±181	6700-7480
Swales et al (2005)	Karehana Bay	H	-41.0729, 174.8579	*A. stutchburyi*	IE	NZ7379	Tidal flat	0.63 [m]	0.30	0.33	0.20	-0.31 [s]	0.34	0.32	0.60	→	3290±78	2890-3360
	Pauatahanui Inlet	F	-41.1089, 174.9184	*A. stutchburyi*	IE	NZ7381	Tidal flat	0.18	0.30	0.33	0.10	0.00	0.00	0.18	0.46	→	6985±106	7270-7680
	Pauatahanui Inlet	F	-41.1089, 174.9184	*A. stutchburyi*	IE	NZ7383	Tidal flat	0.99 [n]	0.30	0.33	0.10	0.00	0.00	0.99	0.46	→	7058±107	7340-7780
	Pauatahanui Inlet	F	-41.0850, 174.8927	Shell [b]	UE	NZ7387	Tidal flat	0.48	0.30	0.33	0.30	0.00	0.00	0.48	0.54	→	5079±90	5210-5660
	Pauatahanui Inlet	F	-41.0850, 174.8927	Shell [b]	UE	NZ7393	Tidal flat	0.93	0.30	0.33	0.10	0.00	0.00	0.93	0.46	→	3285±78	2880-3350
	Pauatahanui Inlet	F	-41.0850, 174.8927	Shell [b]	UE	NZ7421	Tidal flat	0.93	0.30	0.33	0.10	0.00	0.00	0.93	0.46	→	3487±88	3130-3630
Canterbury																		
Gibb (1986)	Christchurch	K	-43.4466, 172.9467	Shell	IE	NZ1816	Estuarine	0.84	2.03 [q]	-	-	1.32 [s]	0.70	2.16	2.15	5830±90	6151±59	6410-6770
	Christchurch	K	-43.4784, 172.6056	Shell	IE	NZ4711	Estuarine	-5.47	2.47 [q]	-	-	1.49 [s]	0.79	-3.98	2.59	6600±140	6936±130	7180-7680
	Christchurch	K	-43.2117, 172.9174	Shell	IE	NZ117	Estuarine	-5.47	3.05 [q]	-	-	1.44 [s]	0.76	-4.03	3.14	6750±90	6679±58	7030-7380
	Christchurch	K	-43.2126, 172.9186	Shell	IE	NZ1245	Estuarine	-9.47	2.83 [q]	-	-	1.62 [s]	0.87	-7.85	2.96	7350±130	7655±144	7820-8420
	Christchurch	K	-43.2513, 172.9112	Shell	IE	NZ1244	Estuarine	-11.47	2.83 [q]	-	-	1.63 [s]	0.87	-9.84	2.96	7370±110	7678±140	7850-8430
	Christchurch	K	-43.5588, 172.7065	Shell	IE	NZ4851	Estuarine	-9.07	2.24 [q]	-	-	1.65 [s]	0.87	-7.42	2.40	7470±120	7777±97	8000-8450
	Christchurch	K	-43.1397, 172.9482	Shell	IE	NZ4045	Beach	-9.87	2.83 [q]	-	-	1.66 [s]	0.89	-8.21	2.97	7490±150	7823±143	7960-8600
	Christchurch	K	-43.4286, 172.9430	*A. stutchburyi*	IE	NZ1817	Estuarine	-15.67	2.26 [q]	-	-	1.68 [s]	0.88	-13.99	2.43	7670±110	7939±84	8190-8610
	Christchurch	K	-43.4322, 172.9282	Shell	IE	NZ691	Estuarine	-15.17	2.29 [q]	-	-	1.73 [s]	0.91	-13.44	2.46	7820±70	8129±48	8430-8860
	Christchurch	K	-43.5362, 172.6893	Shell	IE	NZ4524	Estuarine	-18.47	2.43 [q]	-	-	1.76 [s]	0.93	-16.71	2.60	7940±90	8274±73	8570-9040
	Christchurch	K	-43.4632, 172.6576	Shell	IE	NZ4712	Estuarine	-12.77	2.24 [q]	-	-	1.79 [s]	0.98	-10.98	2.44	8030±170	8367±149	8550-9370
	Christchurch	K	-43.4903, 172.6982	Shell	IE	NZ4319	Estuarine	-15.77	2.24 [q]	-	-	1.82 [s]	0.99	-13.95	2.45	8180±70	8514±163	8670-9510
	Christchurch	K	-43.4903, 172.6982	*A. stutchburyi*	IE	NZ4318	Estuarine	-26.47	2.24 [q]	-	-	1.85 [s]	0.96	-24.62	2.44	8280±70	8617±51	9090-9450
	Christchurch	K	-43.4993, 172.6808	Shell	IE	NZ4713	Estuarine	-23.57	2.9 [q]	-	-	1.88 [s]	1.03	-21.69	3.08	8410±70	8744±154	9000-9840
	Christchurch	K	-43.3746, 172.9653	Shell	IE	NZ276	Beach	-25.97	2.24 [q]	-	-	1.92 [s]	1.00	-24.05	2.45	8530±100	8872±66	9390-9780
	Christchurch	K	-43.4286, 172.9430	Peat	PT	NZ1819	Estuarine	-25.1	1.25 [q]	-	-	2.05 [s]	1.09	-23.05	1.66	9180±140	9173±118	9910-10590
	Christchurch	K	-43.5362, 172.6893	Peat	PT	NZ4485	Estuarine	-29.20	1.14 [q]	-	-	2.17 [s]	1.15	-27.03	1.62	9520±140	9518±116	10480-11170
	Christchurch	K	-43.5210, 172.7055	Peat	PT	NZ5158	Estuarine	-32.60	2.37 [q]	-	-	2.21 [s]	1.18	-30.39	2.65	9850±140	9796±118	10700-11410
Shulmeister and Kirk (1993)	Pegasus Bay	K	-43.2528, 172.7166	*P. australis*	IE	NZA2546	Transgressive barrier	-10.40 [h]	0.32	0.69	0.10	1.74 [s]	0.92	-8.66	1.20	→	8150±94	8420-8960
	Pegasus Bay	K	-43.2528, 172.7166	Shell	UE	NZ7955	Marine sand	-2.52 [h]	0.32	0.54	0.10	0.84 [s]	0.47	-1.68	0.79	→	4138±71	3960-4430
Shulmeister and Kirk (1997)	Pegasus Bay	K	-43.2528, 172.7166	*M. discors*	DW	NZA2607	Beach/nearshore	2.35 [h]	0.32	0.69	0.10	0.33 [s]	0.21	2.68	0.79	→	2090±80	1450-1890
	Pegasus Bay	K	-43.2528, 172.7166	Shell	MX	NZ7953	Beach ridge	0.88 [h]	0.32	0.1	0.10	0.31 [s]	0.19	1.19	0.39	→	1958±70	1330-1720
	Pegasus Bay	K	-43.2528, 172.7166	Shell	UE	NZ7956	Beach/nearshore	-2.37 [h]	0.32	0.54	0.10	0.52 [s]	0.31	-1.85	0.70	→	2895±88	2360-2860
	Pegasus Bay	K	-43.2528, 172.7166	Shell	UE	NZA2606	Beach/nearshore	-1.82 [h]	0.32	0.54	0.10	0.76 [s]	0.43	-1.06	0.76	→	3810±83	3530-4040
Soons et al (1997)	Kaitorete Barrier	K	-43.7954, 172.6930	*P. australis*	MX	NZA3791	Barrier	3.73	0.25	0.1	0.10	0.03 [s]	0.05	3.76	0.29	→	561±57	0-330
	Kaitorete Barrier	K	-43.8089, 172.6854	*P. australis*	MX	NZA3751	Barrier	2.93	0.25	0.1	0.10	0.08 [s]	0.06	3.01	0.29	→	775±48	290-510
	Kaitorete Barrier	K	-43.8346, 172.5448	Shell	UE	NZ7929 [g]	Not reported	-35.55	0.25	0.54	0.10	2.07 [s]	1.07	-33.48	1.23	→	9483±59	10200-10510
	Kaitorete Barrier	K	-43.8346, 172.5448	Shell	UE	NZ7928	Not reported	-26.55	0.25	0.54	0.10	1.84 [s]	0.95	-24.71	1.12	→	8530±43	9010-9360
	Kaitorete Barrier	K	-43.8346, 172.5448	Shell	UE	NZ7927	Not reported	-18.55	0.25	0.54	0.10	1.69 [s]	0.87	-16.86	1.06	→	7990±50	8330-8600
Stephenson and Shulmeister (1999)	Okains Bay	K	-43.7072, 173.0446	Shell	MX	NZA6074	Beach ridge	0.93	0.53	0.1	0.10	0.24 [s]	0.16	1.17	0.58	→	1674±76	1030-1410
	Okains Bay	K	-43.6969, 173.0585	Shell	MX	NZA3750	Base of dune	0.93	0.53	0.1	0.10	0.06 [s]	0.07	0.99	0.56	→	672±63	140-480

Source / Region	Locality	Tectonic regime (cf. Table 4)	Lat/long (Decimal degrees, WGS 1984)	Indicator	Indicator category	Radiocarbon laboratory code	Environment / Facies	Indicated RSL (m)	L (m)	D (m)	B (m)	Tectonic correction (m)	Tectonic correction error, V (m)	Corrected RSL (m)	Total vertical error (m)	Reported age (years BP)	Conventional radiocarbon age (^{14}C years)	Sidereal age range (cal yr BP)
East Otago																		
Ensor (1986)	Blueskin Bay	L	-45.7380, 170.5784	*A. stutchburyi*	IE	NZ6853	Estuary	0.05 [g]	0.32	0.53	0.05	0.00	0.00	0.05	0.61	4010±20	3925±72	3680-4150
	Blueskin Bay	L	-45.7242, 170.5754	*A. stutchburyi*	IE	NZ6866	Estuary	-0.46 [g]	0.32	0.53	0.05	0.00	0.00	-0.46	0.61	5880±230	5316±142	5320-6000
	Blueskin Bay	L	-45.7242, 170.5754	*A. stutchburyi*	IE	NZ6867	Estuary	-0.91 [g]	0.32	0.53	0.05	0.00	0.00	-0.91	0.61	3760±430	3728±331	2840-4540
	Blueskin Bay	L	-45.7177, 170.5795	Peat	PT	NZ6953	Deltaic channel	-0.74 [g]	0.32	0.61	0.05	0.00	0.00	-0.74	0.68	2850±150	1907±352	1170-2620
	Blueskin Bay	L	-45.7177, 170.5795	Peat	PT	NZ6952	Deltaic channel	-0.89 [g]	0.32	0.61	0.10	0.00	0.00	-0.89	0.69	2410±510	2661±137	2340-3010
Gibb (1986)	Blueskin Bay	L	-45.7126, 170.5895	*P. subtriangulata*	IE	NZ5270	Beach	0.00	0.50 [q]	-	-	0.00	0.00	0.00	0.50	413±30	751±28	290-490
	Blueskin Bay	L	-45.7153, 170.5893	*A. stutchburyi*	IE	NZ6485	Tidal flat	0.55	0.90 [q]	-	-	0.00	0.00	0.55	0.90	907±62	1243±59	660-930
	Blueskin Bay	L	-45.7675, 170.5885	*A. stutchburyi*	IE	NZ1973	Tidal flat	0.03	0.90 [q]	-	-	0.00	0.00	0.03	0.90	1970±50	2290±44	1750-2090
	Blueskin Bay	L	-45.7154, 170.5945	*P. subtriangulata*	IE	NZ5269	Beach	0.00	0.50 [q]	-	-	0.00	0.00	0.00	0.50	2250±50	2591±35	2120-2420
	Blueskin Bay	L	-45.7639, 170.5899	*A. stutchburyi*	IE	NZ1975	Tidal flat	0.53	0.90 [q]	-	-	0.00	0.00	0.53	0.90	3240±60	3556±47	3320-3620
	Blueskin Bay	L	-45.7675, 170.5885	*M. liliana*	IE	NZ1974	Tidal flat	0.03	0.90 [q]	-	-	0.00	0.00	0.03	0.90	3440±60	3754±48	3520-3880
	Blueskin Bay	L	-45.7694, 170.5961	*P. subtriangulata*	IE	NZ1978	Tidal flat	0.2	0.90 [q]	-	-	0.00	0.00	0.20	0.90	5600±70	5913±56	6190-6490
	Blueskin Bay	L	-45.7694, 170.5961	*A. stutchburyi*	IE	NZ1977	Tidal flat	0.73	0.90 [q]	-	-	0.00	0.00	0.73	0.90	6000±70	6338±57	6630-7000
	Blueskin Bay	L	-45.7135, 170.5907	Shell	IE	NZ6484	Upper tidal flat	-0.97	0.50 [q]	-	-	0.00	0.00	-0.97	0.50	6750±150	7084±117	7360-7830
	Blueskin Bay	L	-45.7685, 170.5949	Shell	MX	NZ1976	Beach ridge	0.30	0.50 [q]	-	-	0.00	0.00	0.30	0.50	5640±70	5956±56	6240-6560
Rayns (1985)	Hoopers Inlet	L	-45.8541, 170.6633	*A. stutchburyi*	IE	NZ6634	Estuary	-0.97 [p]	0.50	0.15	0.10	0.00	0.00	-0.97	0.53	3530±80	3565±37	3340-3610
	Hoopers Inlet	L	-45.8681, 170.6649	*A. stutchburyi*	IE	NZ6635	Estuary	-0.67 [p]	0.50	0.15	0.10	0.00	0.00	-0.67	0.53	1645±35	1936±29	1350-1630
	Hoopers Inlet	L	-45.8668, 170.6648	*A. stutchburyi*	IE	NZ6750	Estuary	-0.72 [p]	0.50	0.15	0.10	0.00	0.00	-0.72	0.53	1250±65	1571±58	970-1270
	Hoopers Inlet	L	-45.8668, 170.6648	*A. stutchburyi*	IE	NZ6783	Estuary	-0.72 [p]	0.50	0.15	0.10	0.00	0.00	-0.72	0.53	1105±40	1404±33	820-1100
	Hoopers Inlet	L	-45.8668, 170.6648	*A. stutchburyi*	IE	NZ6780	Estuary	-0.72 [p]	0.50	0.15	0.10	0.00	0.00	-0.72	0.53	1450±35	1745±34	1170-1420
	Hoopers Inlet	L	-45.8603, 170.6830	*A. stutchburyi*	IE	NZ6638	Estuary	-0.77 [p]	0.50	0.15	0.08	0.00	0.00	-0.77	0.53	2970±70	3122±36	2760-3070
	Papanui Inlet	L	-45.8505, 170.7025	*A. stutchburyi*	IE	NZ6637	Estuary	-0.81 [p]	0.53	0.39	0.15	0.00	0.00	-0.81	0.67	6020±70	5499±41	5720-6050
	Papanui Inlet	L	-45.8431, 170.6875	*A. stutchburyi*	IE	NZ6636	Estuary	0.14 [p]	0.53	0.39	0.04	0.00	0.00	0.14	0.66	3780±60	3777±37	3570-3880
	Papanui Inlet	L	-45.8416, 170.7045	*A. stutchburyi*	IE	NZ6775	Estuary	0.04 [p]	0.53	0.39	0.10	0.00	0.00	0.04	0.66	505±63	827±58	300-570
	Papanui Inlet	L	-45.8416, 170.7045	*A. stutchburyi*	IE	NZ6749	Estuary	0.04 [p]	0.53	0.39	0.10	0.00	0.00	0.04	0.66	945±62	1272±57	670-960
	Papanui Inlet	L	-45.8416, 170.7045	*A. stutchburyi*	IE	NZ6786	Estuary	0.04 [p]	0.53	0.39	0.10	0.00	0.00	0.04	0.66	683±59	1000±55	490-690
	Papanui Inlet	L	-45.8416, 170.7045	*A. stutchburyi*	IE	NZ6789	Estuary	0.04 [p]	0.53	0.39	0.10	0.00	0.00	0.04	0.66	673±36	990±33	500-660
Thomas (2000)	Blueskin Bay	L	-45.7207, 170.5917	*A. stutchburyi* [a]	IE	NZ3547	Estuary	-0.43 [r]	0.30	0.53	0.10	0.00	0.00	-0.43	0.61	4400±140	4572±30	4620-4940

Footnotes:

a Articulated.

b Estuarine.

c Disarticulated.

d Not reported. Dated by Waikato Radiocarbon Laboratory.

e Given incorrectly in source as NZ5128.

f Given incorrectly in source as NZ7994.

g Inferred from log given in source.

h Inferred from fence diagram given in source.

i Elevation converted from chart datum (Chart NZ5321) to mean sea-level.

j Elevation converted from mean high tide to mean sea-level using tides for Whangateau Harbour.

k Elevation converted from mean high tide to mean sea-level using tides for Coromandel Harbour.

l Elevation is given as "above mean low water springs". L is therefore spring tidal range.

m Gibb and Cox (2009) give the elevation of this index point as +0.96 m.

n Gibb and Cox (2009) give the elevation of this index point as -0.66 m.

o RTK-dGPS determination. Elevation relative to WVD1953.

p Inferred from bathymetry with 1 m depth intervals given in source.

q Includes vertical error components D and B (see Gibb, 1986).

r Includes vertical error components D and B (see Gibb, 1986; Thomas, 2000).

s Based on a long-term rate of tectonic deformation. See Table 4 for details for tectonic deformation rates.

t Event tectonic deformation. See Table 4 for details for tectonic deformation rates.

Table 2

Table 2: Summary of the ecological ranges of fossil shell species used as palaeo sea level indicators.

Indicator / species	Habitat / formation summary	Vertical range (upper to lower)	Sources
A. stutchburyi	Sheltered, intertidal lower foreshore	MSL to MLWS	Gibb (1979); Wilson et al. (2007b)
M. liliana	Sheltered, intertidal lower foreshore	MSL to MLWS	Morton and Miller (1986); Nipper and Roper (1995); Hogg et al. (1998); Thrush et al. (1999); Norkko et al. (2001); Grant and Hay 2003; Cummings and Thrush (2004); Lelieveld et al. (2004); Lundquist et al. (2004)
M. ovata	Sheltered, intertidal lower foreshore	MSL to MLWS	Morton and Miller (1968); Powell (1979); Leach and Anderson (1974)
P. australis	Sheltered, intertidal, sometimes subtidal	MHWN to MLWN	Powell (1979); Carroll and Wells (1995); Hogg et al. (1998); Cummings and Thrush (2004)
P. subtriangulata	Beachface, intertidal	MHWN to MLWN	Powell (1979); Pillans and Huber (1995); Herzer (1981); Carter et al. (1986)
Unidentified estuarine shell	Sheltered, intertidal lower foreshore	MSL to MLWS	As for A. stutchburyi and M. ovata, as these account for 90 per cent of identified species (cf. Gibb, 1986)
D. zealandica	Shallow water down to 130 m depth	MLWS to -130 m	Morton and Miller (1968); Powell (1979); Brook and Grace (1981); Beu and Kitamura(1998); Hayward et al. (2001); Abrahim (2005)
M. roseus	Low tide level down to 200 m depth	MLWS to -200 m	Powell (1979); Allmon et al. (1994); Bax et al. (2003); Probst and Crawford (2008)
Volutidae spp.	Spring tidal flat to beyond low water	MSL to LAT	Powell (1979); Beu and Maxwell (1990)
D. lambata	Depths of 1-50 m	MLWS to -50 m	Estcourt (1967); McKnight (1969); Brook and Grace (1981); Powell (1979)
M. discors	From 3-7 below lowest astronomical tide (LAT)	-3 m LAT to -7 m LAT	Powell (1979); Cranfield et al. (1994); Haddon et al. (1996); Cranfield and Michael (2001a, b)
Unidentified deepwater shell	Tidal flat to mid shelf	MLWS to mid shelf	-
Peat	Intertidal, upper foreshore	HAT - MTL	Barlow et al. (2013)

Table 3

Table 3: Tidal ranges for each of the sites throughout the New Zealand region from which palaeo sea-level indicators listed in Table 1 were recovered. Tide gauge levels are taken from the New Zealand Nautical Almanac unless otherwise indicated.

Locality	Tide data source	Mean spring tidal range (m)	Mean neap tidal range (m)	Proximity of tide data source to locality (km)
Awana	Typhena tidal gauge	1.80	1.30	7
Blueskin Bay Estuary	Ensor (1986)	2.10	1.00	--
Bream Bay	Nichol (2002)	2.60	1.10	13
Christian Bay	Mansion House Bay tidal gauge	2.10	1.50	6
Coromandel Harbour	Coromandel Harbour tidal gauge	2.30	1.70	--
Firth of Thames	Thames (Rocky Point) tidal gauge	2.70	2.10	--
Hoopers Inlet	Albrect and Vennell (2007)	0.60	0.34	--
Kaitorete Barrier	Lyttelton tidal gauge	2.14	1.38	28
Kaituna Bay	Russell tidal gauge	2.10	1.20	32
Karehana Bay	Gibb and Cox (2009)	1.32	0.22	--
Kowhai Beach	Hicks and Nichol (2007)	1.80	1.20	--
Mahurangi Estuary	Oldman et al. (2003)	3.00	2.00	--
Manawatu	Manawatu River Entrance tidal gauge	2.20	0.90	--
Mangatawhiri Spit	Whangateau Harbour tidal gauge	2.50	1.70	8
Matai Bay	Rangaunu Harbour tidal gauge	2.10	1.50	12
Matauri Bay	Russell tidal gauge	2.10	1.20	27
Mirada	Thames (Rocky Point) tidal gauge	2.70	2.10	--
Northern Kaitoke	Typhena tidal gauge	1.80	1.30	7
Okahu Bay	Auckland tidal gauge	2.84	1.76	8
Okupe Lagoon	Waiorua Bay (Kapiti Island) tidal gauge	1.30	0.30	1
Papanui Inlet	Albrect and Vennell (2007)	1.56	0.86	--
Pauanui Beach	Tairua tidal gauge	1.80	1.20	--
Pauatahanui Inlet	Gibb and Cox (2009)	1.32	0.24	--
Pegasus Bay	Lyttelton tidal gauge	2.14	1.38	45
Puhoi River Estuary	Weiti River Mouth tidal gauge	2.20	1.60	13
Southern Kaitoke	Typhena tidal gauge	1.80	1.30	7
Tamaki Estuary	Auckland tidal gauge	2.84	1.76	8
Tapora Flats	Tinopai tidal gauge	3.30	1.70	14
Tauhara	Tinopai tidal gauge	3.30	1.70	11
Tokerau Beach	Rangaunu Harbour tidal gauge	2.10	1.50	4
Waitamata Harbour	Hume and McGlone (1986)	3.00	2.00	--
Weiti River Estuary	Weiti River Mouth tidal gauge	2.20	1.60	--
Whangapoua Estuary	Thrush et al. (2000)	1.70	1.30	--
Whitianga	Woods (2011)	1.60	1.20	--

Table 4

Table 4: Summary of long-term and event tectonic deformation for localities and regions within the New Zealand archipelago from which the palaeo sea level indicators detailed in Table 1 were recovered.

	Area / Site	Region	Analysis of tectonic regime	Range of suggested tectonic deformation rates	Adopted tectonic deformation rate and error	Principal sources
A	Northland / Auckland	Northern North Island	Stable	-	-	Clement (2011); Beavan and Litchfield (2012); and many references therein
B	Coromandel Peninsula	Northern North Island	Long-term uplift	0.25-0.30 mm yr^{-1}	0.275 ± 0.025 mm yr^{-1}	Pillans (1986); Abrahamson (1987); Clement (2011); Beavan and Litchfield (2012)
C	Miranda / Kaiaua	Northern North Island	Stable	-	-	Schofield (1960); Woodroffe et al. (1983); Clement (2011)
D	Manawatu, sites proximal to MIS 5e marine terrace	Southwest North Island	Long-term uplift	0-0.06 mm yr^{-1}	0.03 ± 0.03 mm yr^{-1}	Hesp and Shepherd (1978); Clement (2011)
E	Manawatu, sites distal from MIS5e marine terrace	Southwest North Island	Stable	-	-	Pillans (1986); Williams (1991); Clement (2011)
F	Pauatahanui Inlet (east)	Southwest North Island	Stable	-	-	Healy (1980); Wynne (1981); Eiby (1990); Gibb and Cox (2009)
G	Taupo Swamp	Southwest North Island	Long-term uplift	0.3-0.5 mm yr^{-1}	0.4 ± 0.1 mm yr^{-1}	Swales et al. (2005); Gibb and Cox (2009)
H	Karahana Bay	Southwest North Island	Long-term uplift	0-0.2 mm yr^{-1}	0.1 ± 0.1 mm yr^{-1}	Healy (1980); Wynne (1981); Eiby (1990); Gibb and Cox (2009)
I	Okupe Lagoon	Southwest North Island	Event uplift	1.5-3.0 m in an earthquake c. 3300 cal yr BP	2.25 ± 0.75 m	Goff et al. (2000)
J	Kumenga	Southwest North Island	Event uplift	0.2-0.3 m in AD1855 earthquake	0.25 ± 0.05 m	Leach and Anderson (1974); Grapes and Downes (1997); Clement (2011); Beavan and Litchfield (2012)
K	Canterbury	Canterbury	Subsidence	-0.1 - -0.3 mm yr^{-1}	-0.2 ± 0.1 mm yr^{-1}	Lensen (1975); Wellman (1979); Lambeck et al. (2002); Clement (2011); Beavan and Litchfield (2012)
L	Otago	Otago	Stable	-	-	Clement (2011); Beavan and Litchfield (2012); and many references therein

Figure 1

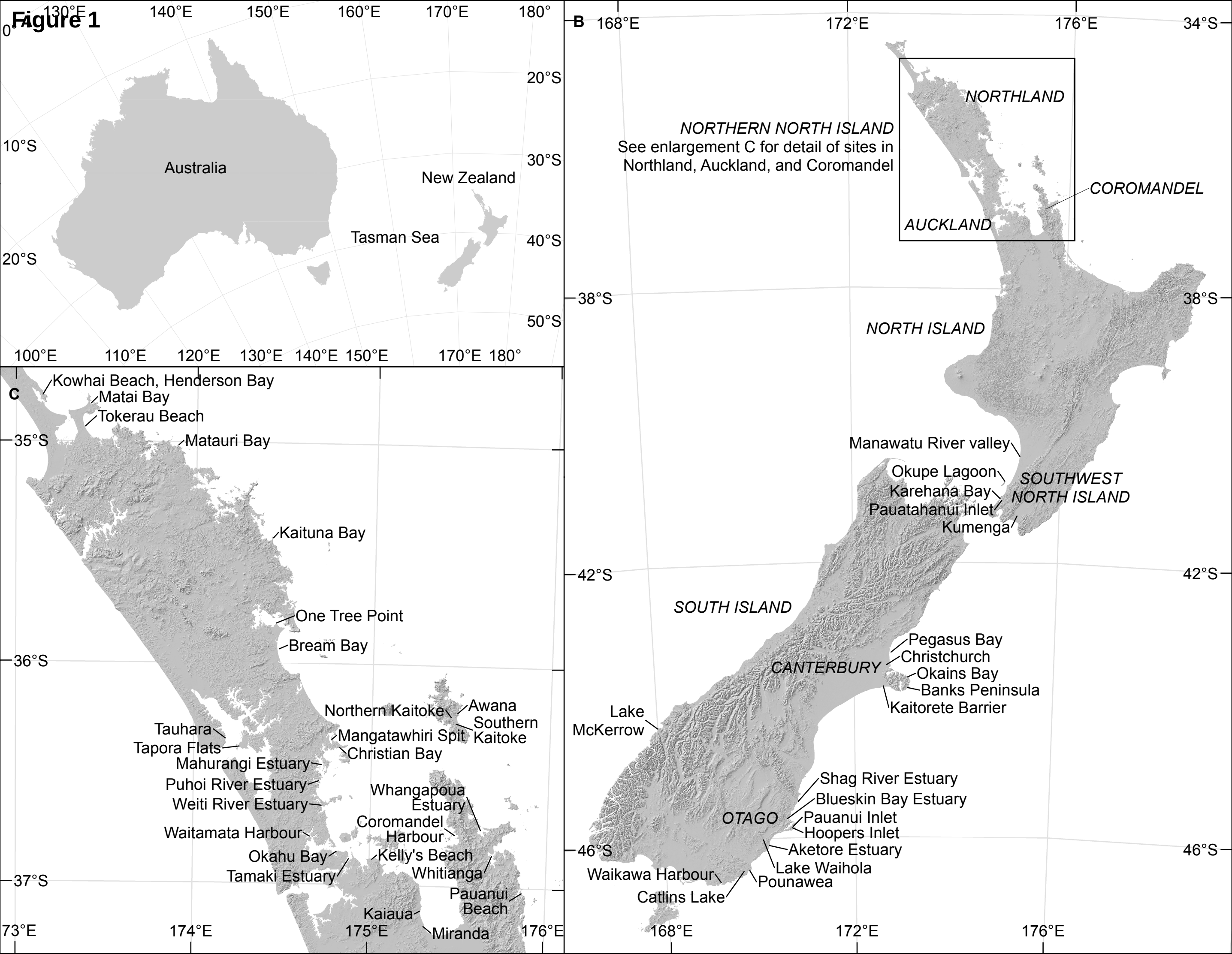
A
130°E
140°E
150°E
160°E
170°E
180°
0°
10°S
20°S
20°S
30°S
40°S
50°S
Australia
New Zealand
Tasman Sea
100°E
110°E
120°E
130°E
140°E
150°E
170°E
180°
B
168°E
172°E
176°E
34°S
38°S
38°S
42°S
42°S
46°S
46°S
NORTHLAND
NORTHERN NORTH ISLAND
See enlargement C for detail of sites in
Northland, Auckland, and Coromandel
COROMANDEL
AUCKLAND
NORTH ISLAND
Manawatu River valley
Okupe Lagoon
SOUTHWEST
NORTH ISLAND
Karehana Bay
Pauatahanui Inlet
Kumenga
SOUTH ISLAND
Pegasus Bay
Christchurch
CANTERBURY
Okains Bay
Banks Peninsula
Kaitorete Barrier
Lake
McKerrow
Shag River Estuary
Blueskin Bay Estuary
OTAGO
Pauanui Inlet
Hoopers Inlet
Aketore Estuary
Lake Waihola
Waikawa Harbour
Pounawea
Catlins Lake
168°E
172°E
176°E
C
Kowhai Beach, Henderson Bay
Matai Bay
Tokerau Beach
35°S
Matauri Bay
Kaituna Bay
One Tree Point
Bream Bay
36°S
Northern Kaitoke
Awana
Southern
Kaitoke
Tauhara
Mangatawhiri Spit
Tapora Flats
Christian Bay
Mahurangi Estuary
Puhoi River Estuary
Whangapoua
Estuary
Weiti River Estuary
Coromandel
Harbour
Waitamata Harbour
Okahu Bay
Kelly's Beach
Tamaki Estuary
Whitianga
37°S
Pauanui
Beach
Kaiaua
Miranda
73°E
174°E
175°E
176°E

Figure 2

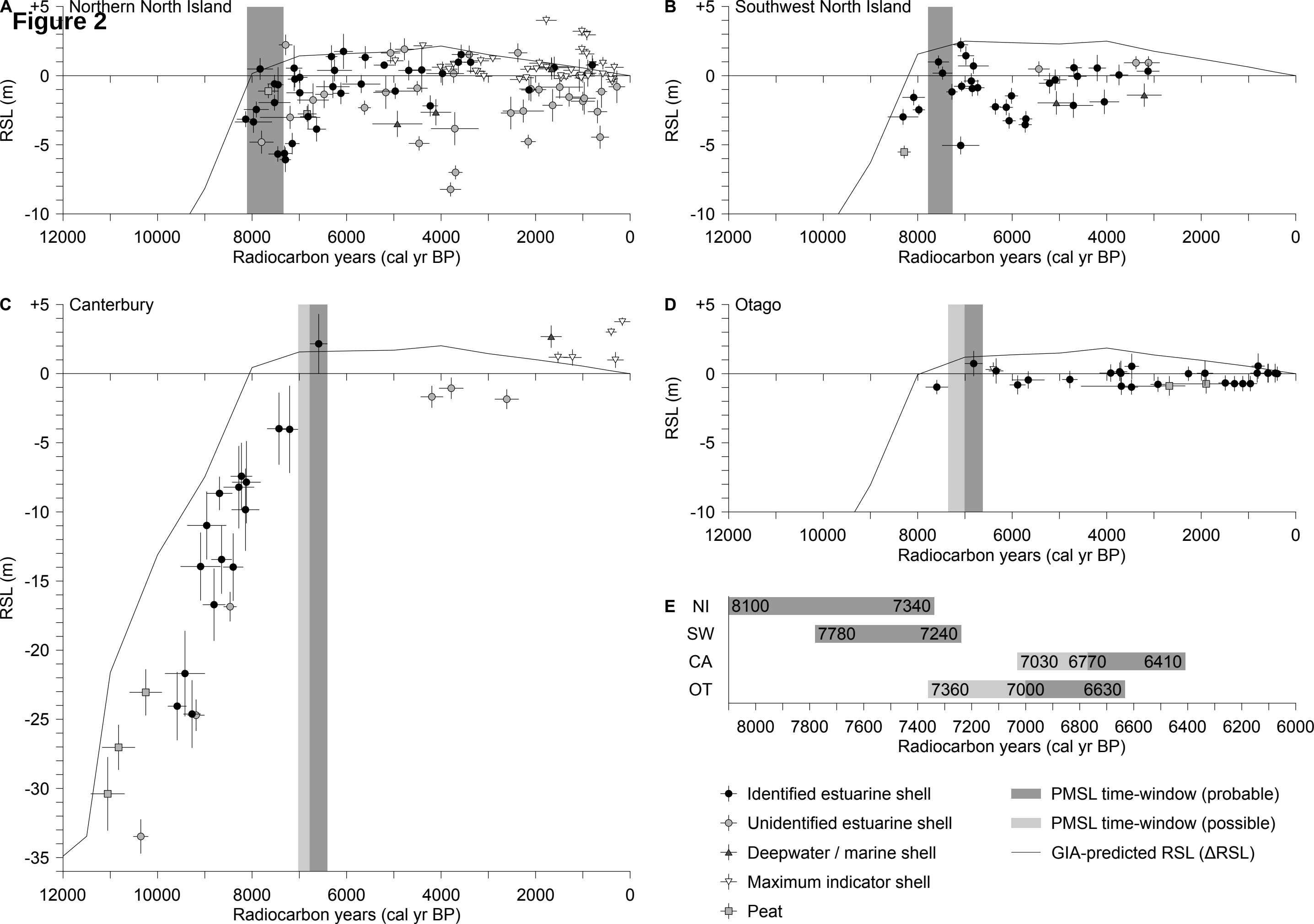

A
Northern North Island
B
Southwest North Island
C
Canterbury
D
Otago
E
RSL (m)
Radiocarbon years (cal yr BP)
NI
8100
7340
SW
7780
7240
CA
7030
6770
6410
OT
7360
7000
6630
Identified estuarine shell
Unidentified estuarine shell
Deepwater / marine shell
Maximum indicator shell
Peat
PMSL time-window (probable)
PMSL time-window (possible)
GIA-predicted RSL (ΔRSL)

Figure 3

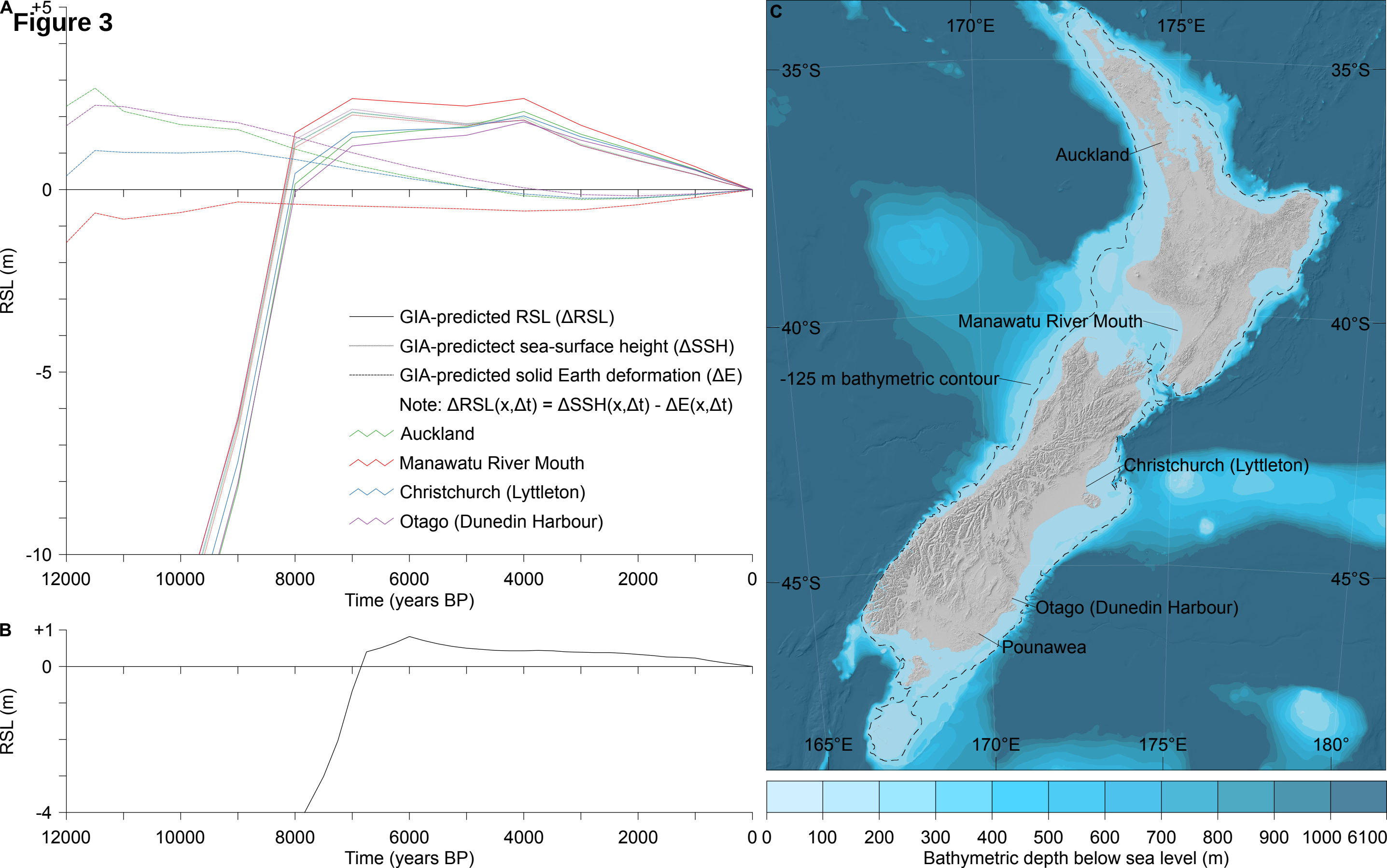
A
+5
0
-5
-10
RSL (m)
12000
10000
8000
6000
4000
2000
0
Time (years BP)
GIA-predicted RSL (ΔRSL)
GIA-predictect sea-surface height (ΔSSH)
GIA-predicted solid Earth deformation (ΔE)
Note: ΔRSL(x,Δt) = ΔSSH(x,Δt) - ΔE(x,Δt)
Auckland
Manawatu River Mouth
Christchurch (Lyttleton)
Otago (Dunedin Harbour)
B
+1
0
-4
RSL (m)
12000
10000
8000
6000
4000
2000
0
Time (years BP)
C
170°E
175°E
35°S
40°S
45°S
165°E
170°E
175°E
180°
Auckland
Manawatu River Mouth
-125 m bathymetric contour
Christchurch (Lyttleton)
Otago (Dunedin Harbour)
Pounawea
0
100
200
300
400
500
600
700
800
900
1000
6100
Bathymetric depth below sea level (m)

Figure 4

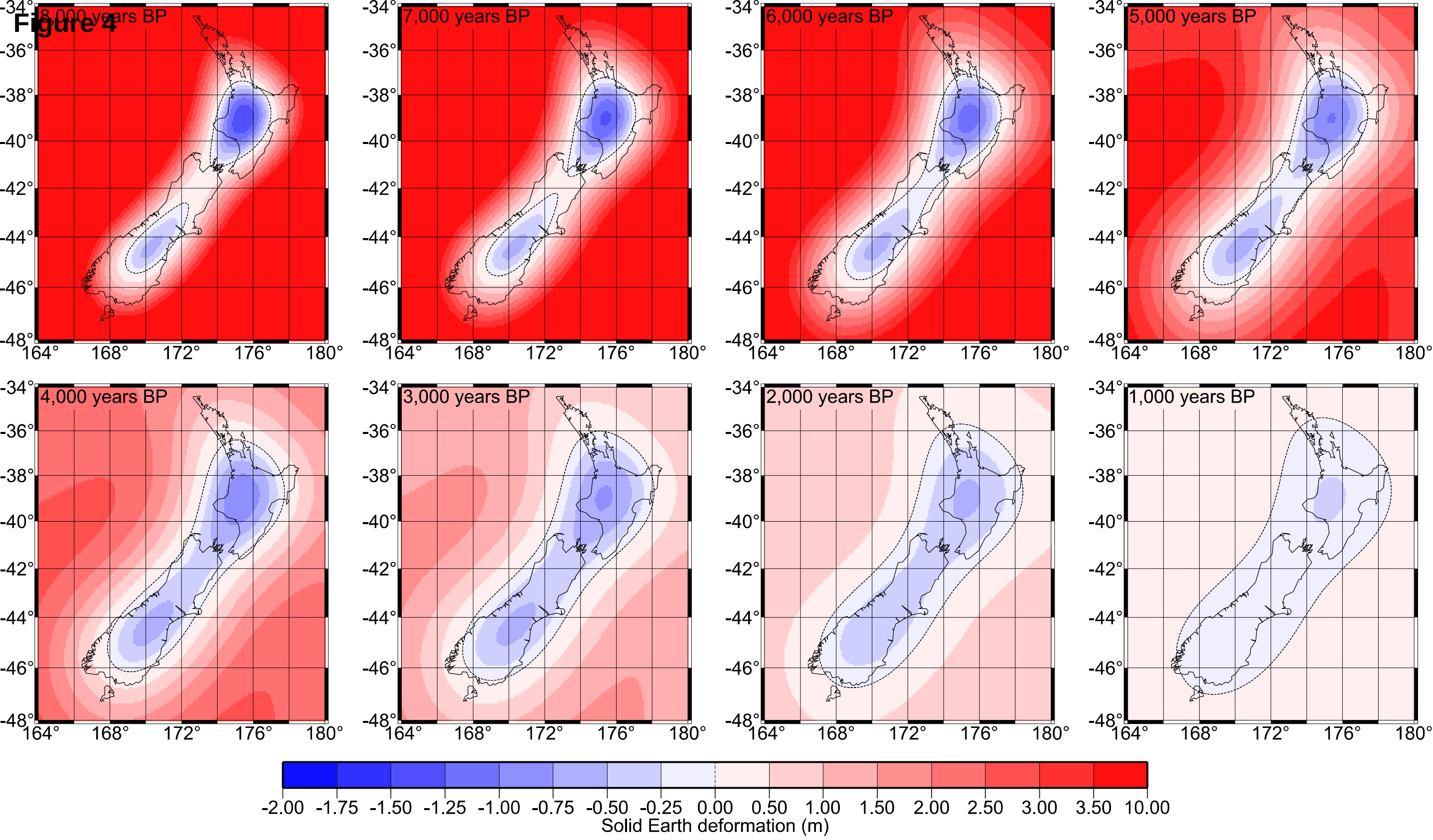
8,000 years BP
7,000 years BP
6,000 years BP
5,000 years BP
4,000 years BP
3,000 years BP
2,000 years BP
1,000 years BP
-34°
-36°
-38°
-40°
-42°
-44°
-46°
-48°
164°
168°
172°
176°
180°
-2.00
-1.75
-1.50
-1.25
-1.00
-0.75
-0.50
-0.25
0.00
0.50
1.00
1.50
2.00
2.50
3.00
3.50
10.00
Solid Earth deformation (m)

Figure 5

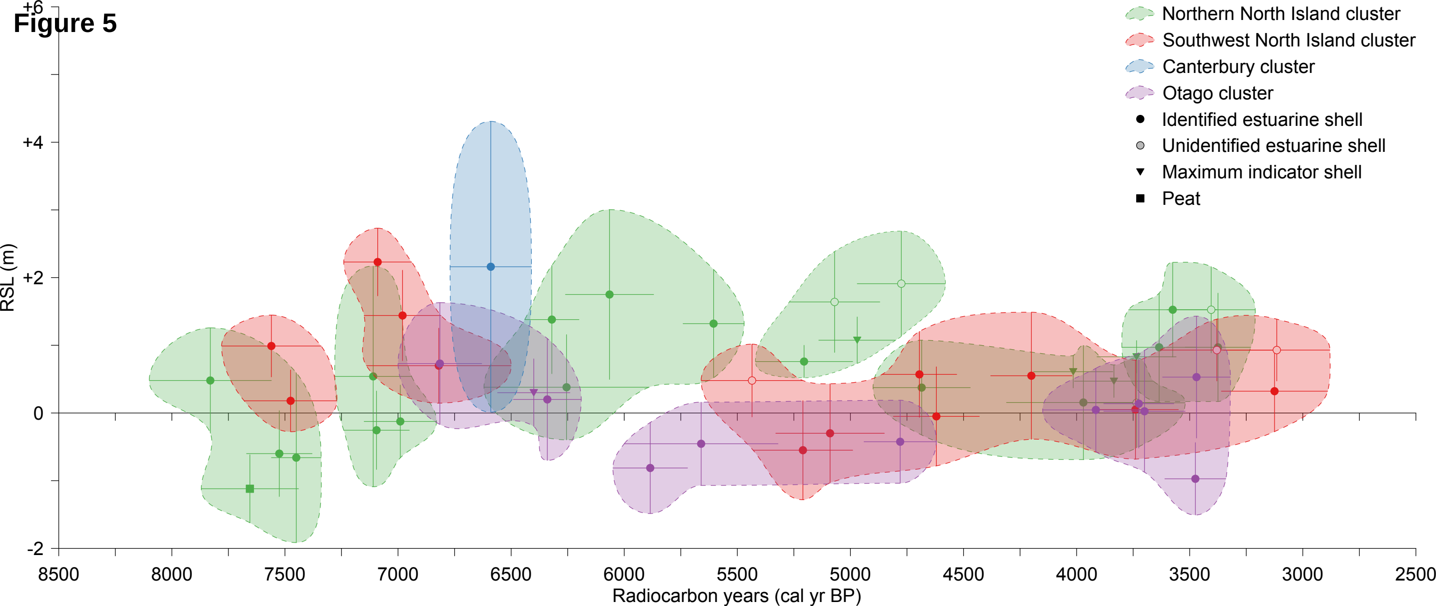

Northern North Island cluster
Southwest North Island cluster
Canterbury cluster
Otago cluster
Identified estuarine shell
Unidentified estuarine shell
Maximum indicator shell
Peat
RSL (m)
+6
+4
+2
0
-2
8500
8000
7500
7000
6500
6000
5500
5000
4500
4000
3500
3000
2500
Radiocarbon years (cal yr BP)

Figure 6

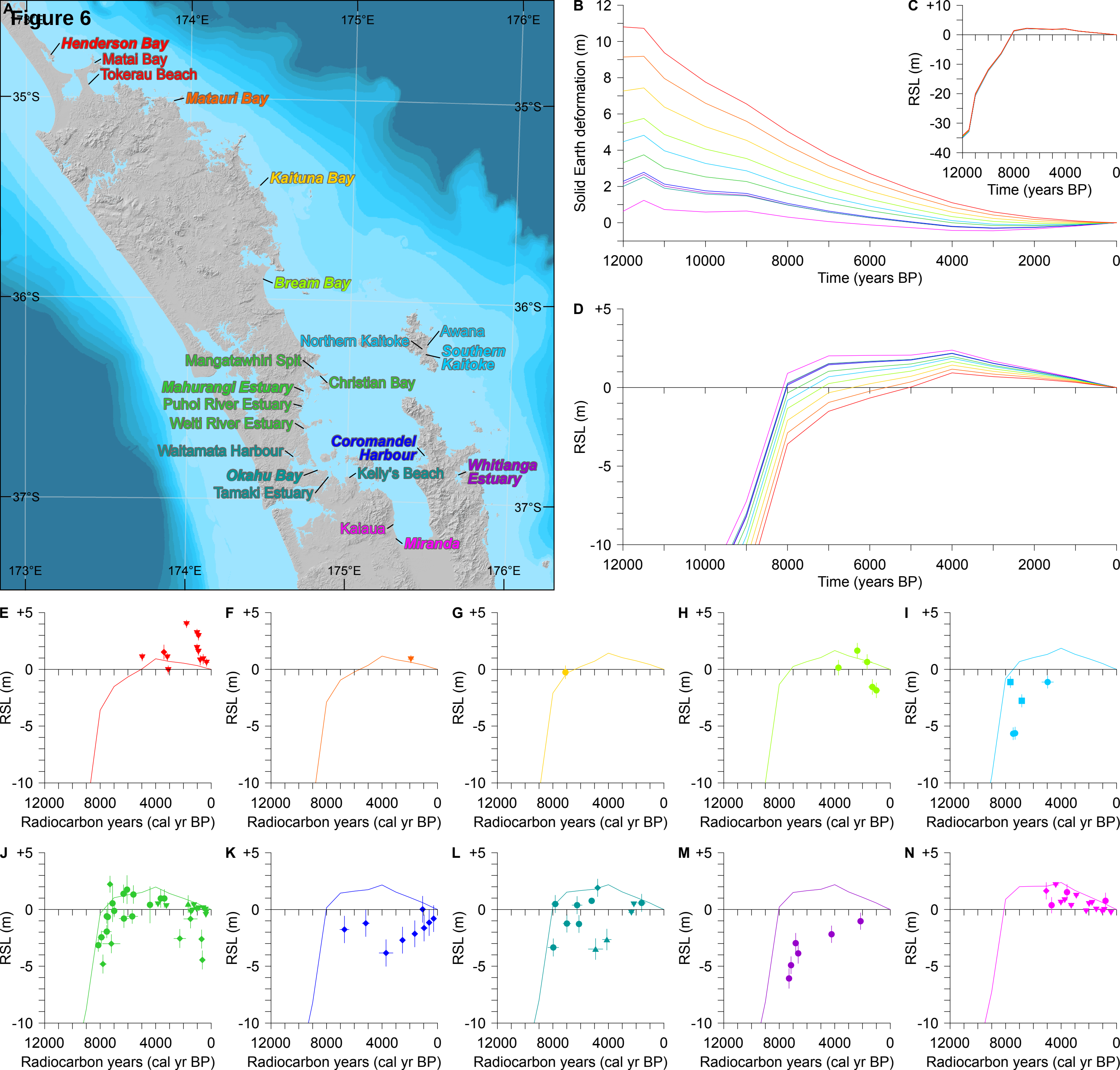
A
173°E
174°E
175°E
176°E
35°S
36°S
37°S
Henderson Bay
Matai Bay
Tokerau Beach
Matauri Bay
Kaituna Bay
Bream Bay
Northern Kaitoke
Awana
Southern Kaitoke
Mangatawhiri Spit
Christian Bay
Mahurangi Estuary
Puhoi River Estuary
Weiti River Estuary
Waitamata Harbour
Coromandel Harbour
Okahu Bay
Kelly's Beach
Tamaki Estuary
Whitianga Estuary
Kaiaua
Miranda
B
Solid Earth deformation (m)
Time (years BP)
C
RSL (m)
Time (years BP)
D
RSL (m)
Time (years BP)
E
F
G
H
I
J
K
L
M
N
RSL (m)
Radiocarbon years (cal yr BP)

Supplementary Figure 1

Click here to download Supplementary Data: Supplementary_Figure_01_RSL_DEF_SSH_definition.pdf

Supplementary Figure 2
Click here to download Supplementary Data: Supplementary_Figure_02_RSL_Maps.pdf

Supplementary Figure 3

Click here to download Supplementary Data: Supplementary_Figure_03_SSH_Maps.pdf